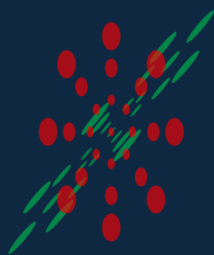


Rapidity scan with DCCI at LHC energy

Shin-ei Fujii¹, Yasuki Tachibana², Tetsufumi Hirano¹

Sophia University¹, Akita International University²



SOPHIA
HADRON
PHYSICS
GROUP

Introduction


Model

Results

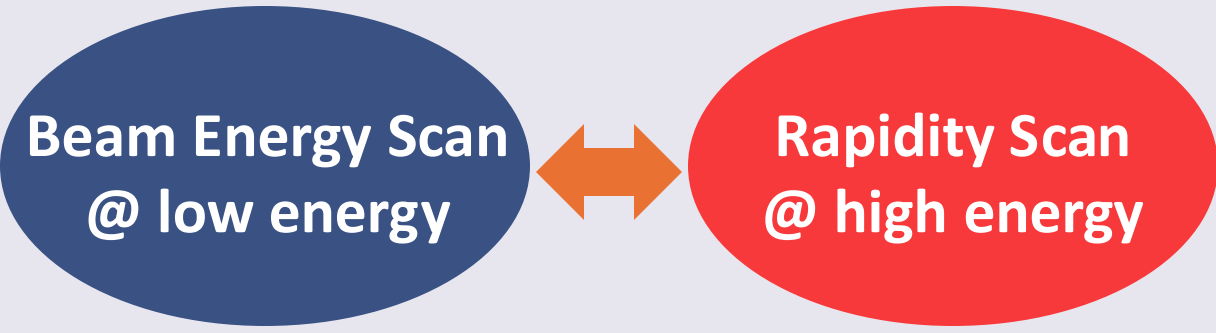
Summary and Outlook

Rapidity Scan

Expected high baryon number density in forward rapidity in high-energy collisions
 M. Li and J. I. Kapusta, Phys. Rev. C **99**, 014906 (2019)

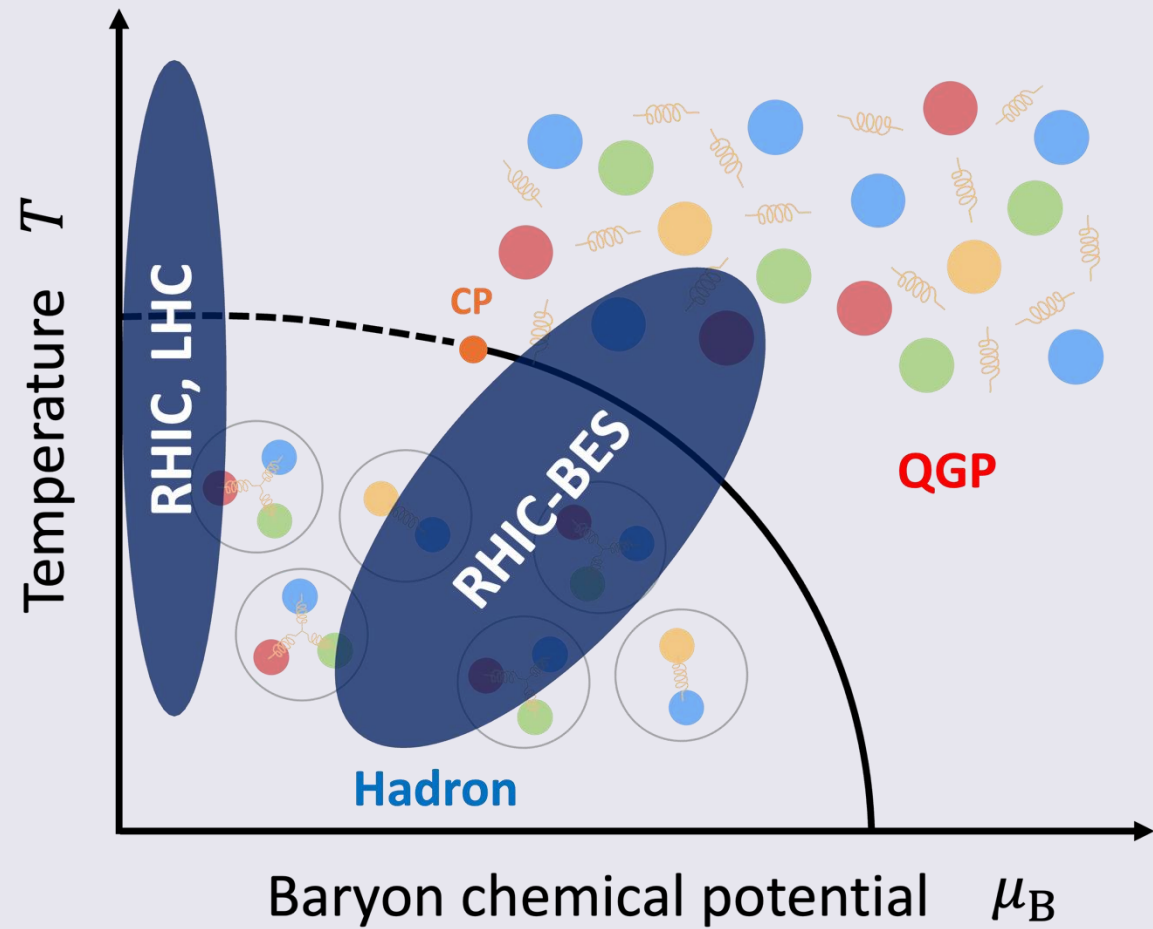

Rapidity Scan

Access high baryon chemical potential region in the QCD phase diagram



Complementary study of QCD phase diagram by BES and Rapidity Scan!

QCD phase diagram and experiments



Rapidity Scan

Expected high baryon number density in forward rapidity in high-energy collisions

M. Li and J. I. Kapusta, Phys. Rev. C **99**, 014906 (2019)



Rapidity Scan

Access high baryon chemical potential region in the QCD phase diagram

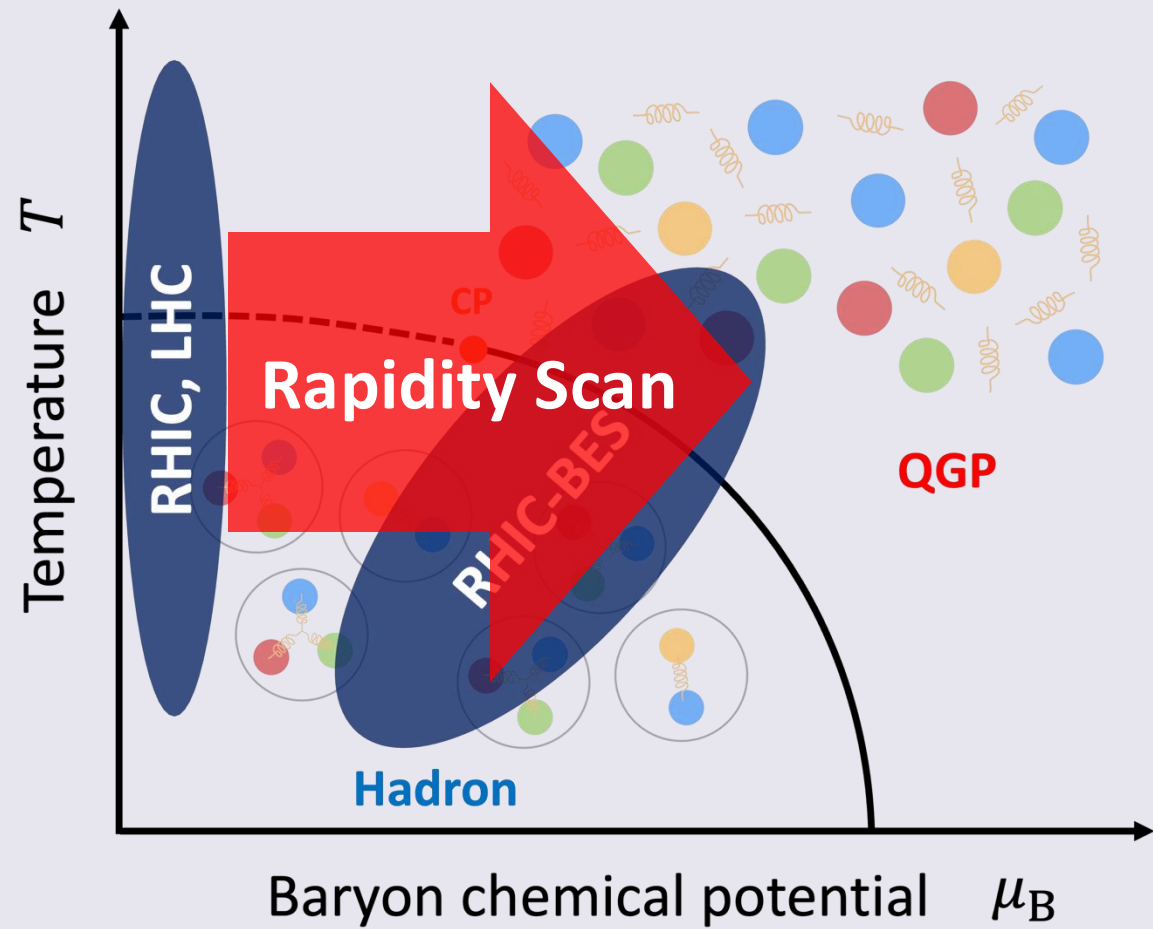
Beam Energy Scan
@ low energy



Rapidity Scan
@ high energy

Complementary study of QCD phase diagram
by BES and Rapidity Scan!

QCD phase diagram and experiments



A fundamental question

How large baryon chemical potential is achieved as equilibrated matter in forward rapidity?

To answer the question, models must describe...

- Equilibrium and non-equilibrium components separately
- Fluidization of baryon number
- Hydrodynamic evolution of baryon number density

A fundamental question

How large baryon chemical potential is achieved as equilibrated matter in forward rapidity?

To answer the question, models must describe...

- Equilibrium and non-equilibrium components separately
- Fluidization of baryon number
- Hydrodynamic evolution of baryon number density

➔ **DCCI + finite n_B extension**

Introduction

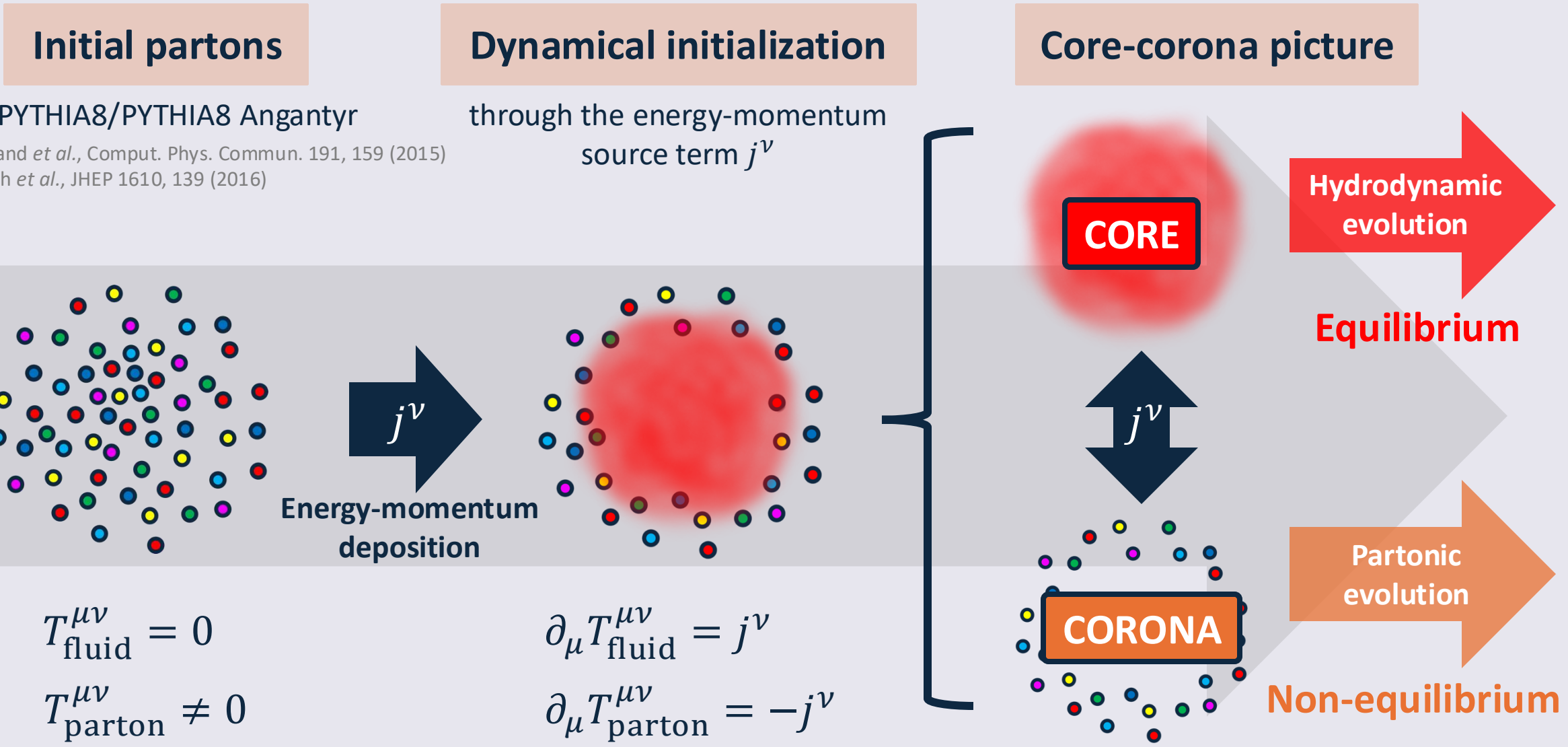
 **Model**

Results

Summary and Outlook

Dynamical Core-Corona Initialization (DCCI) model

Y. Kanakubo *et al.*, Phys. Rev. C **105**, 024905 (2022)



$$T_{\text{fluid}}^{\mu\nu} = 0$$

$$T_{\text{parton}}^{\mu\nu} \neq 0$$

$$\partial_\mu T_{\text{fluid}}^{\mu\nu} = j^\nu$$

$$\partial_\mu T_{\text{parton}}^{\mu\nu} = -j^\nu$$

Source terms

Energy-momentum source term

Y. Kanakubo *et al.*, Phys. Rev. C **105**, 024905 (2022)

$$\partial_\mu T_{\text{fluid}}^{\mu\nu} = j^\nu$$

$$j^\nu = - \sum_i^{N_{\text{parton}}} \frac{dp_i^\nu(t)}{dt} G(\mathbf{x} - \mathbf{x}_i(t))$$

p_i^ν : Four-momentum of i_{th} parton

G : Gaussian function \mathbf{x}_i : Position of i_{th} parton



Baryon number source term

New!!

$$\partial_\mu N_{\text{fluid}}^\mu = \rho$$

$$\rho = - \sum_j^{N_{\text{dead}}} \frac{dB_j}{dt} G(\mathbf{x} - \mathbf{x}_j(t))$$

B_j : Baryon number of j_{th} dead parton

Source terms

Energy-momentum source term

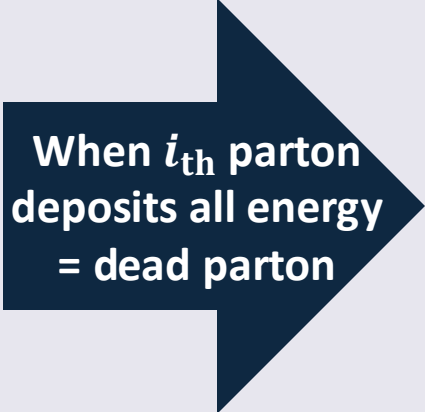
Y. Kanakubo *et al.*, Phys. Rev. C **105**, 024905 (2022)

$$\partial_\mu T_{\text{fluid}}^{\mu\nu} = j^\nu$$

$$j^\nu = - \sum_i^{N_{\text{parton}}} \left[\frac{dp_i^\nu(t)}{dt} \right] G(\mathbf{x} - \mathbf{x}_i(t))$$

p_i^ν : Four-momentum of i_{th} parton

G : Gaussian function \mathbf{x}_i : Position of i_{th} parton



Baryon number source term

New!!

$$\partial_\mu N_{\text{fluid}}^\mu = \rho$$

$$\rho = - \sum_j^{N_{\text{dead}}} \frac{dB_j}{dt} G(\mathbf{x} - \mathbf{x}_j(t))$$

B_j : Baryon number of j_{th} dead parton

Phenomenological fluidization rate per particle in core-corona picture

Low p_T / Dense



High p_T / Dilute



Source terms

Energy-momentum source term

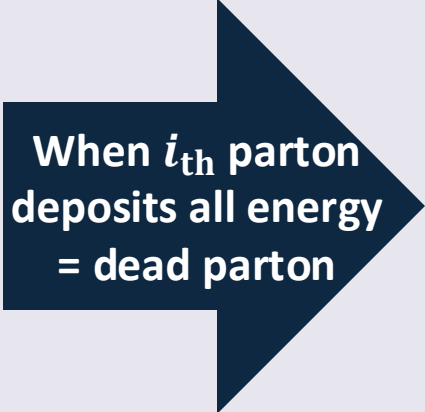
Y. Kanakubo *et al.*, Phys. Rev. C **105**, 024905 (2022)

$$\partial_\mu T_{\text{fluid}}^{\mu\nu} = j^\nu$$

$$j^\nu = - \sum_i^{N_{\text{parton}}} \left[\frac{dp_i^\nu(t)}{dt} \right] G(\mathbf{x} - \mathbf{x}_i(t))$$

p_i^ν : Four-momentum of i_{th} parton

G : Gaussian function \mathbf{x}_i : Position of i_{th} parton



Baryon number source term

New!!

$$\partial_\mu N_{\text{fluid}}^\mu = \rho$$

$$\rho = - \sum_j^{N_{\text{dead}}} \frac{dB_j}{dt} G(\mathbf{x} - \mathbf{x}_j(t))$$

B_j : Baryon number of j_{th} dead parton

- Phenomenological fluidization rate per particle in core-corona picture

Low p_T / Dense



High p_T / Dilute



- Deposition of baryon number into the fluid

Thermalized baryon number in CORE

Introduction

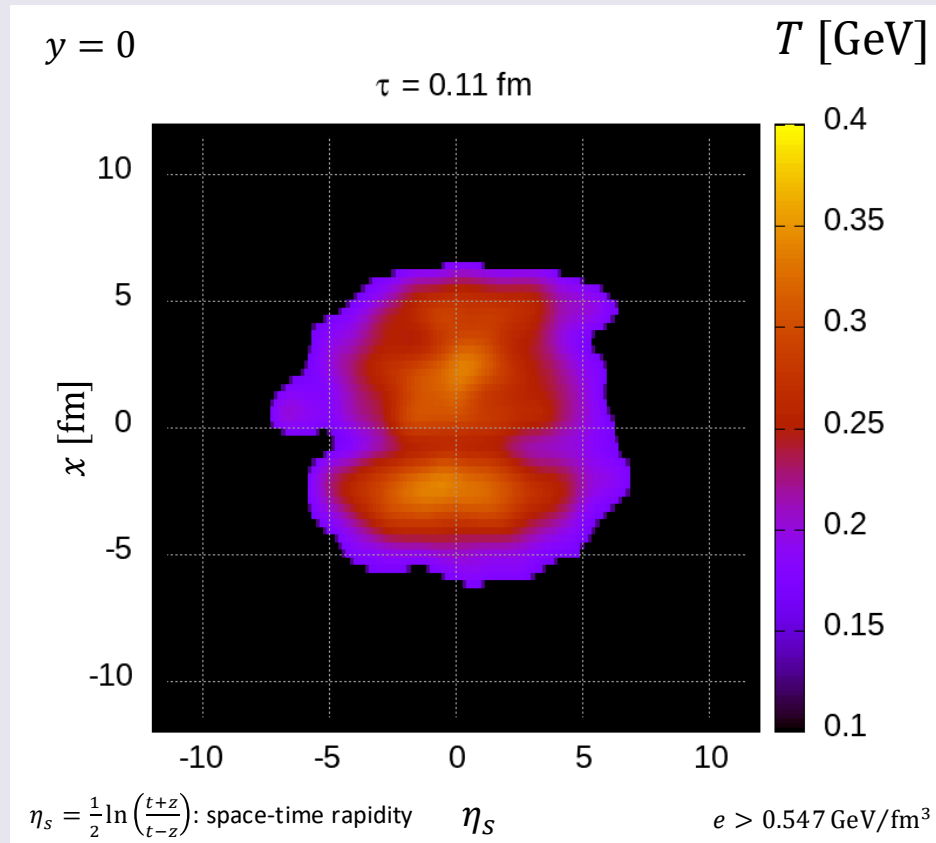
Model

 **Results**

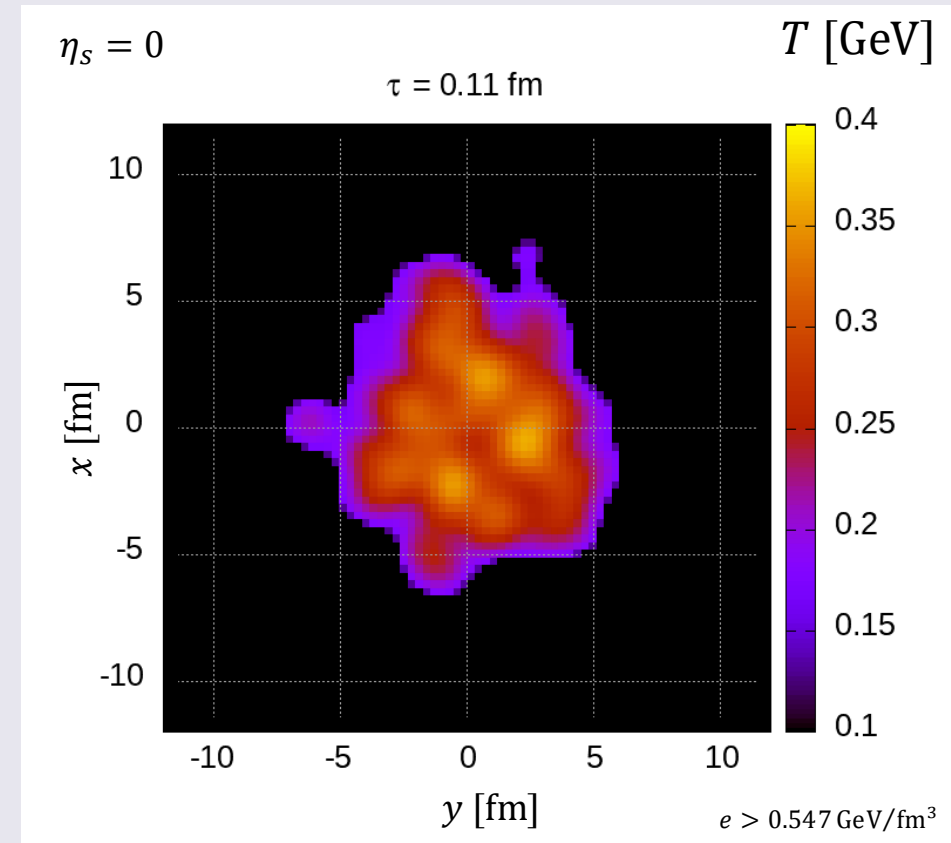
Summary and Outlook

Space-time evolution of core

Temperature (longitudinal profile)



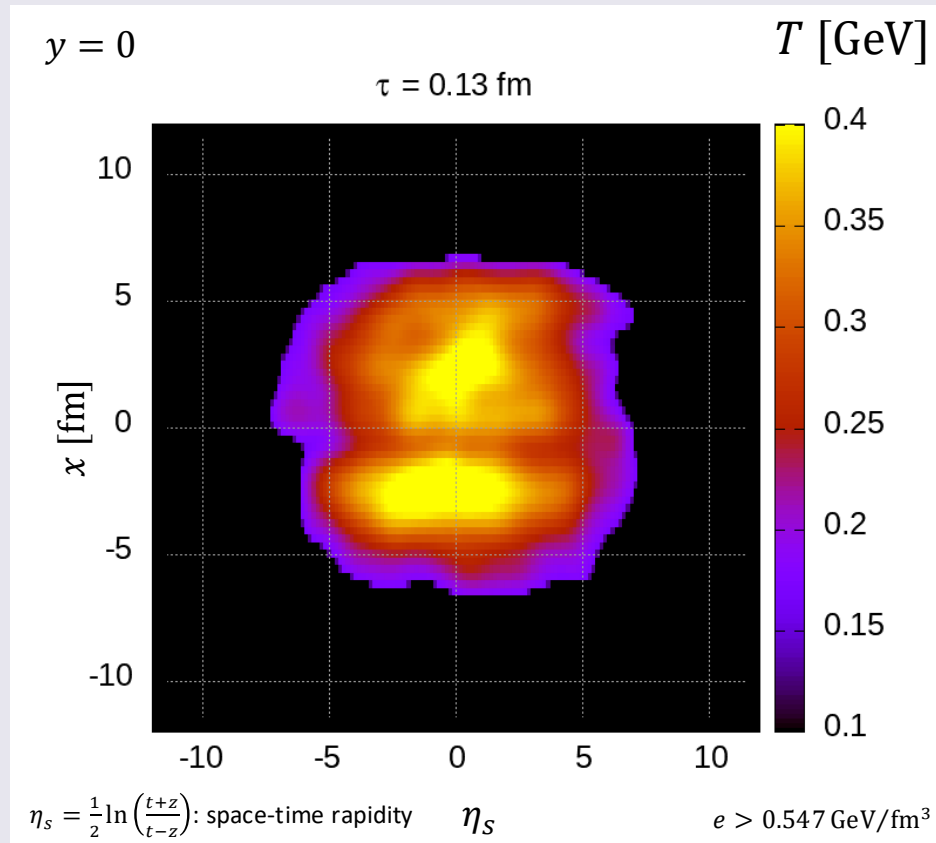
Temperature (transverse profile)



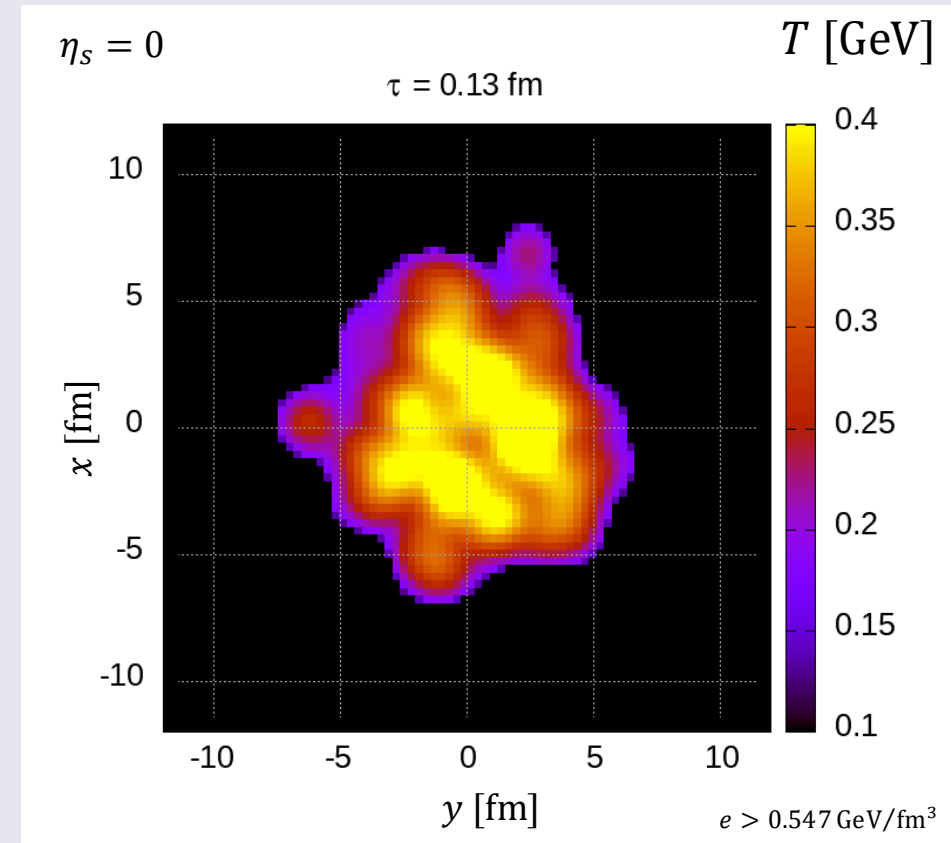
- Gradual formation of the core (QGP fluid) through the energy-momentum source term
- Alongside the fluid formation, the core cools down due to the hydrodynamic evolution

Space-time evolution of core

Temperature (longitudinal profile)



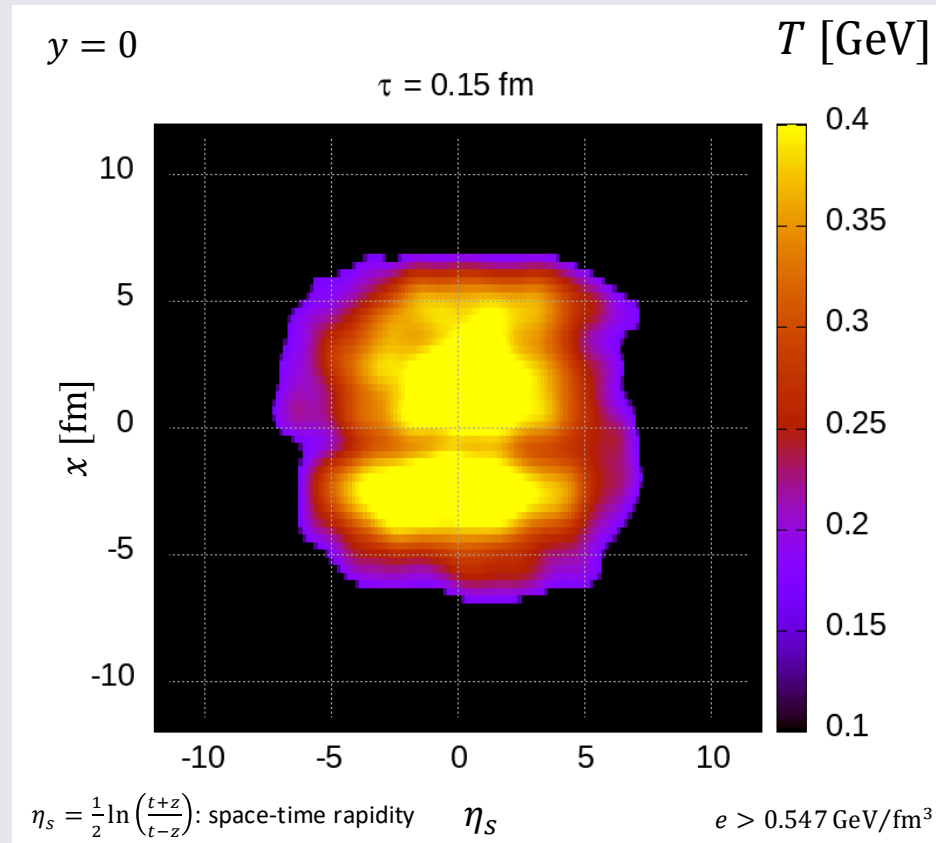
Temperature (transverse profile)



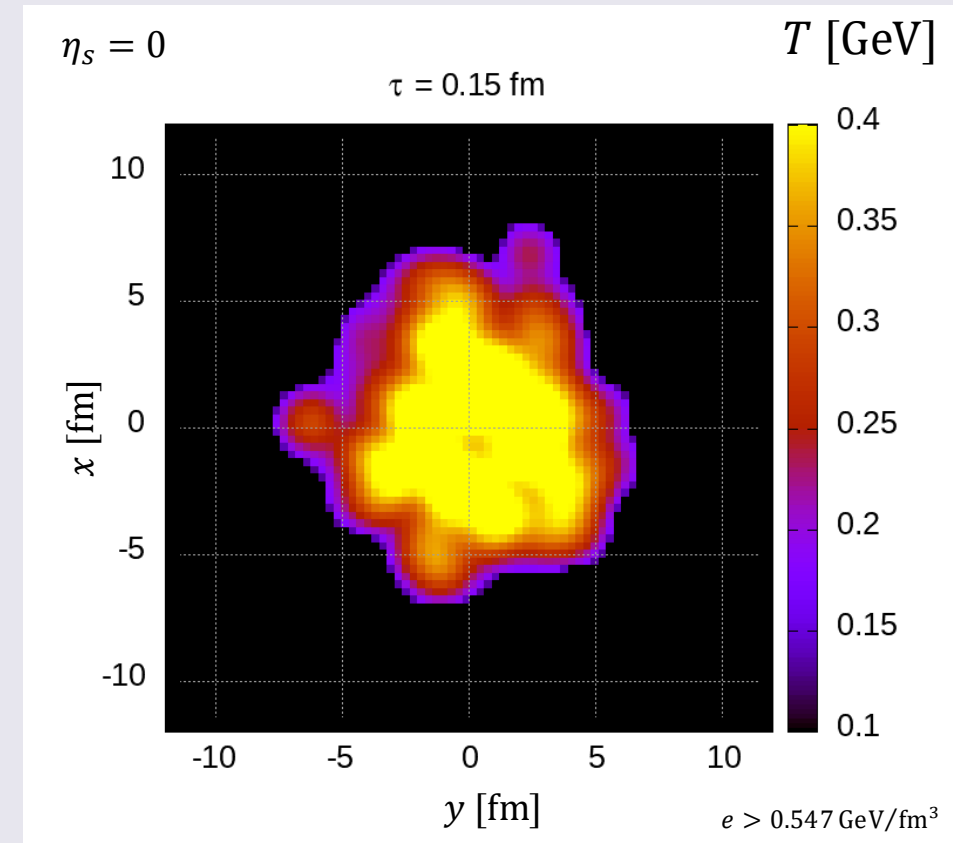
- Gradual formation of the core (QGP fluid) through the energy-momentum source term
- Alongside the fluid formation, the core cools down due to the hydrodynamic evolution

Space-time evolution of core

Temperature (longitudinal profile)



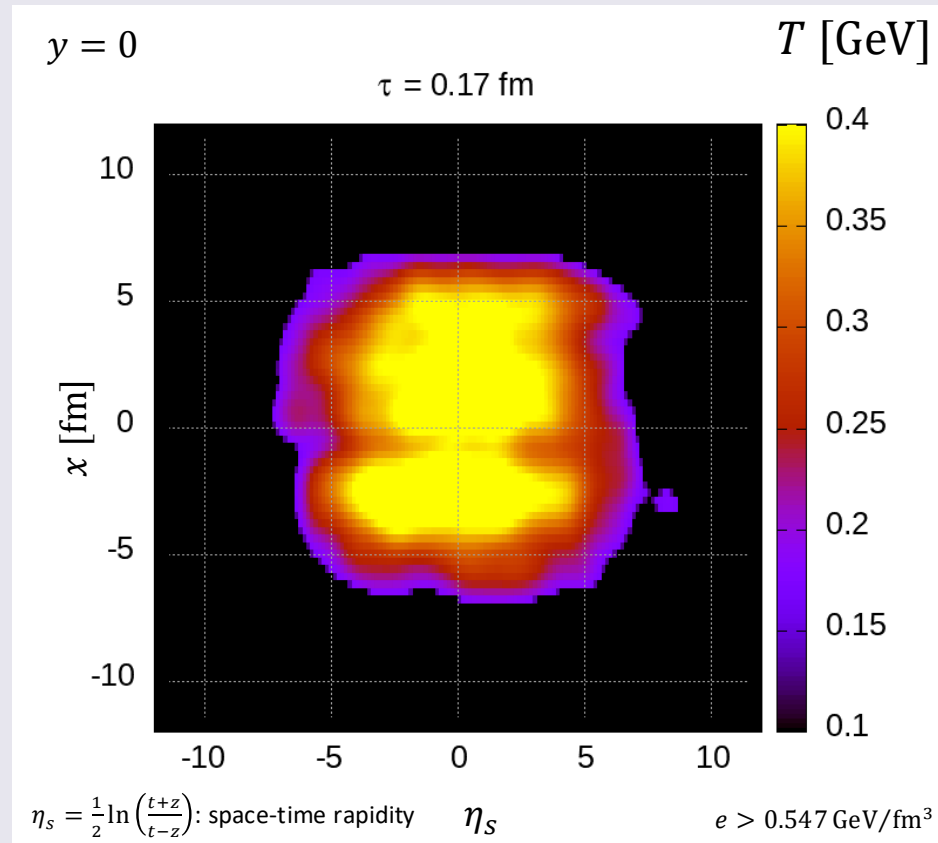
Temperature (transverse profile)



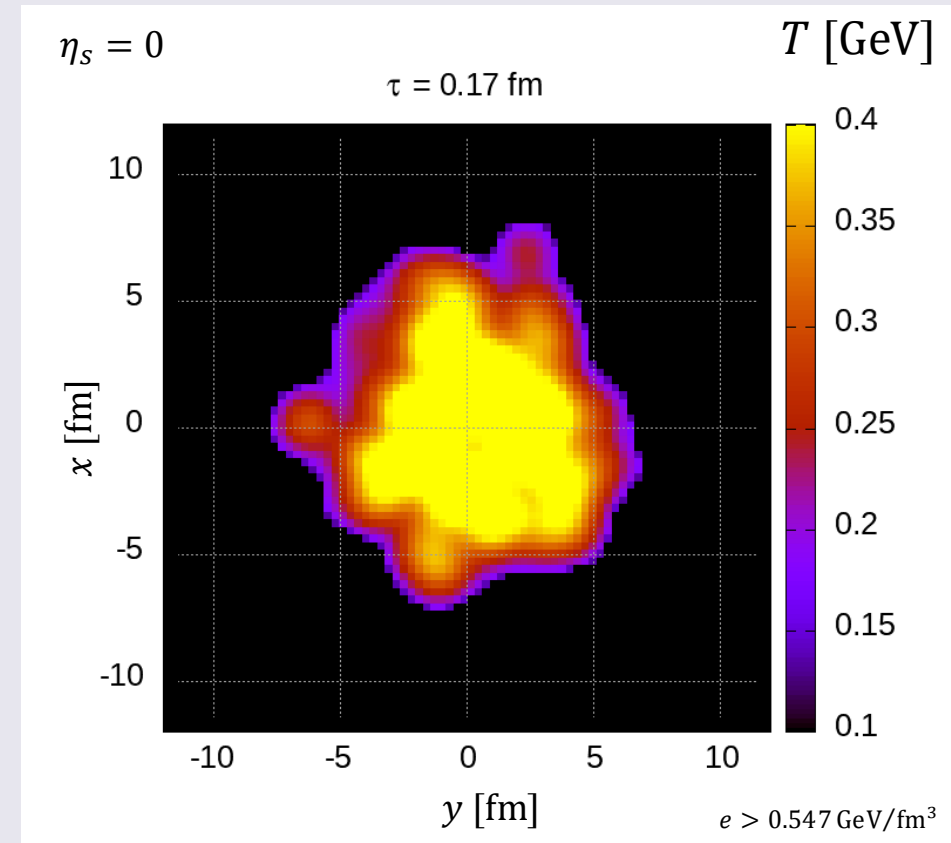
- Gradual formation of the core (QGP fluid) through the energy-momentum source term
- Alongside the fluid formation, the core cools down due to the hydrodynamic evolution

Space-time evolution of core

Temperature (longitudinal profile)



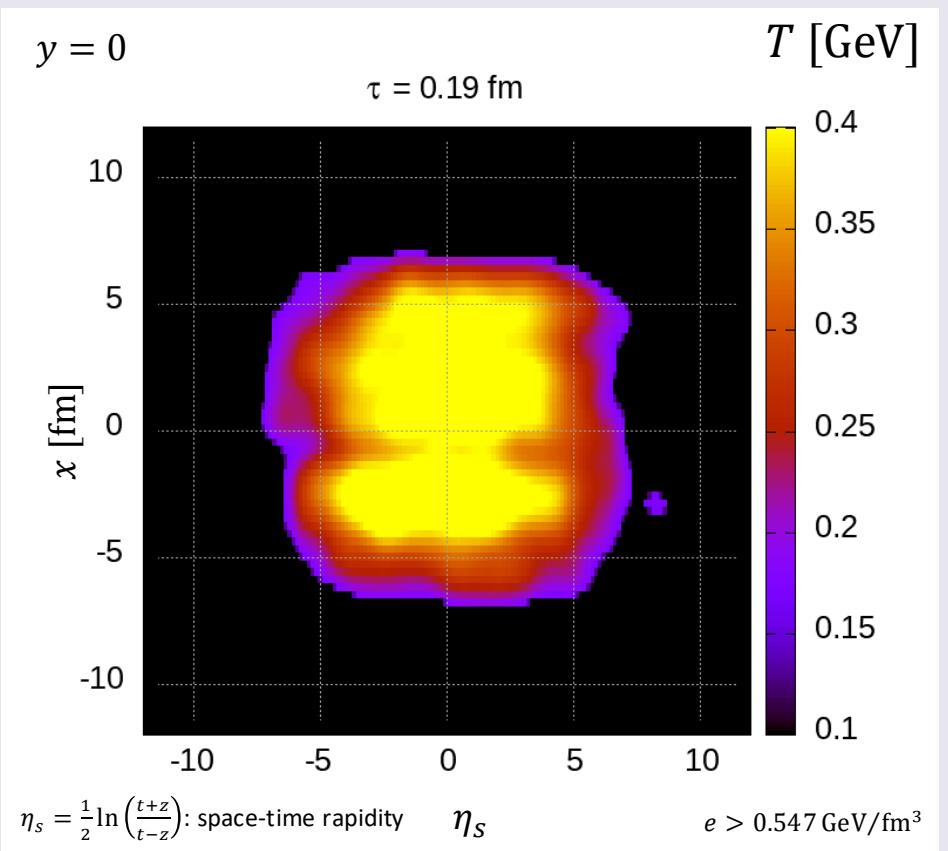
Temperature (transverse profile)



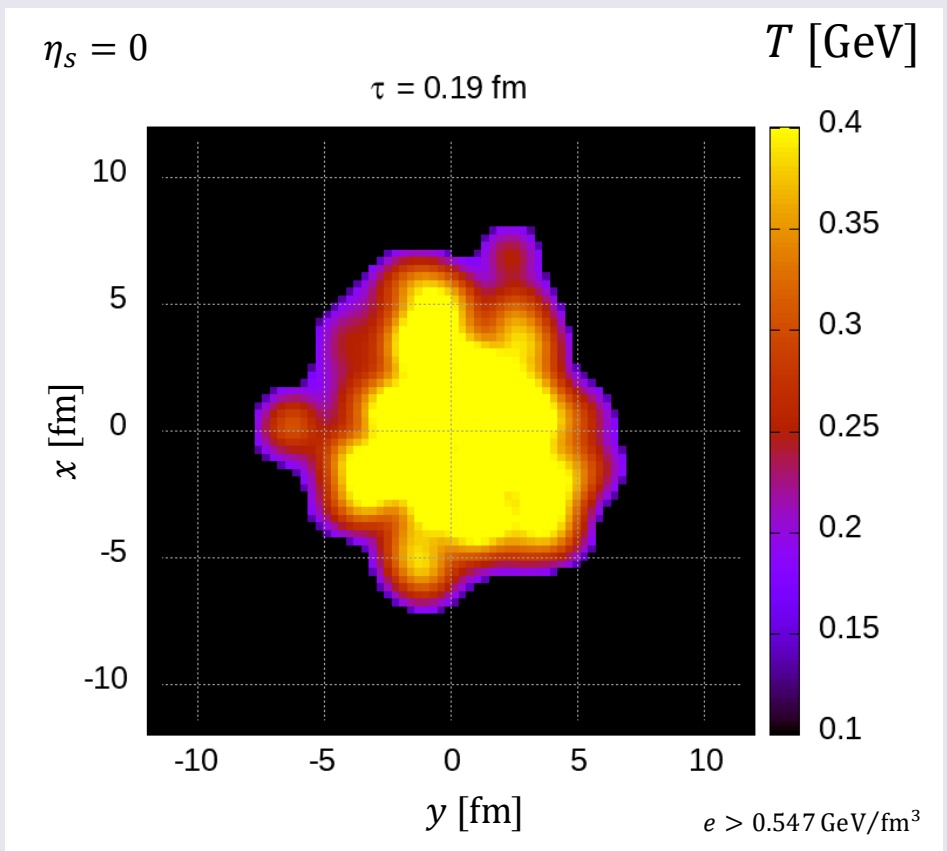
- Gradual formation of the core (QGP fluid) through the energy-momentum source term
- Alongside the fluid formation, the core cools down due to the hydrodynamic evolution

Space-time evolution of core

Temperature (longitudinal profile)



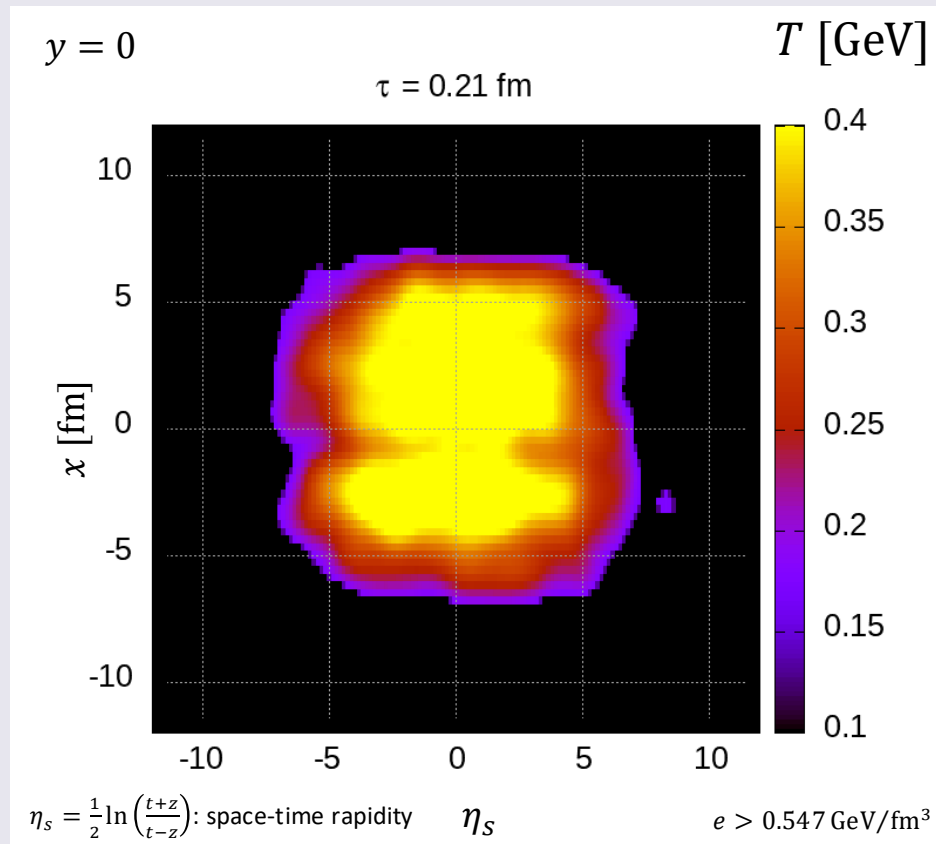
Temperature (transverse profile)



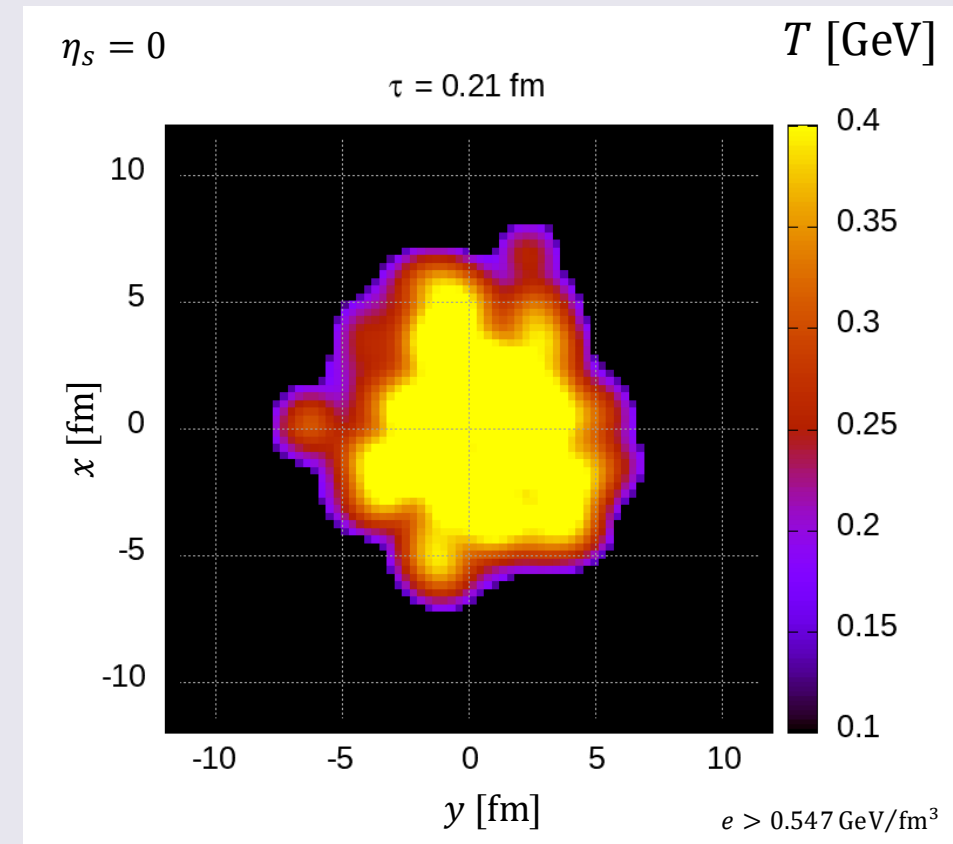
- Gradual formation of the core (QGP fluid) through the energy-momentum source term
- Alongside the fluid formation, the core cools down due to the hydrodynamic evolution

Space-time evolution of core

Temperature (longitudinal profile)



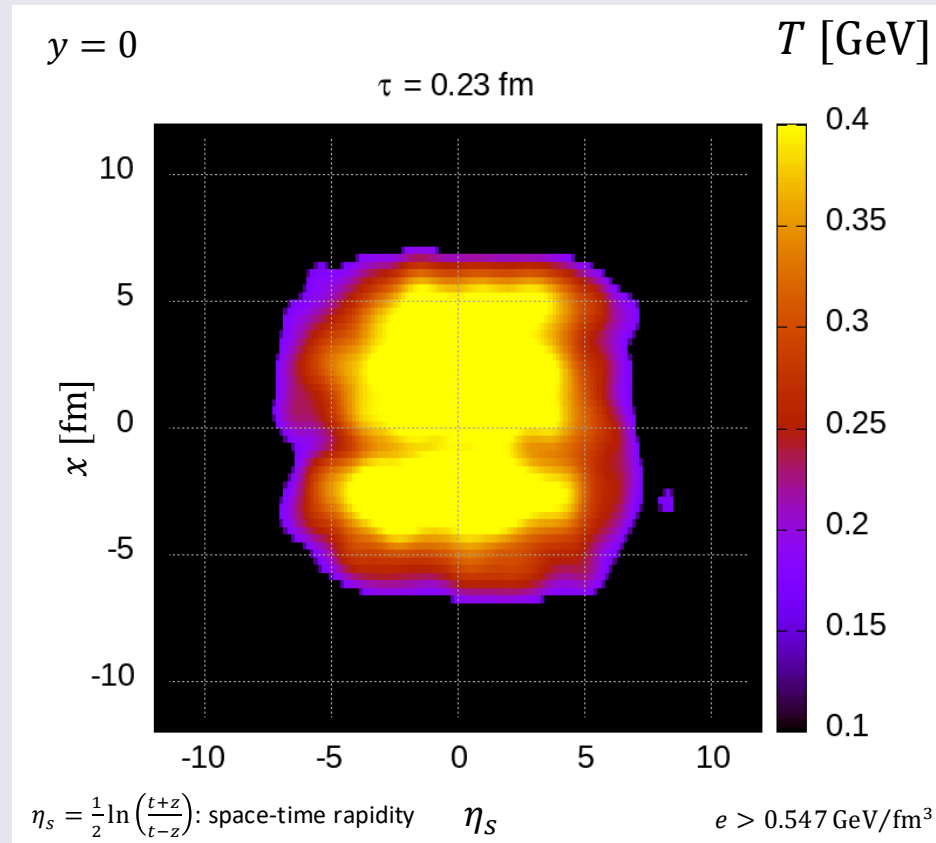
Temperature (transverse profile)



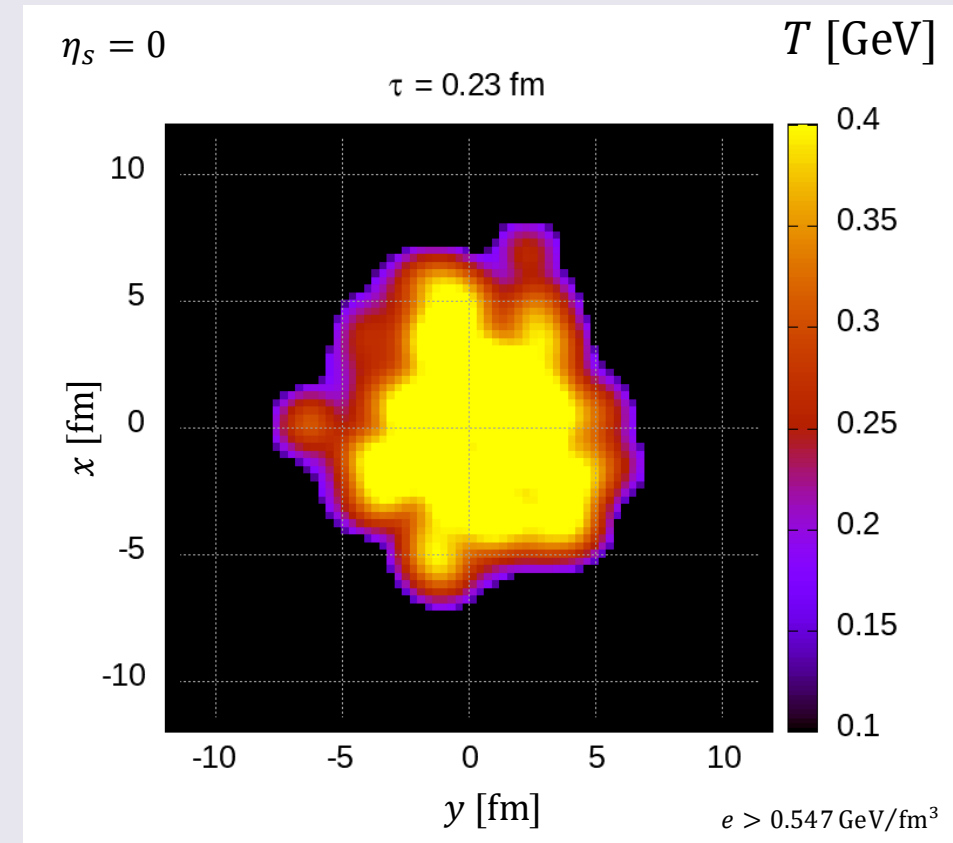
- Gradual formation of the core (QGP fluid) through the energy-momentum source term
- Alongside the fluid formation, the core cools down due to the hydrodynamic evolution

Space-time evolution of core

Temperature (longitudinal profile)



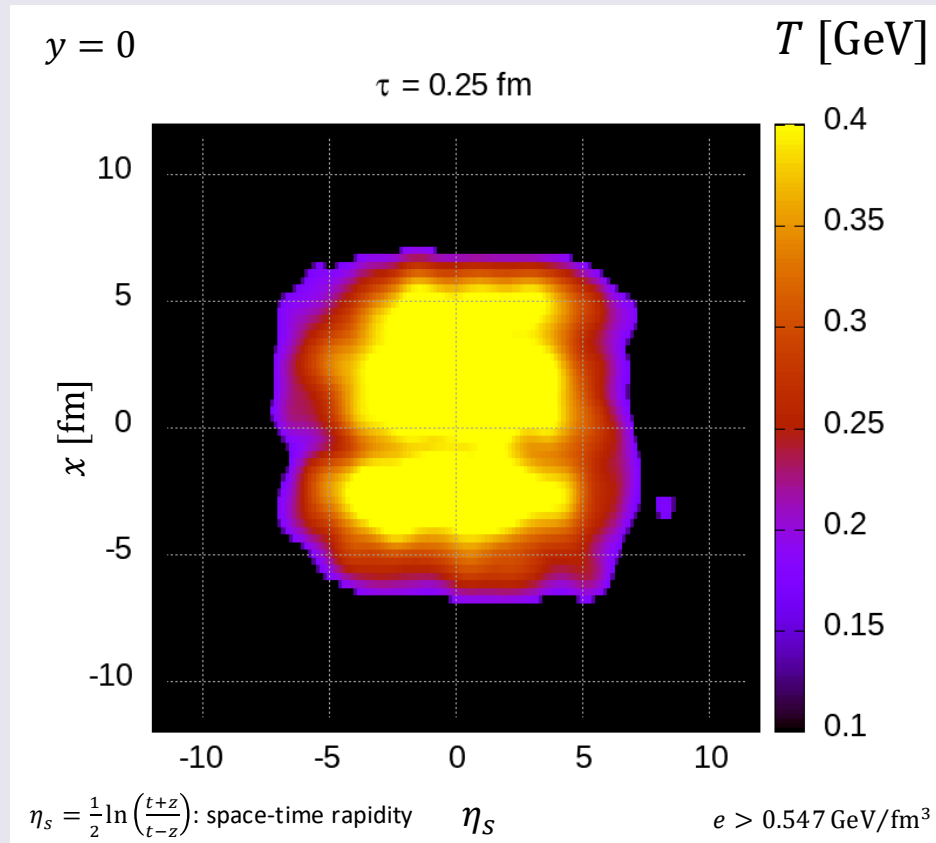
Temperature (transverse profile)



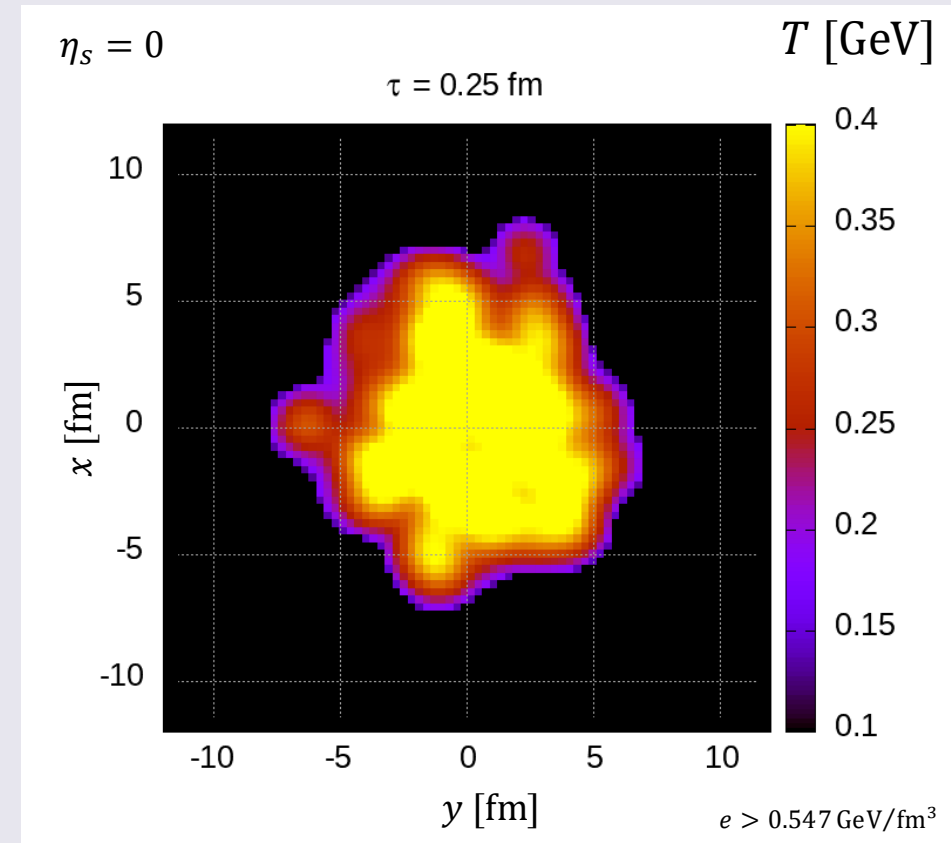
- Gradual formation of the core (QGP fluid) through the energy-momentum source term
- Alongside the fluid formation, the core cools down due to the hydrodynamic evolution

Space-time evolution of core

Temperature (longitudinal profile)



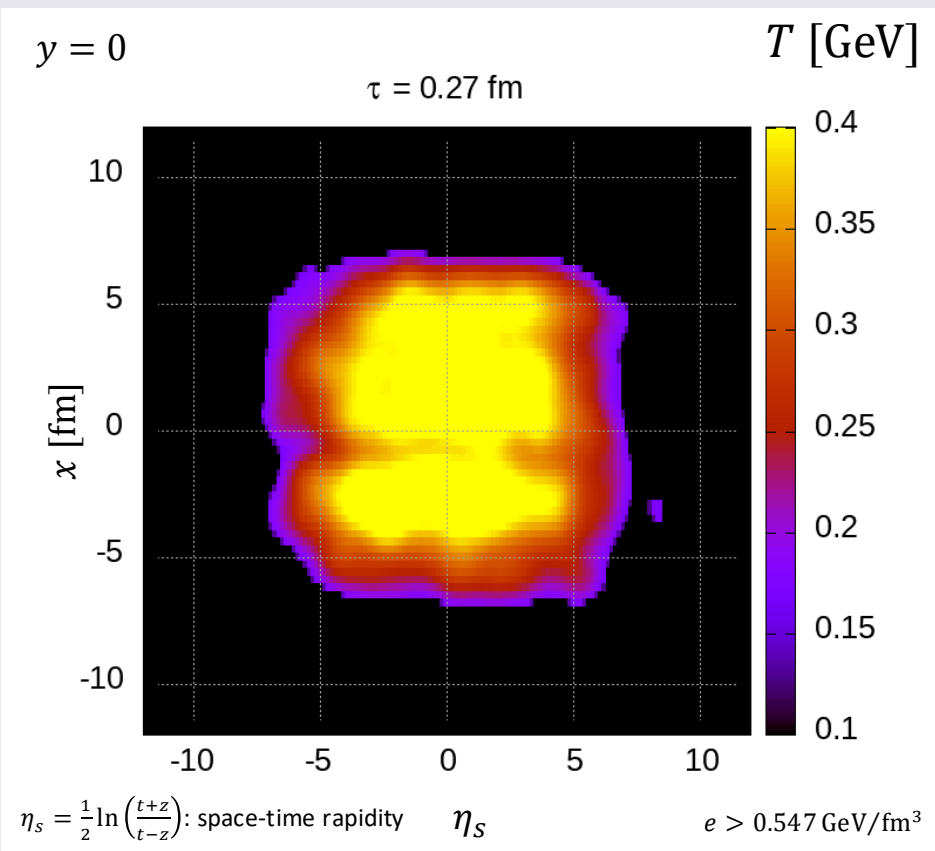
Temperature (transverse profile)



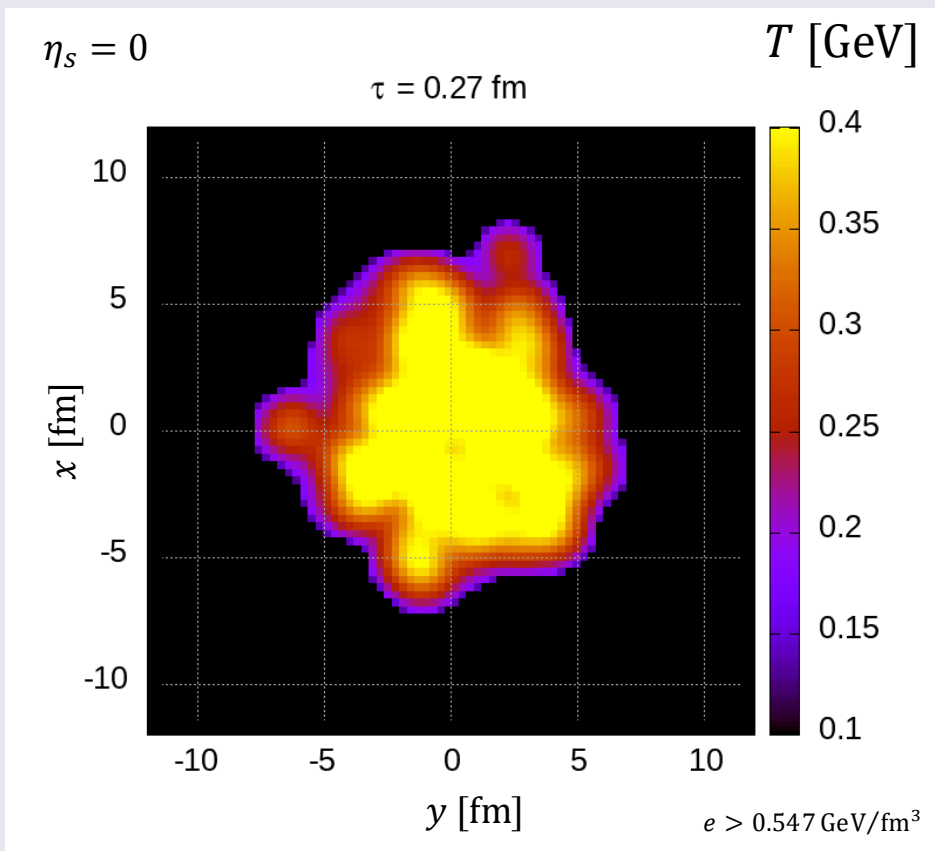
- Gradual formation of the core (QGP fluid) through the energy-momentum source term
- Alongside the fluid formation, the core cools down due to the hydrodynamic evolution

Space-time evolution of core

Temperature (longitudinal profile)



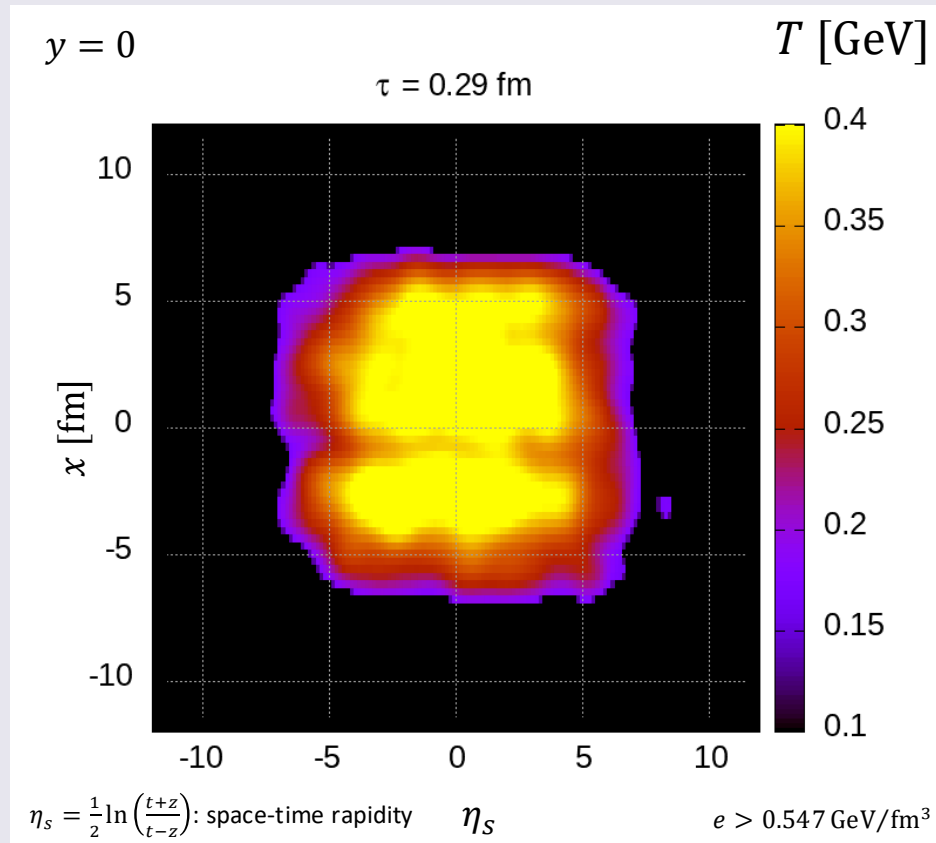
Temperature (transverse profile)



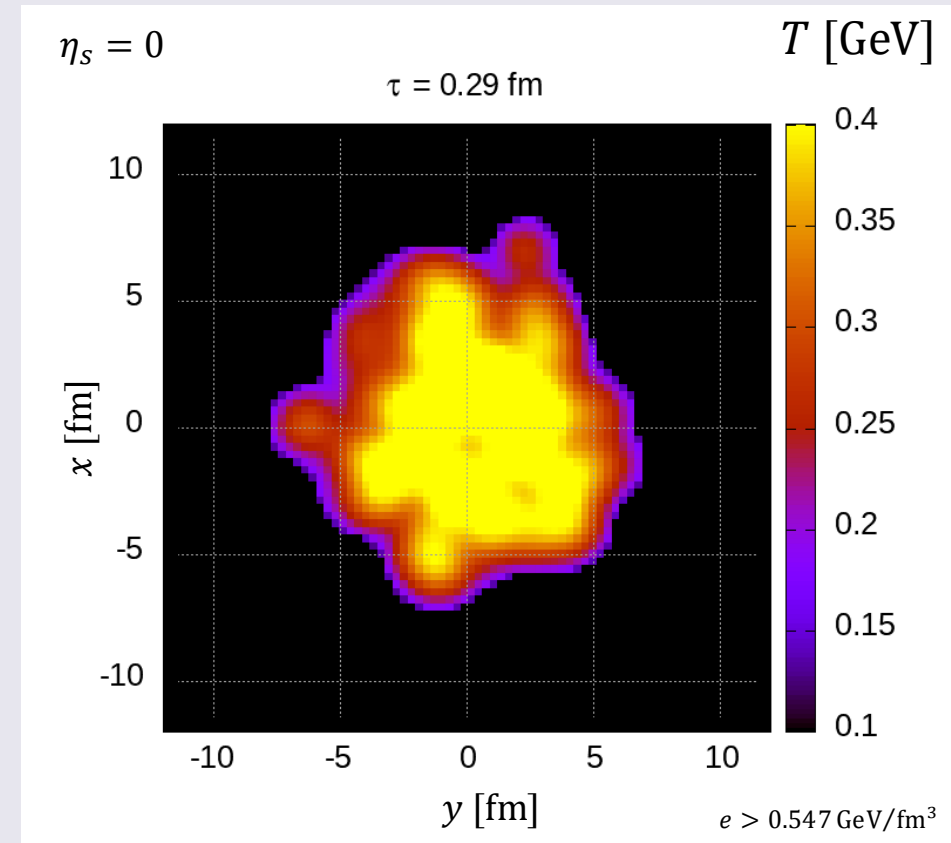
- Gradual formation of the core (QGP fluid) through the energy-momentum source term
- Alongside the fluid formation, the core cools down due to the hydrodynamic evolution

Space-time evolution of core

Temperature (longitudinal profile)



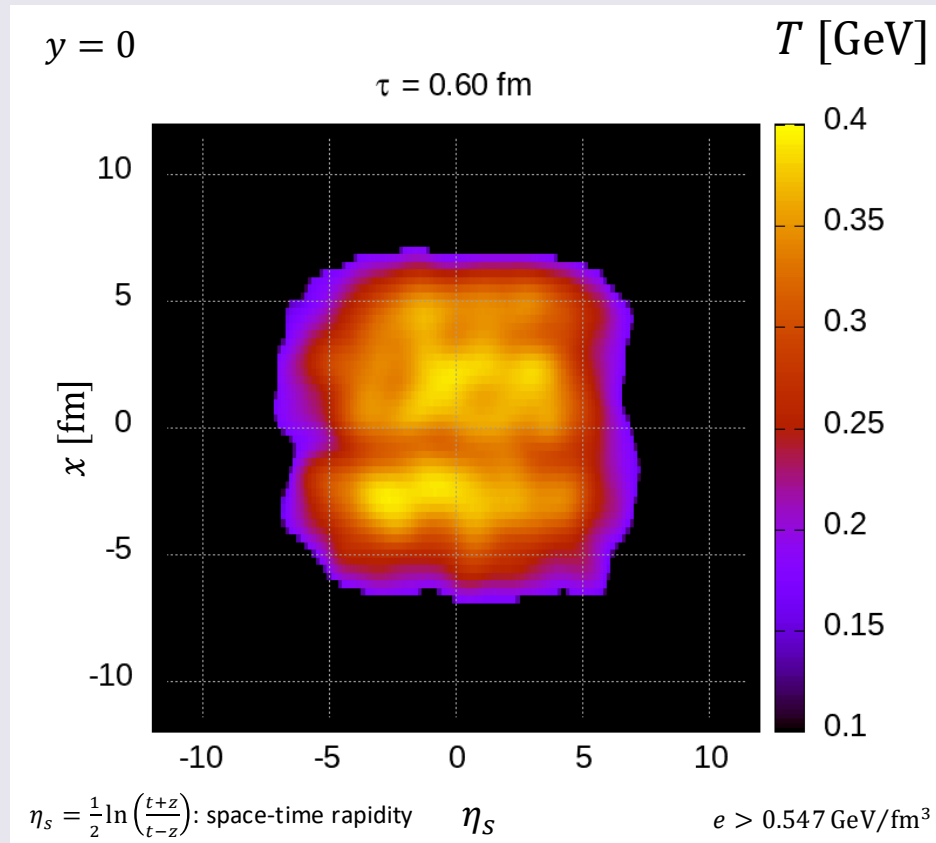
Temperature (transverse profile)



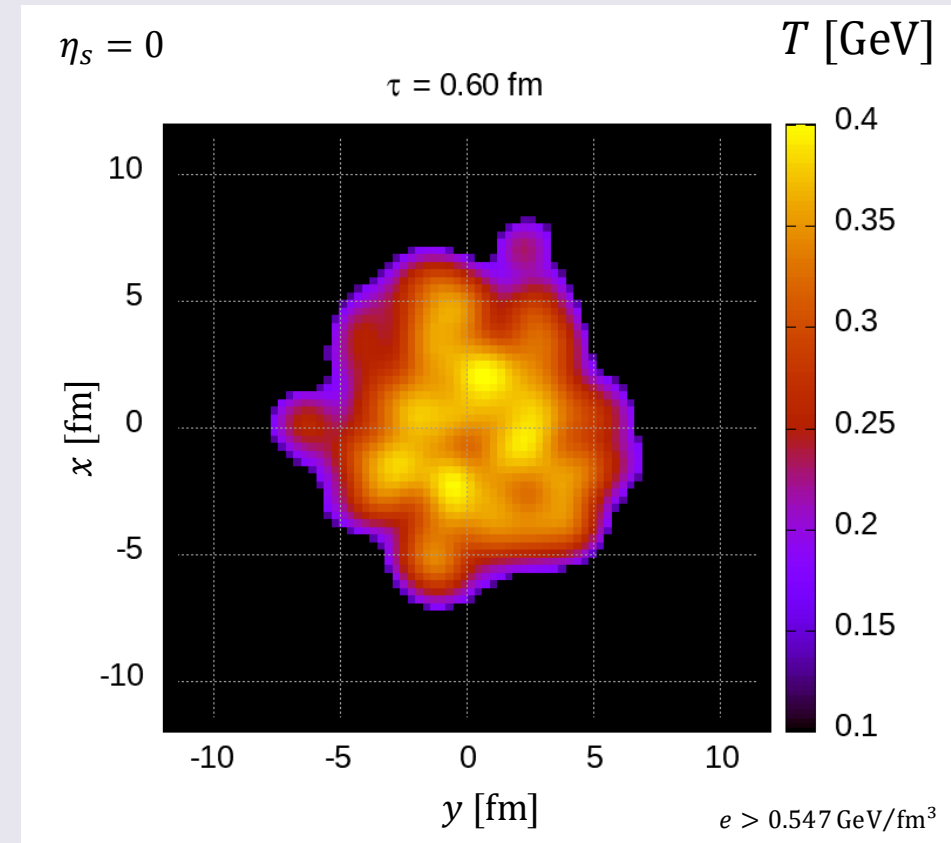
- Gradual formation of the core (QGP fluid) through the energy-momentum source term
- Alongside the fluid formation, the core cools down due to the hydrodynamic evolution

Space-time evolution of core

Temperature (longitudinal profile)



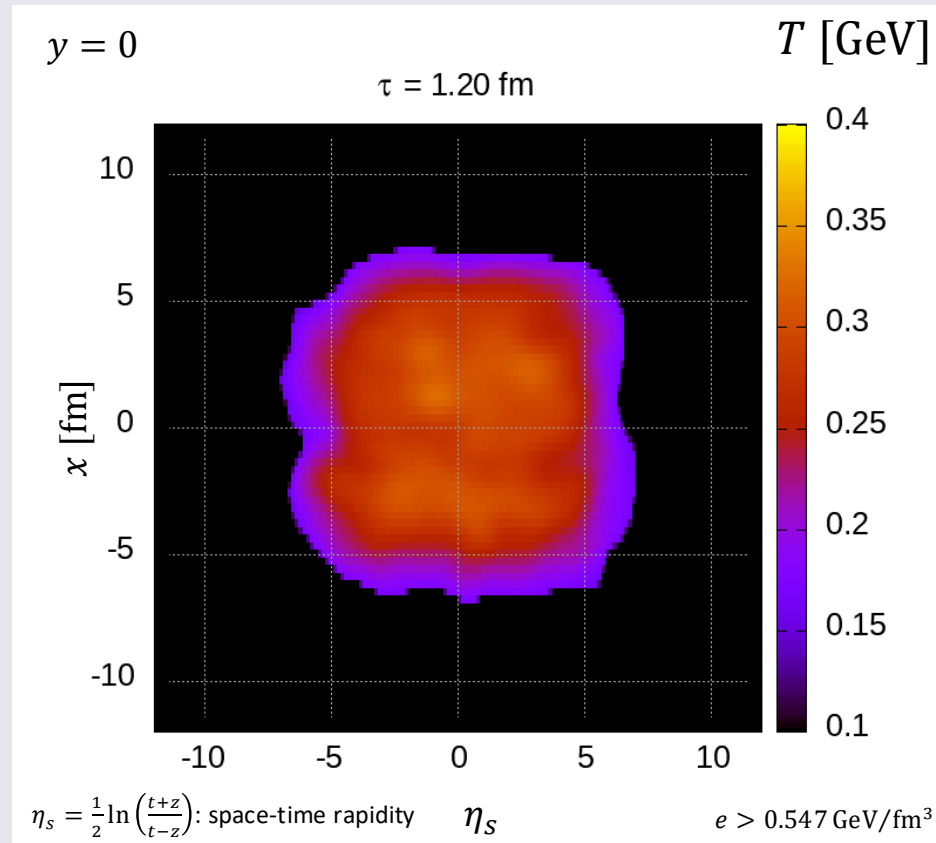
Temperature (transverse profile)



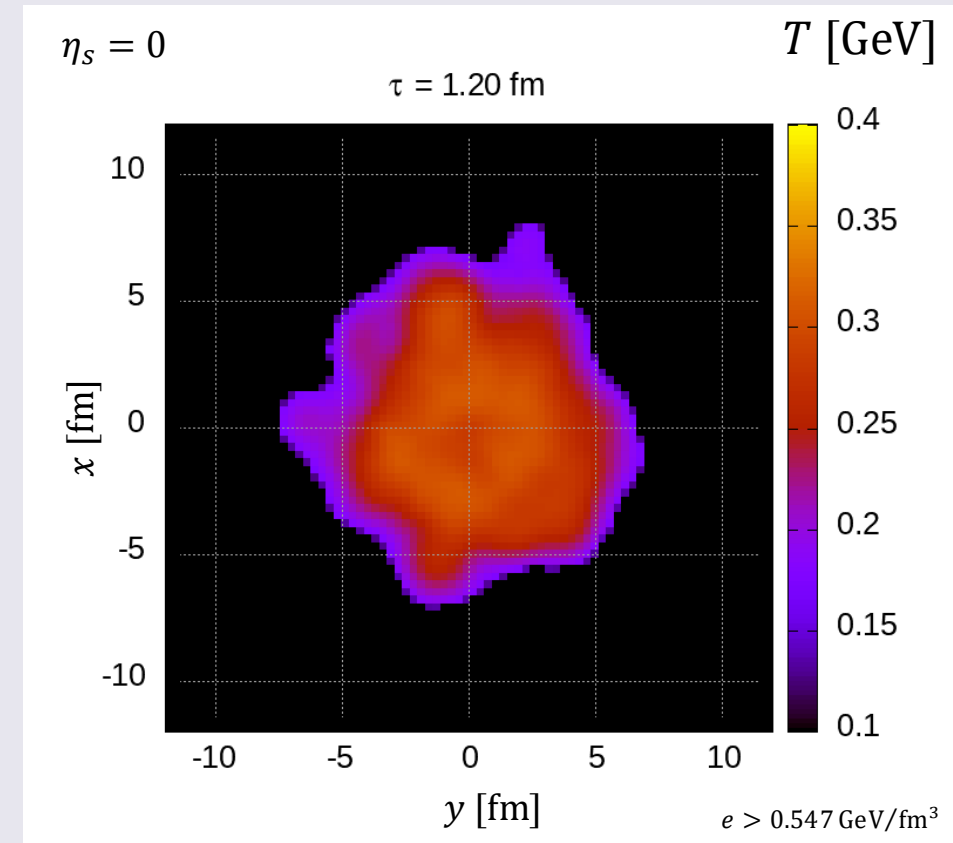
- Gradual formation of the core (QGP fluid) through the energy-momentum source term
- Alongside the fluid formation, the core cools down due to the hydrodynamic evolution

Space-time evolution of core

Temperature (longitudinal profile)



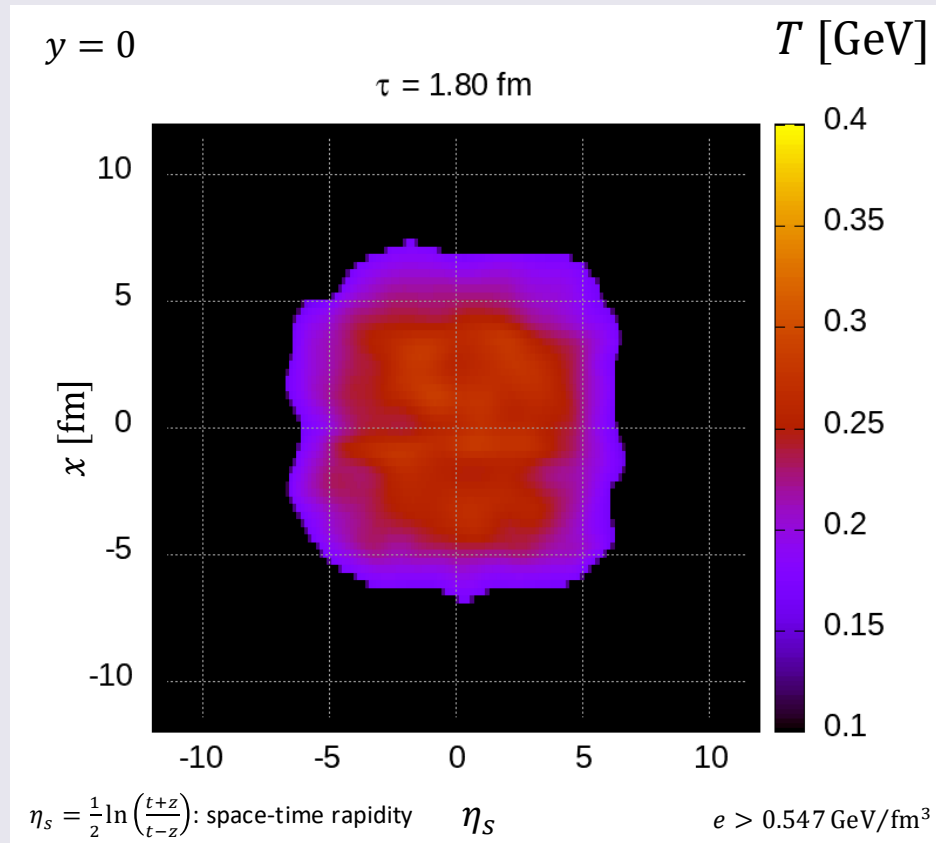
Temperature (transverse profile)



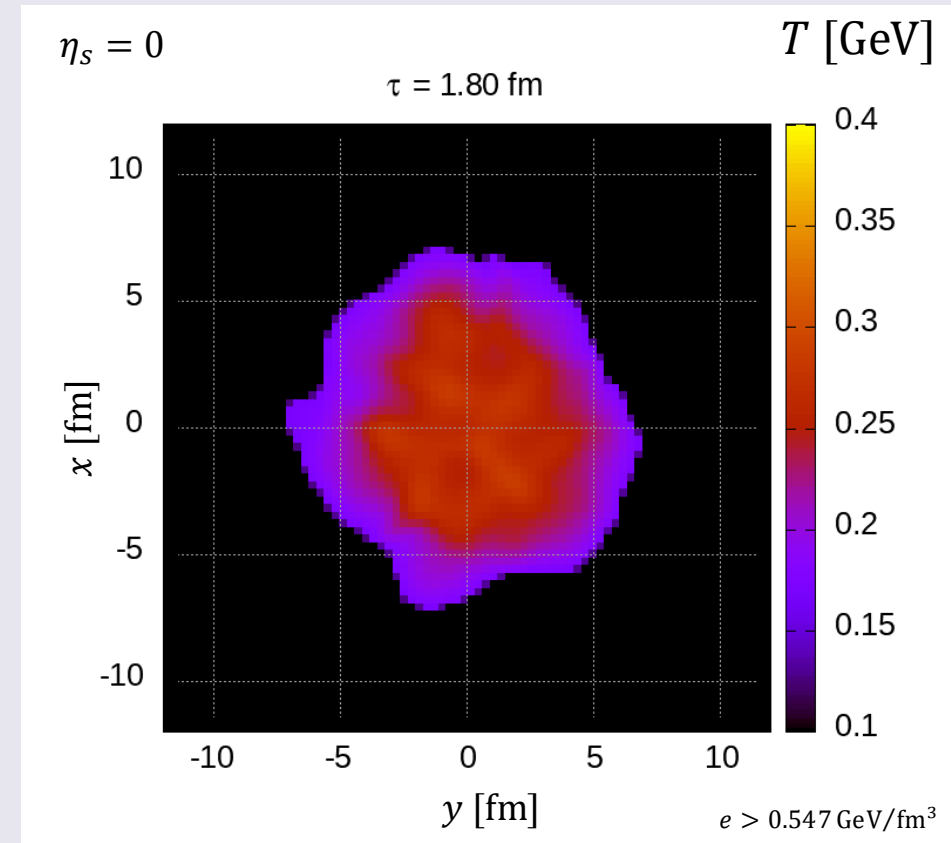
- Gradual formation of the core (QGP fluid) through the energy-momentum source term
- Alongside the fluid formation, the core cools down due to the hydrodynamic evolution

Space-time evolution of core

Temperature (longitudinal profile)



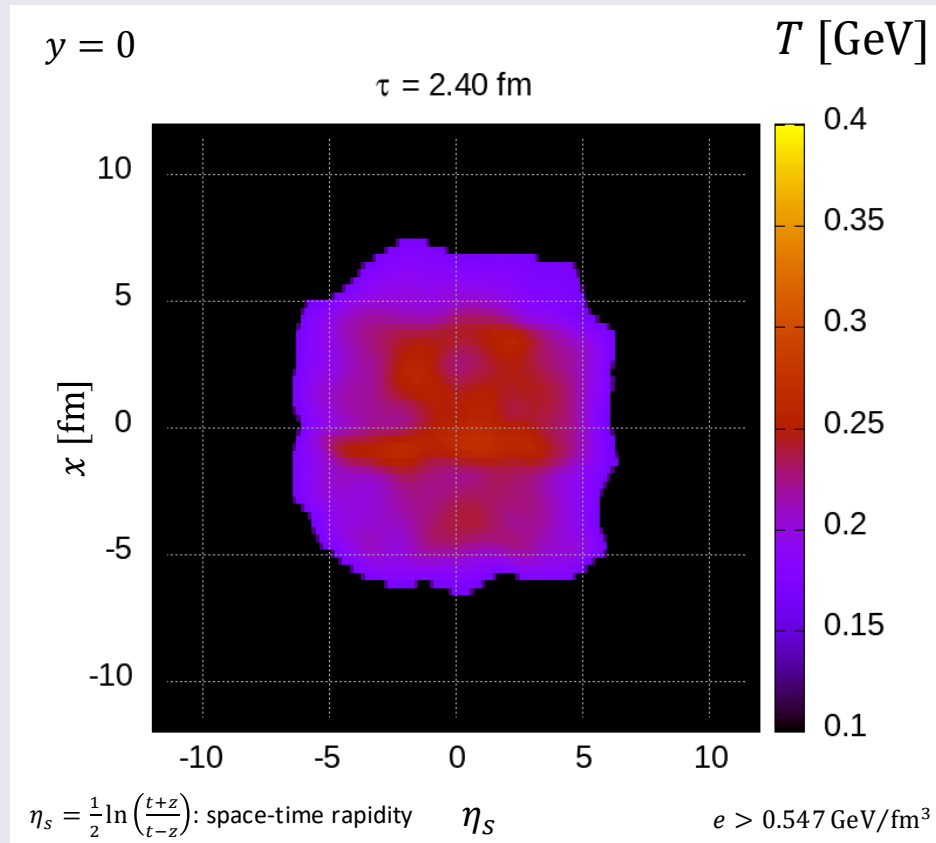
Temperature (transverse profile)



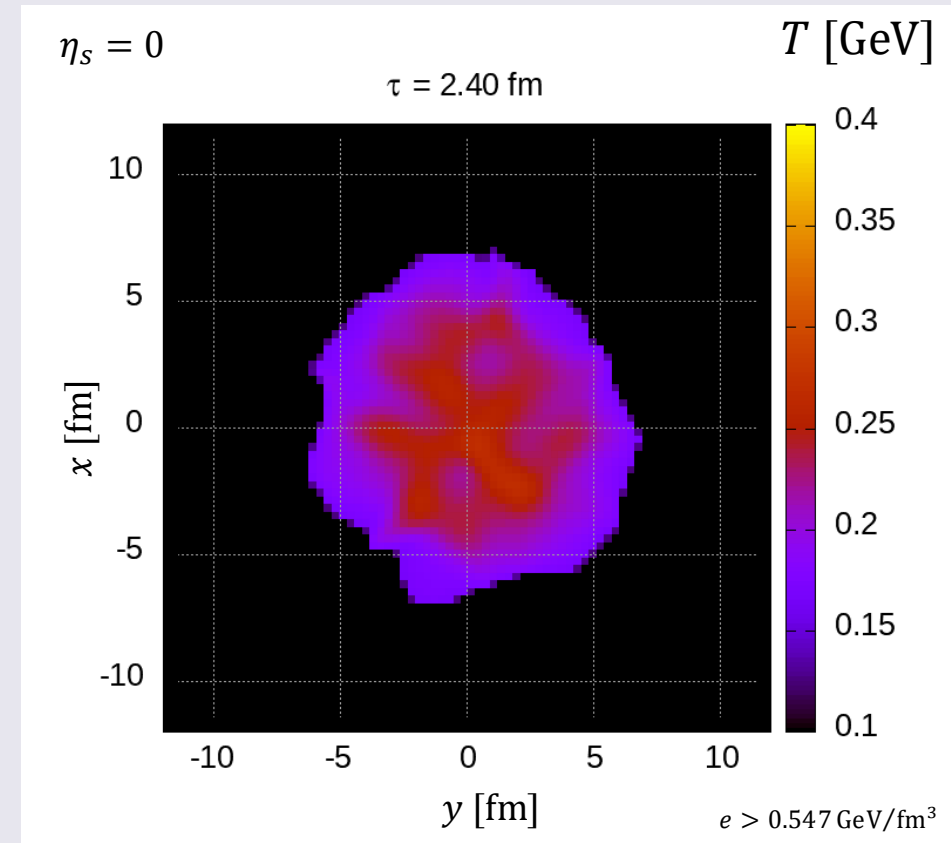
- Gradual formation of the core (QGP fluid) through the energy-momentum source term
- Alongside the fluid formation, the core cools down due to the hydrodynamic evolution

Space-time evolution of core

Temperature (longitudinal profile)



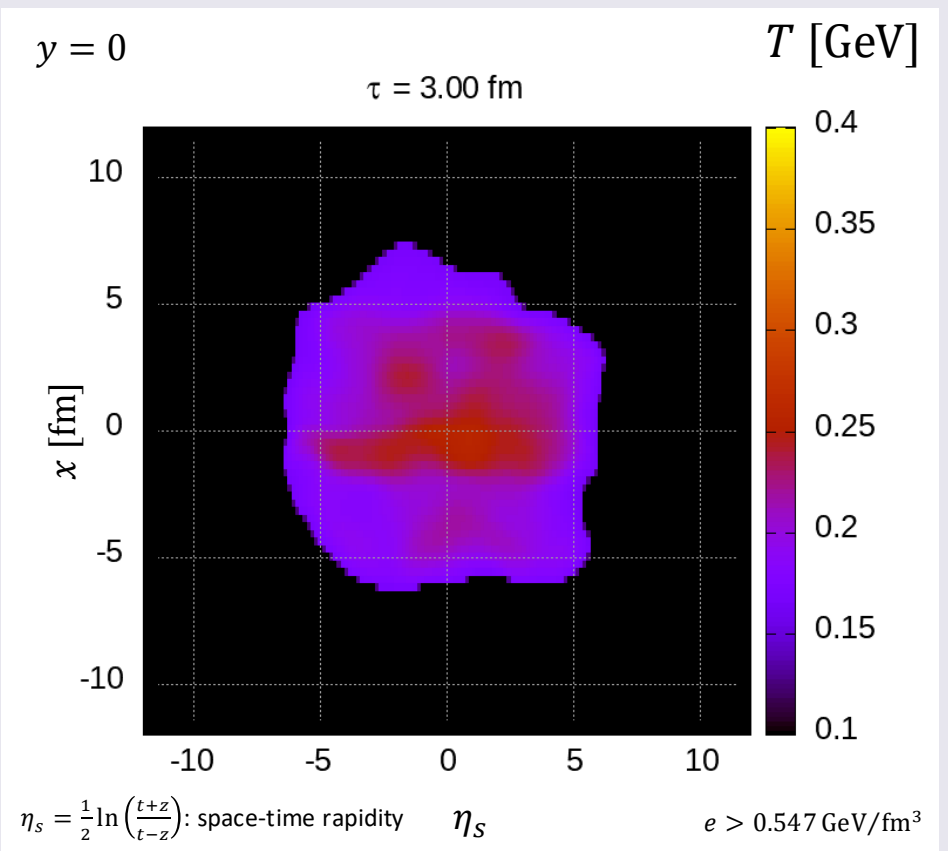
Temperature (transverse profile)



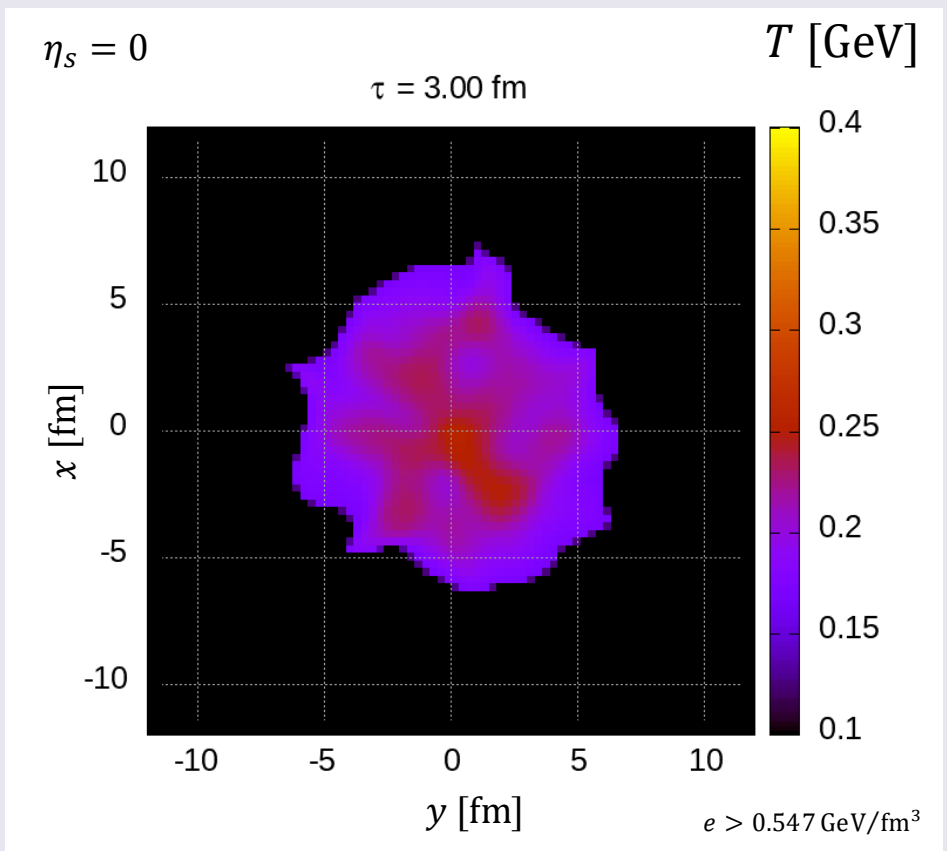
- Gradual formation of the core (QGP fluid) through the energy-momentum source term
- Alongside the fluid formation, the core cools down due to the hydrodynamic evolution

Space-time evolution of core

Temperature (longitudinal profile)



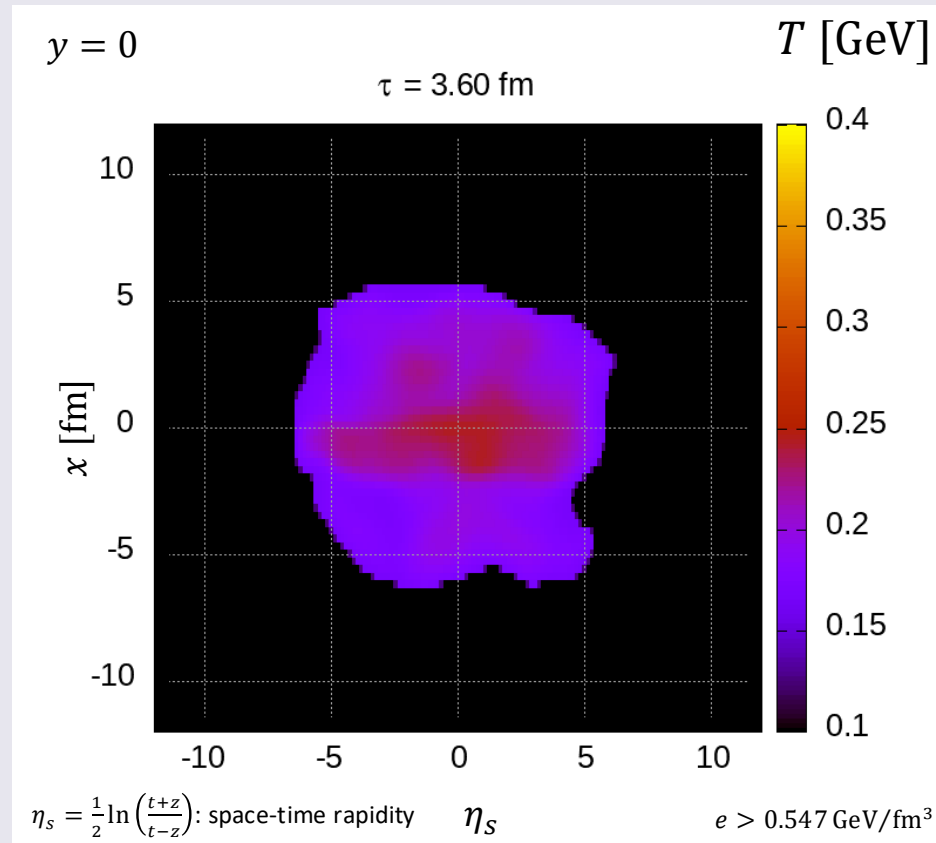
Temperature (transverse profile)



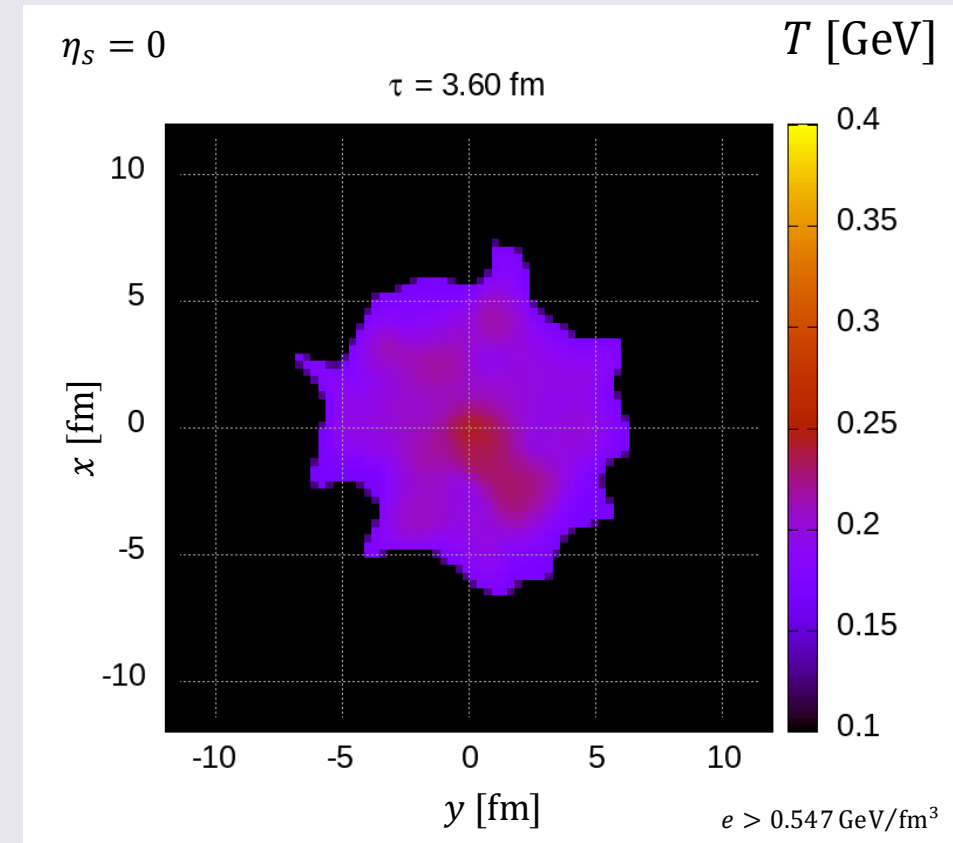
- Gradual formation of the core (QGP fluid) through the energy-momentum source term
- Alongside the fluid formation, the core cools down due to the hydrodynamic evolution

Space-time evolution of core

Temperature (longitudinal profile)



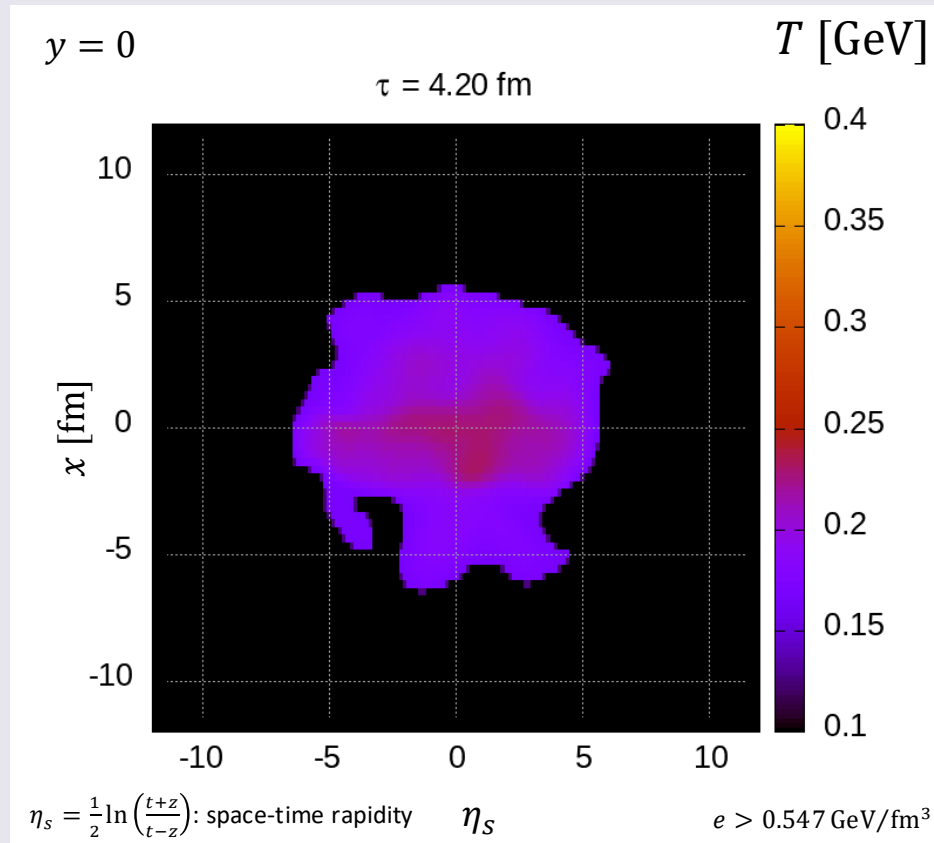
Temperature (transverse profile)



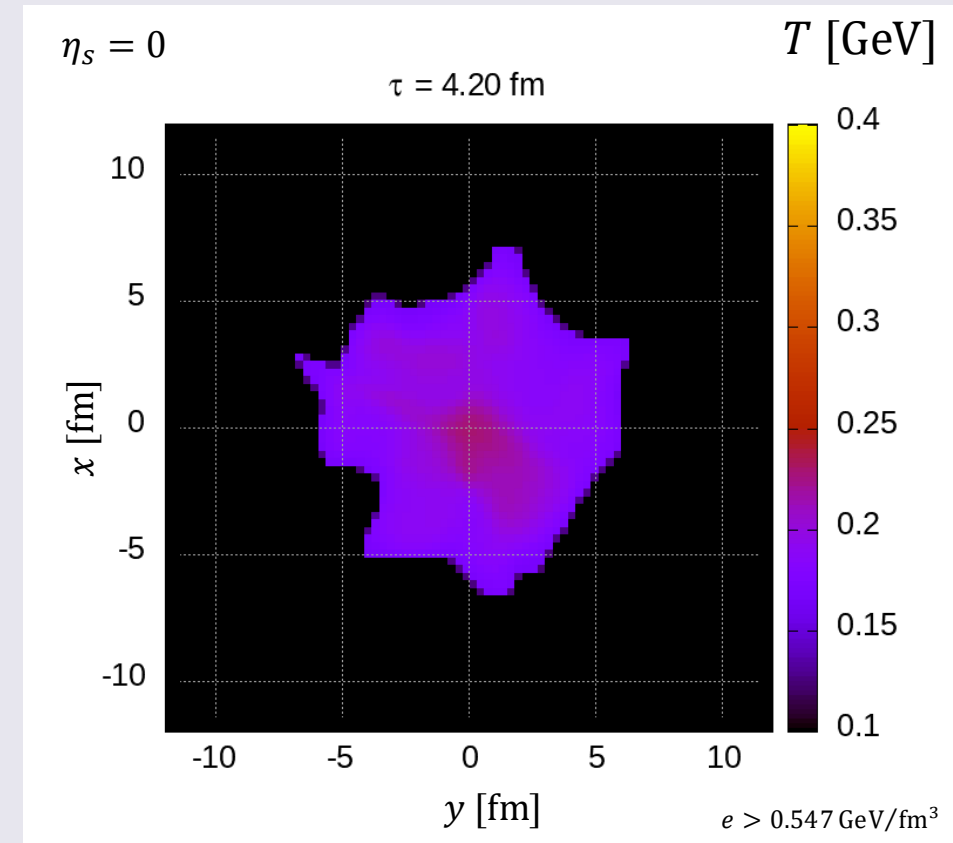
- Gradual formation of the core (QGP fluid) through the energy-momentum source term
- Alongside the fluid formation, the core cools down due to the hydrodynamic evolution

Space-time evolution of core

Temperature (longitudinal profile)



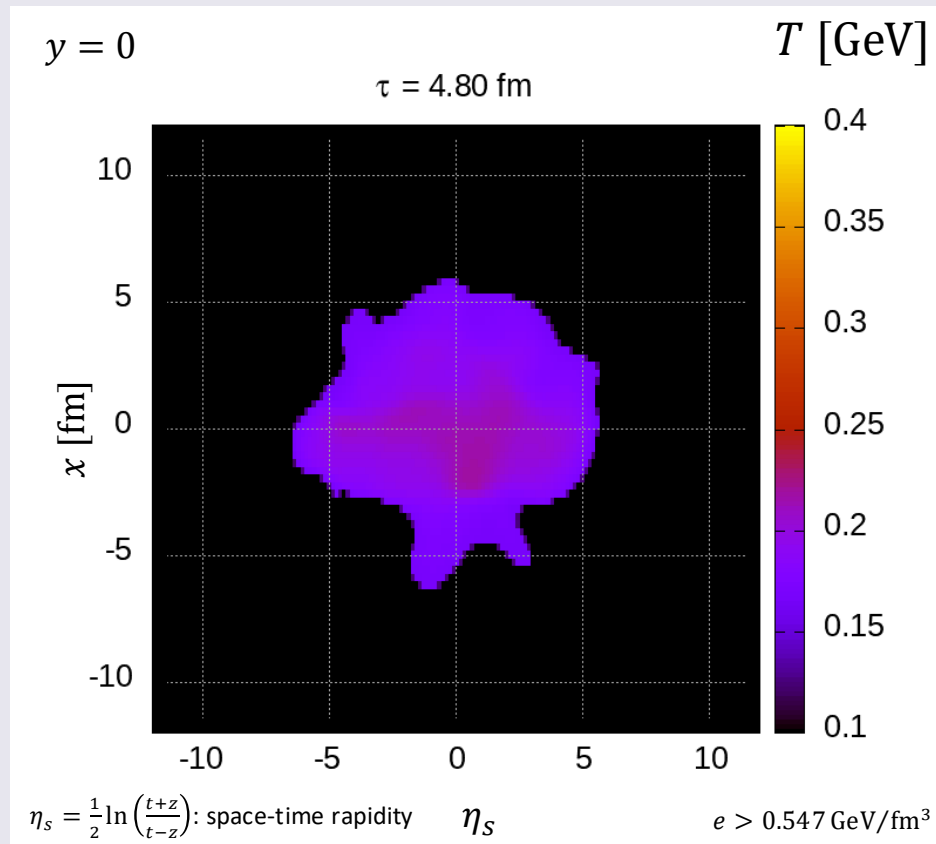
Temperature (transverse profile)



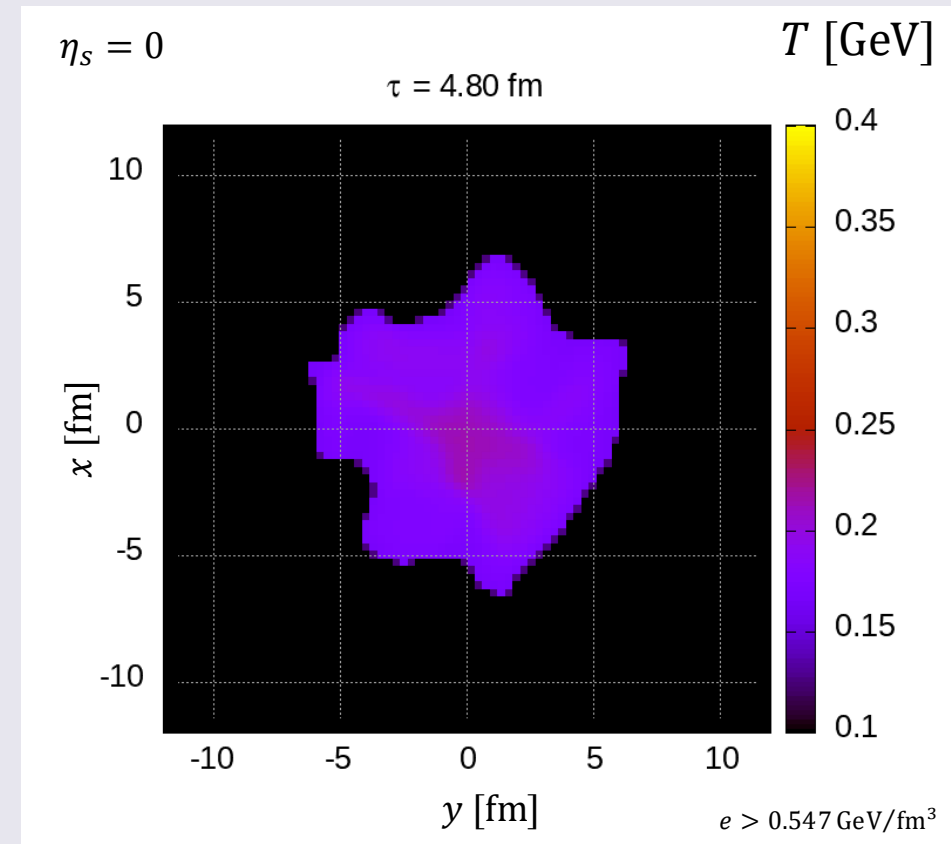
- Gradual formation of the core (QGP fluid) through the energy-momentum source term
- Alongside the fluid formation, the core cools down due to the hydrodynamic evolution

Space-time evolution of core

Temperature (longitudinal profile)



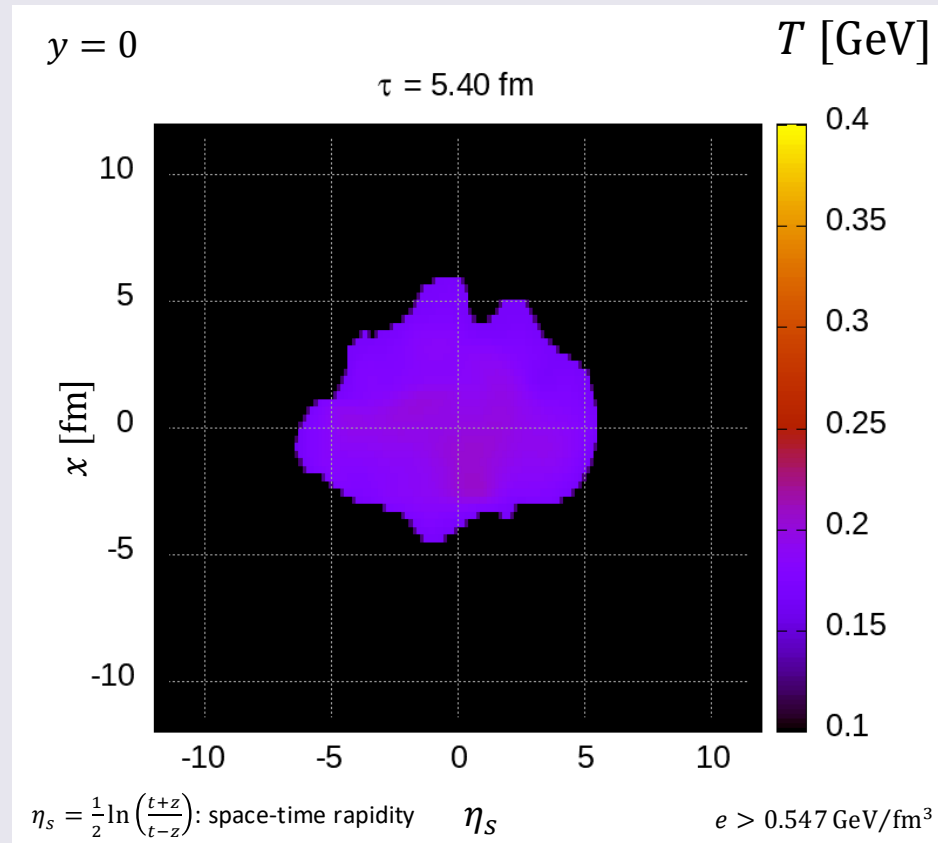
Temperature (transverse profile)



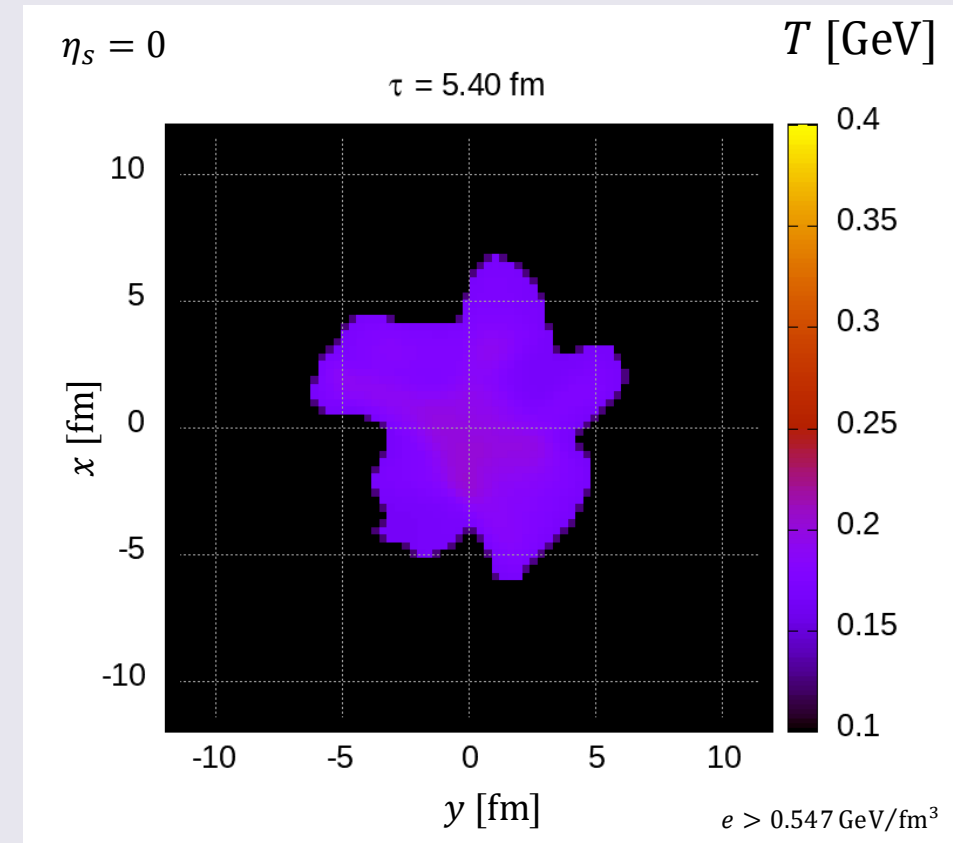
- Gradual formation of the core (QGP fluid) through the energy-momentum source term
- Alongside the fluid formation, the core cools down due to the hydrodynamic evolution

Space-time evolution of core

Temperature (longitudinal profile)



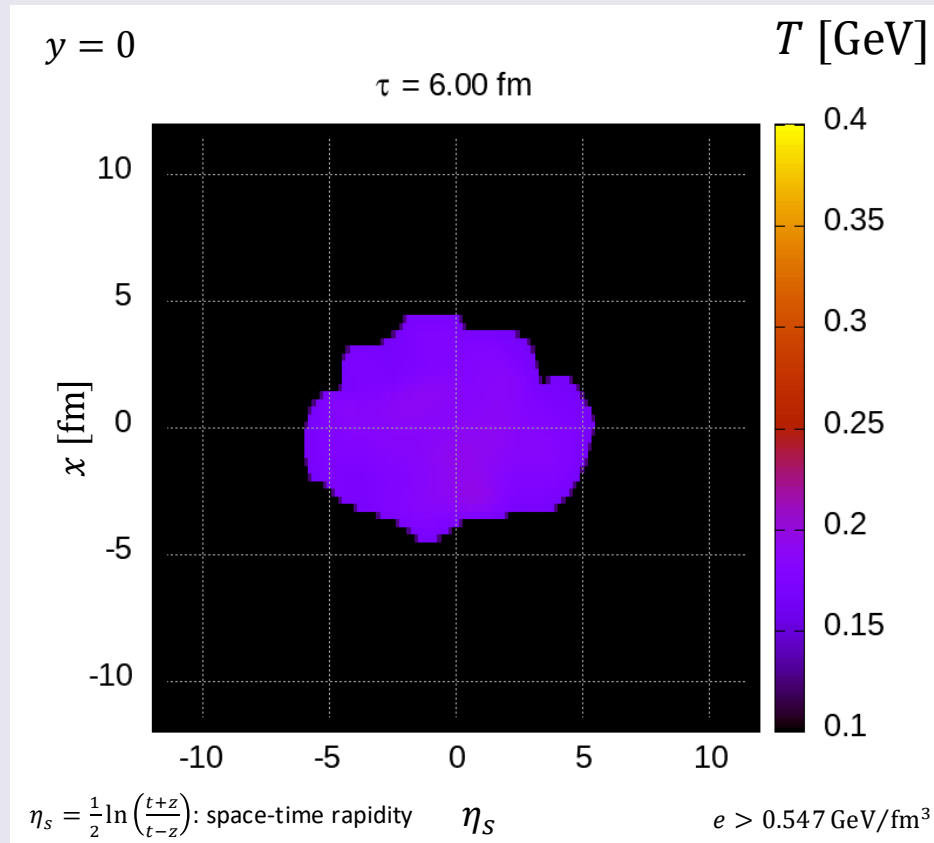
Temperature (transverse profile)



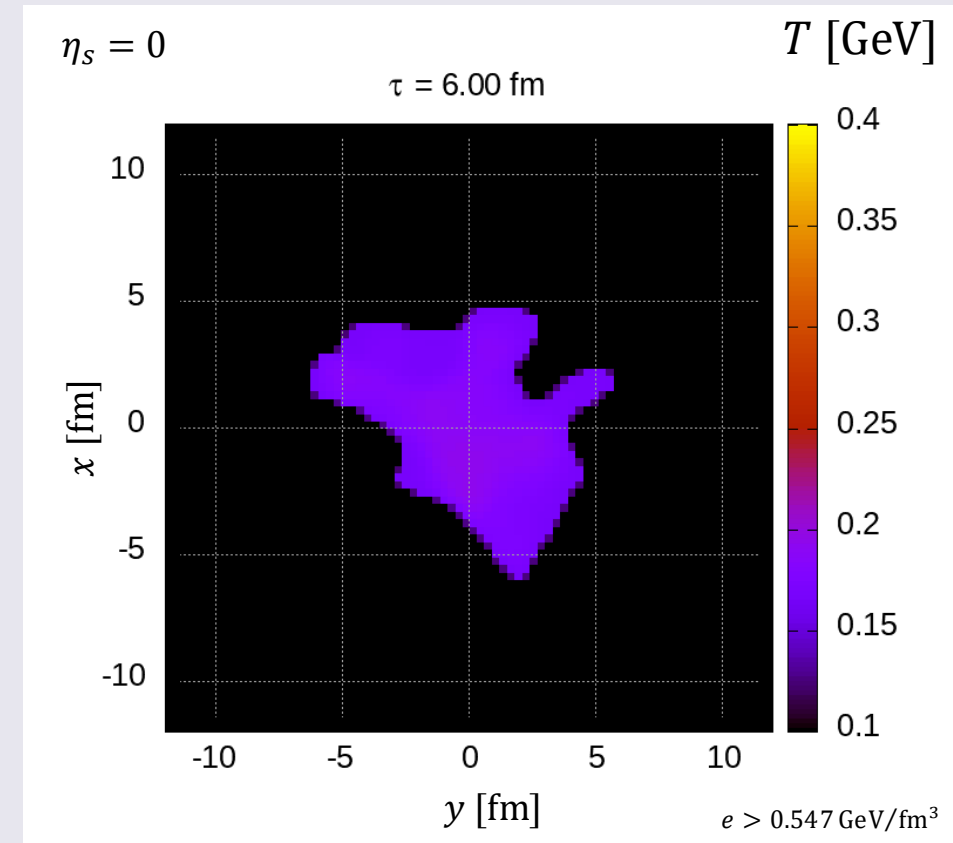
- Gradual formation of the core (QGP fluid) through the energy-momentum source term
- Alongside the fluid formation, the core cools down due to the hydrodynamic evolution

Space-time evolution of core

Temperature (longitudinal profile)



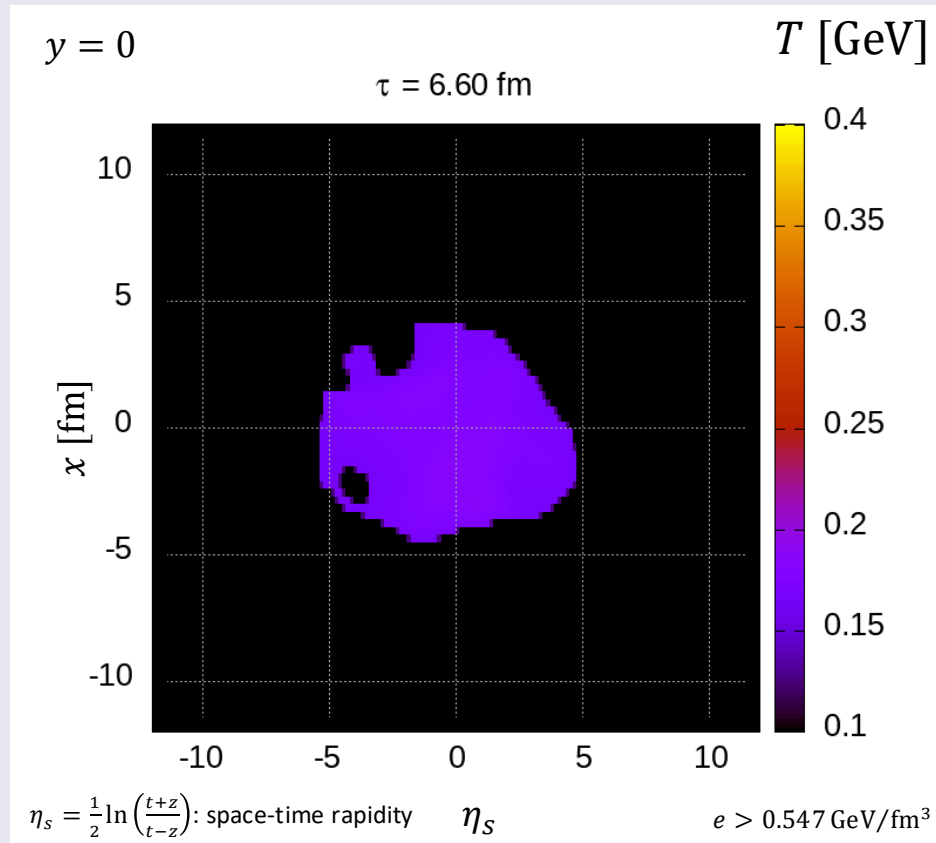
Temperature (transverse profile)



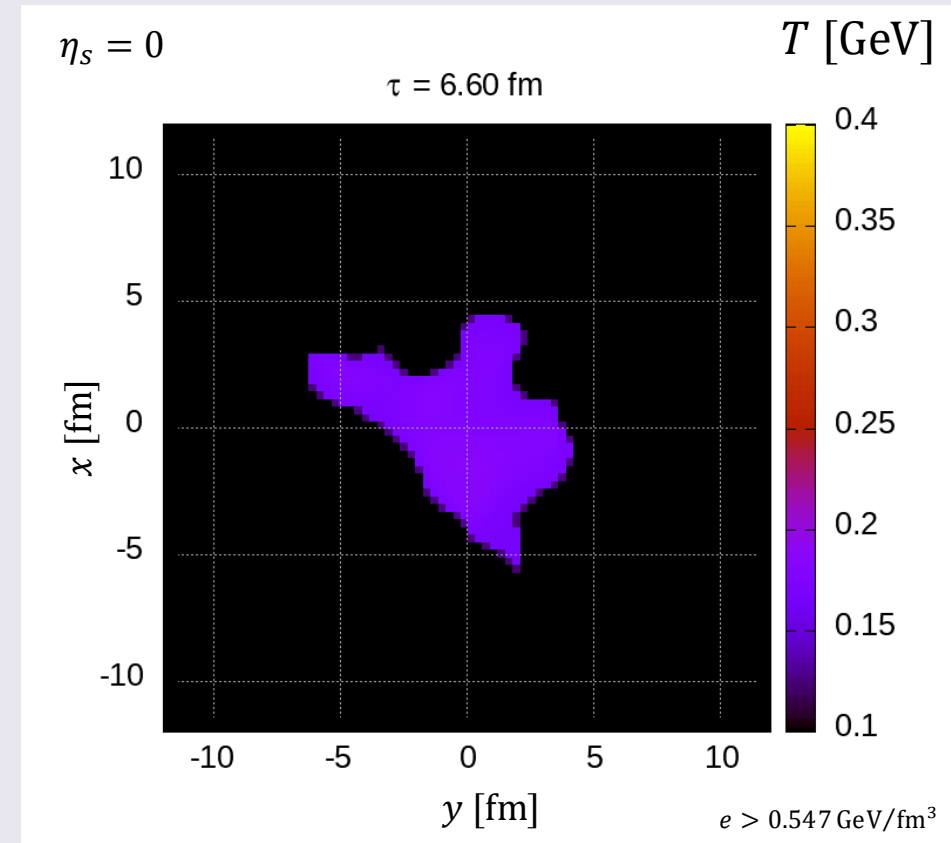
- Gradual formation of the core (QGP fluid) through the energy-momentum source term
- Alongside the fluid formation, the core cools down due to the hydrodynamic evolution

Space-time evolution of core

Temperature (longitudinal profile)



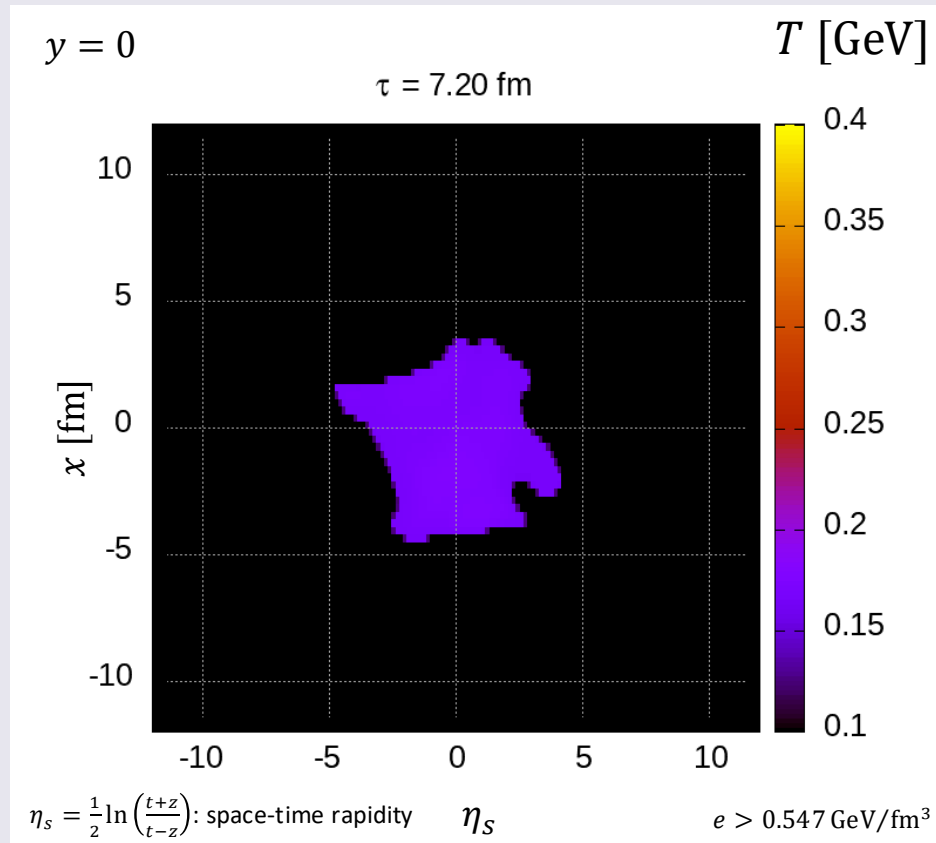
Temperature (transverse profile)



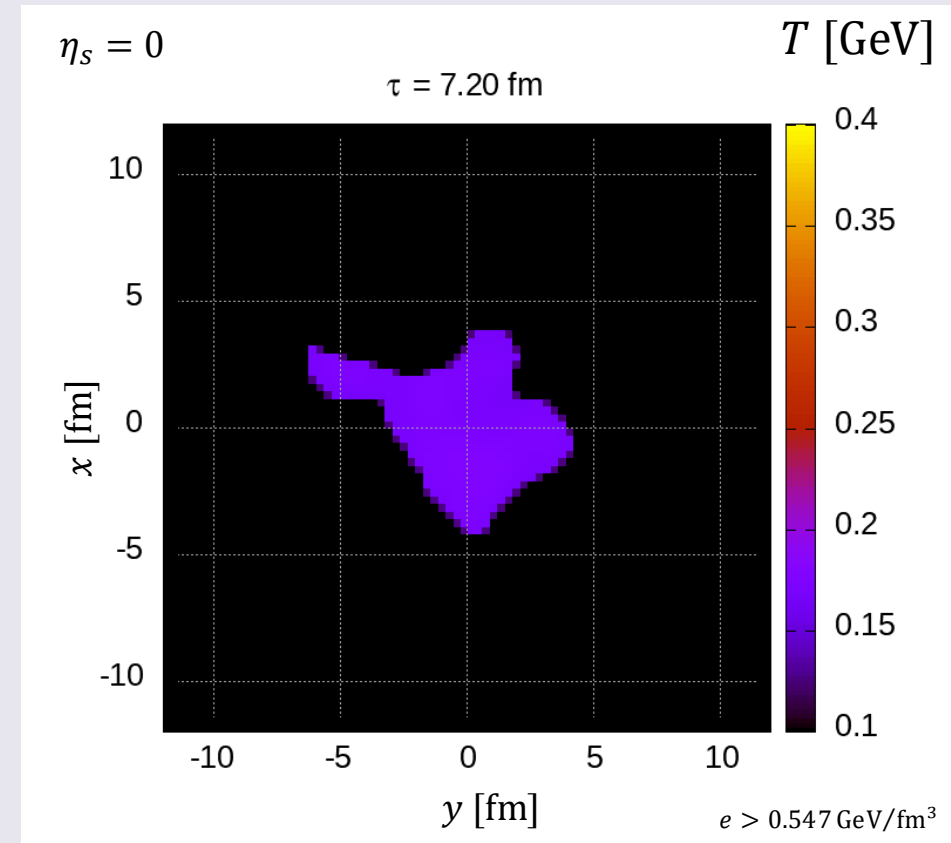
- Gradual formation of the core (QGP fluid) through the energy-momentum source term
- Alongside the fluid formation, the core cools down due to the hydrodynamic evolution

Space-time evolution of core

Temperature (longitudinal profile)



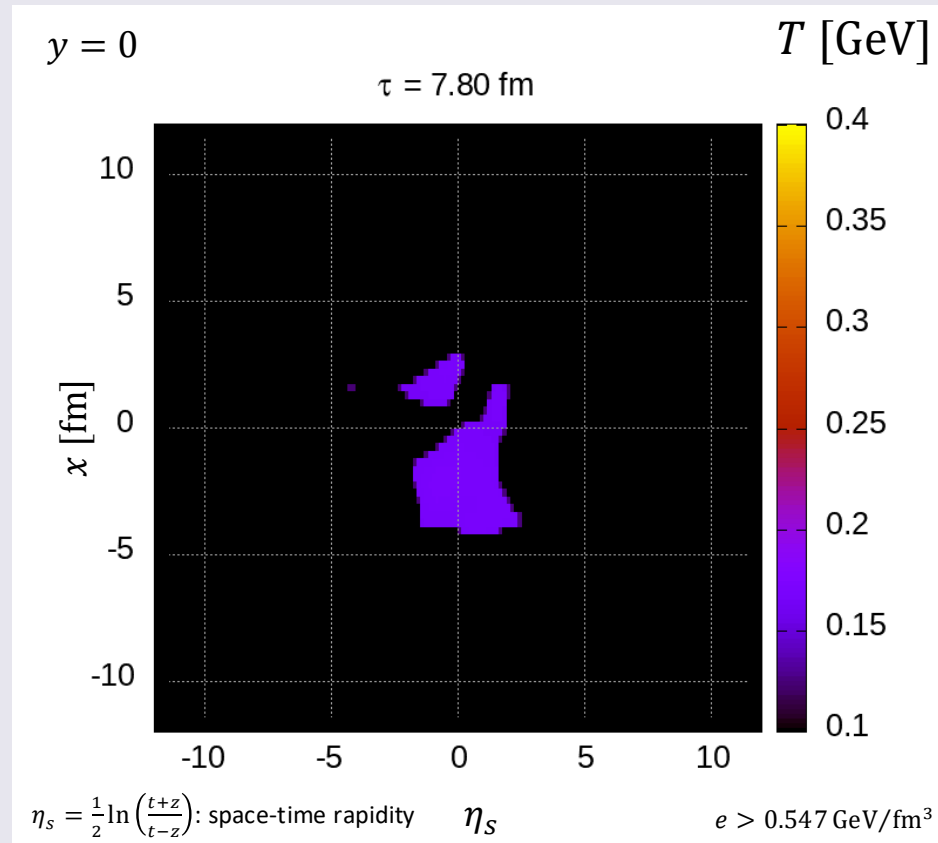
Temperature (transverse profile)



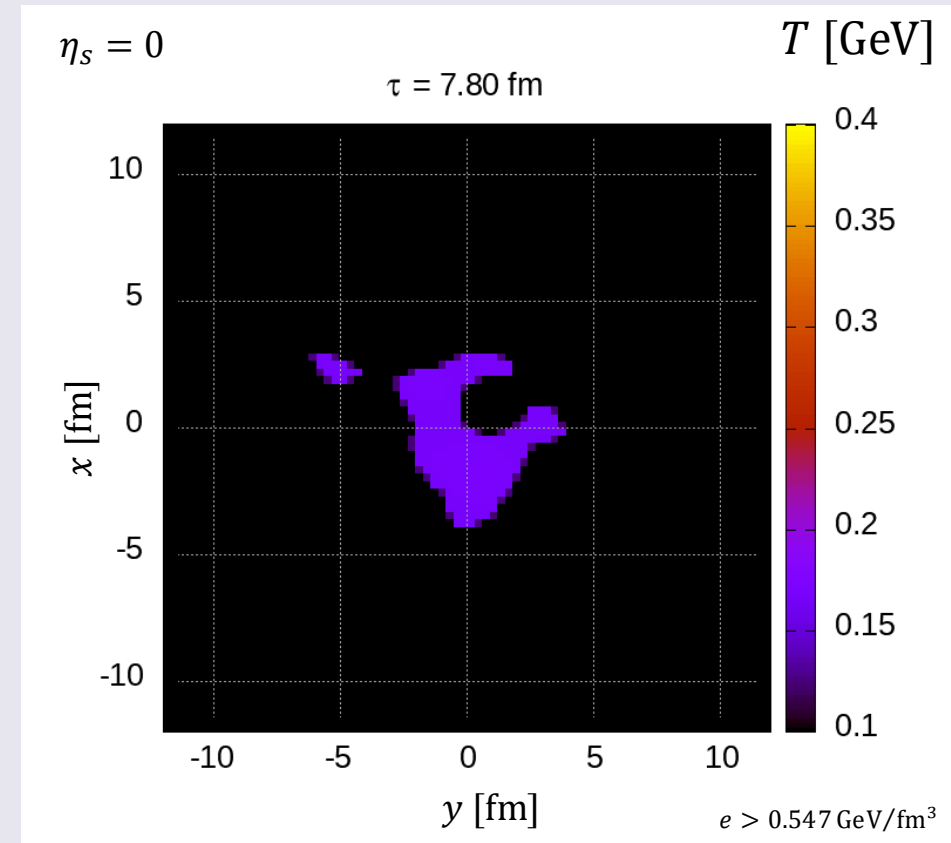
- Gradual formation of the core (QGP fluid) through the energy-momentum source term
- Alongside the fluid formation, the core cools down due to the hydrodynamic evolution

Space-time evolution of core

Temperature (longitudinal profile)



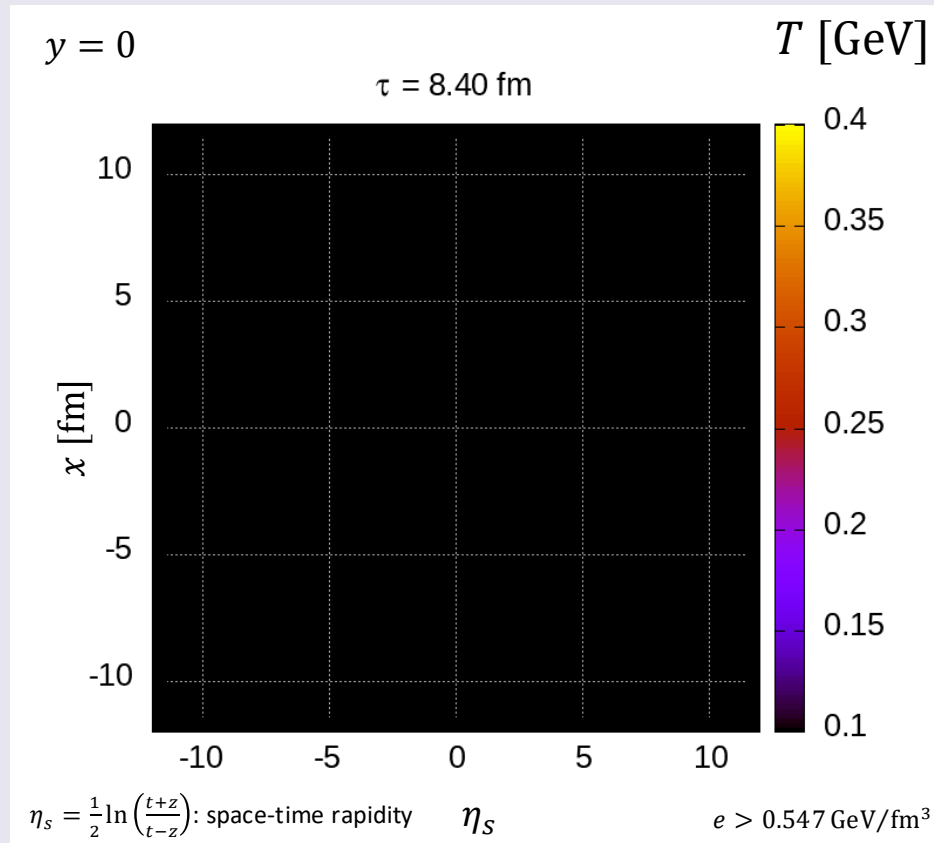
Temperature (transverse profile)



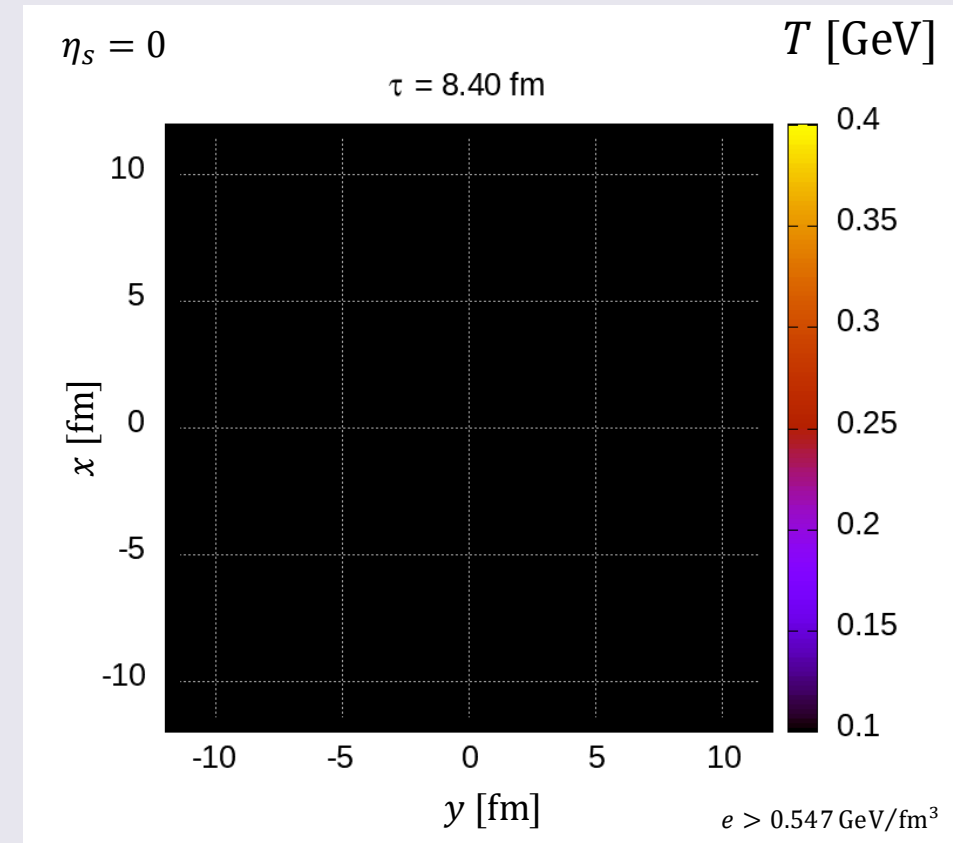
- Gradual formation of the core (QGP fluid) through the energy-momentum source term
- Alongside the fluid formation, the core cools down due to the hydrodynamic evolution

Space-time evolution of core

Temperature (longitudinal profile)



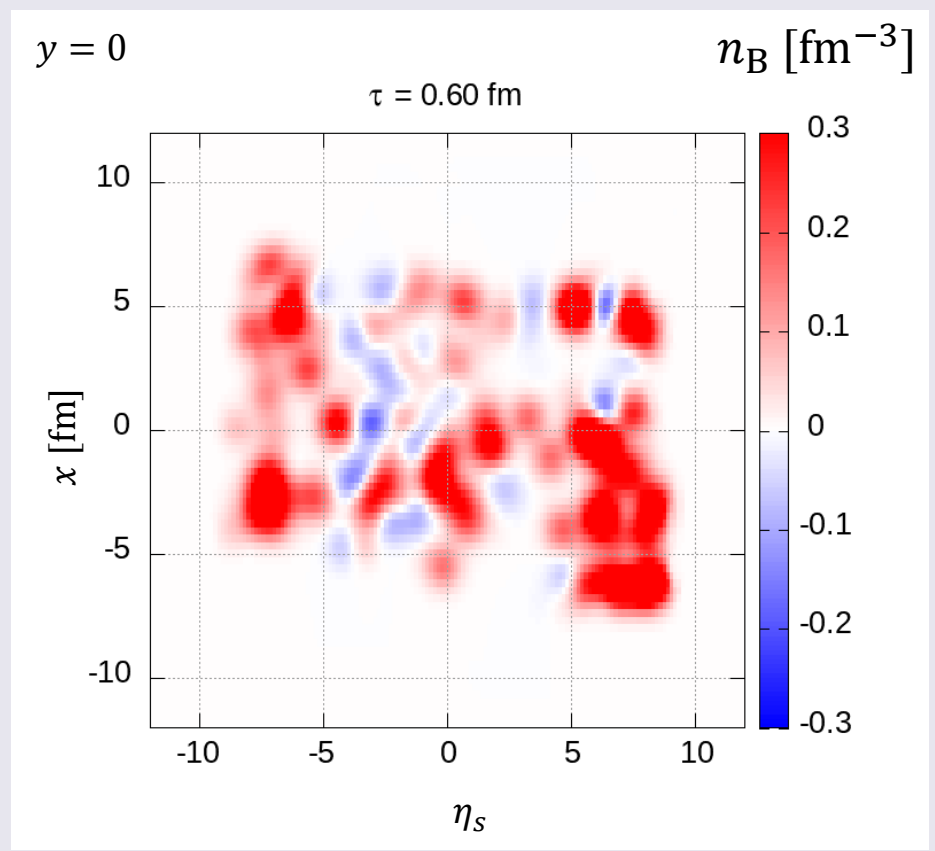
Temperature (transverse profile)



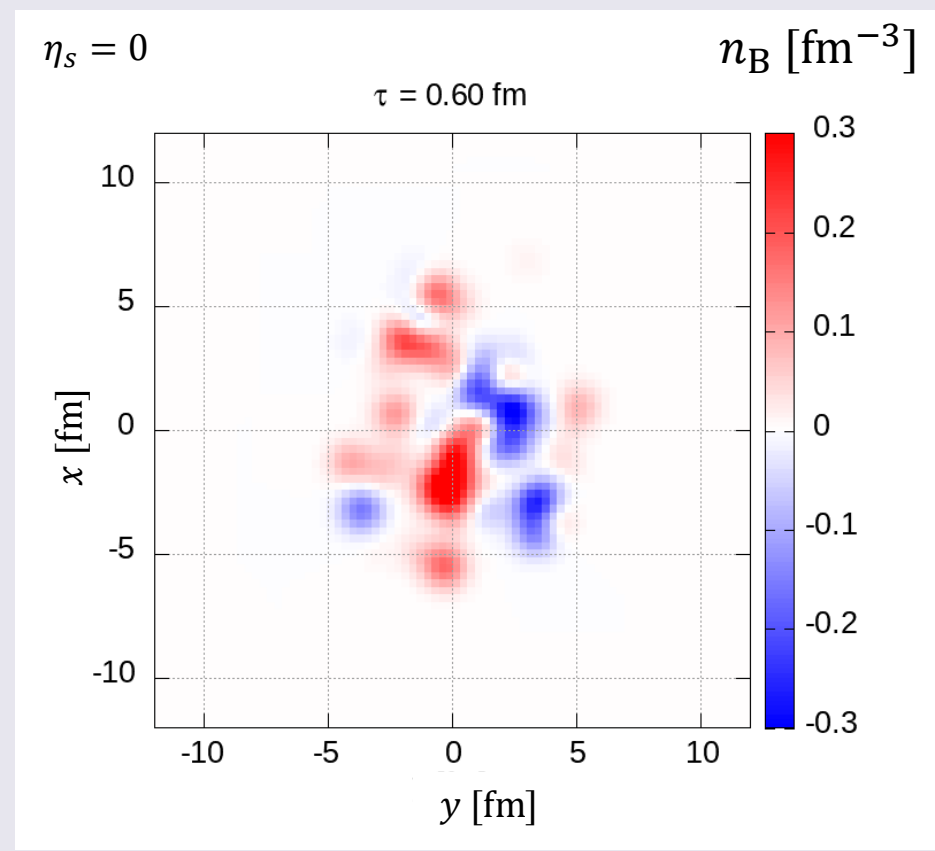
- Gradual formation of the core (QGP fluid) through the energy-momentum source term
- Alongside the fluid formation, the core cools down due to the hydrodynamic evolution

Space-time evolution of core

Baryon number density (longitudinal profile)



Baryon number density (transverse profile)



- Large baryon number density is realized in forward rapidities $5 \lesssim |\eta_s| \lesssim 10$

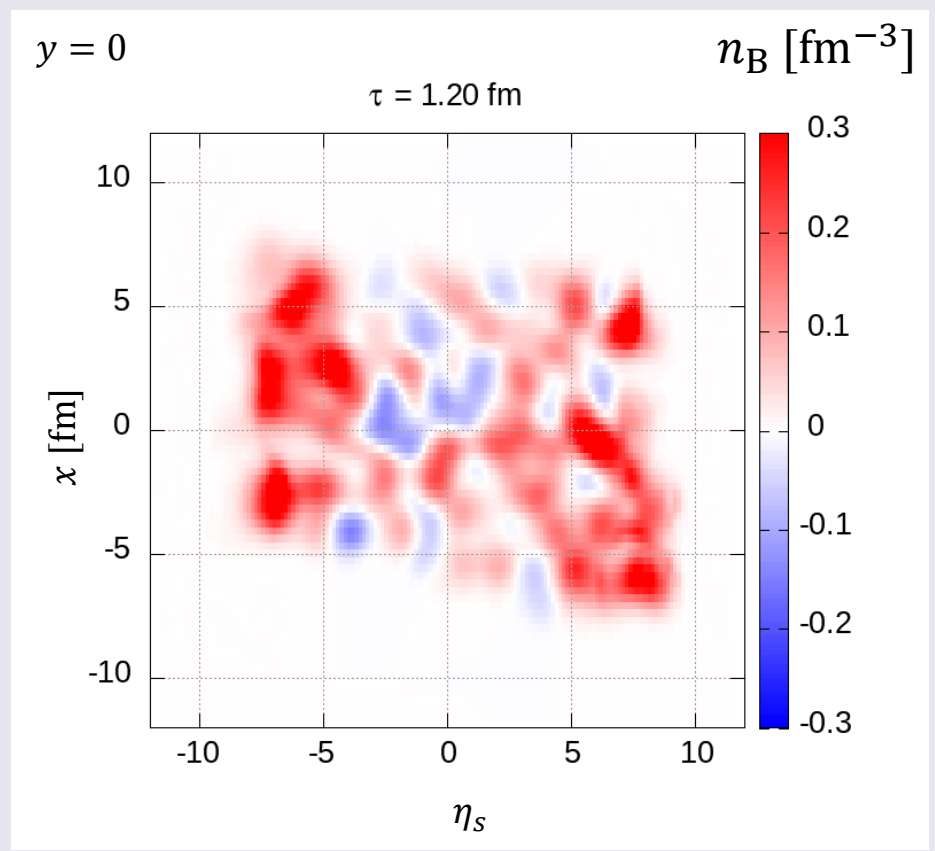
cf.) $y_{\text{beam}}(\sqrt{s_{\text{NN}}} = 2.76 \text{ TeV}) \approx 8$

- Large fluctuations of baryon number density even in midrapidity

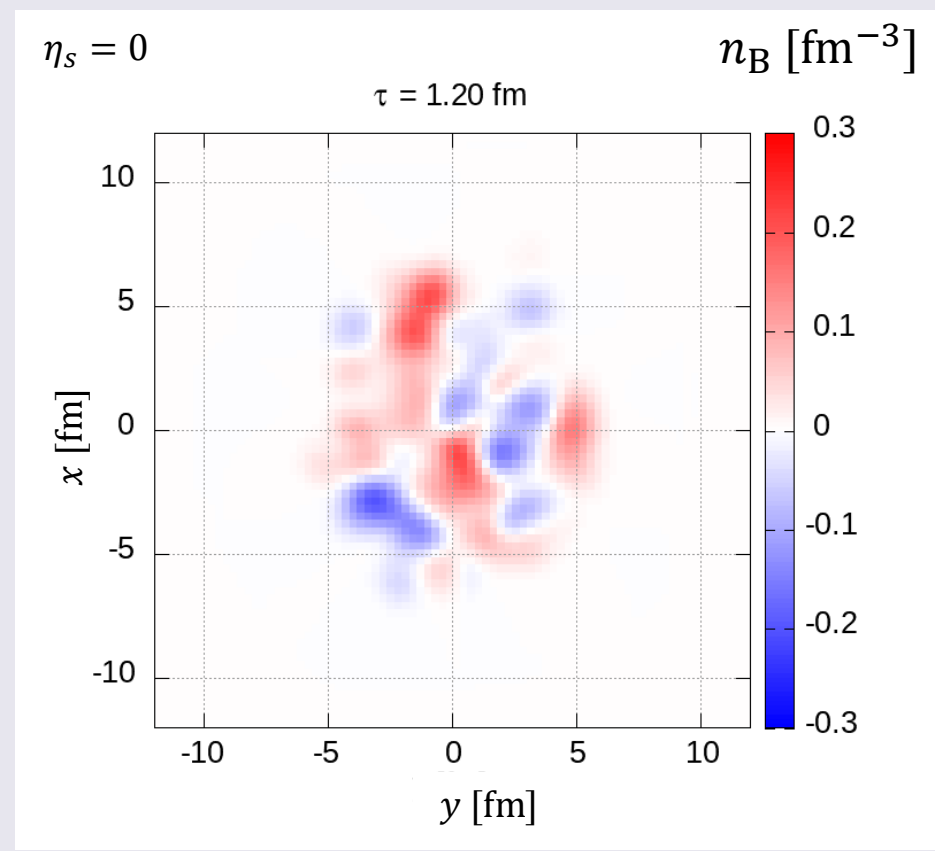
➡ Negative n_B region appears

Space-time evolution of core

Baryon number density (longitudinal profile)



Baryon number density (transverse profile)



- Large baryon number density is realized in forward rapidities $5 \lesssim |\eta_s| \lesssim 10$

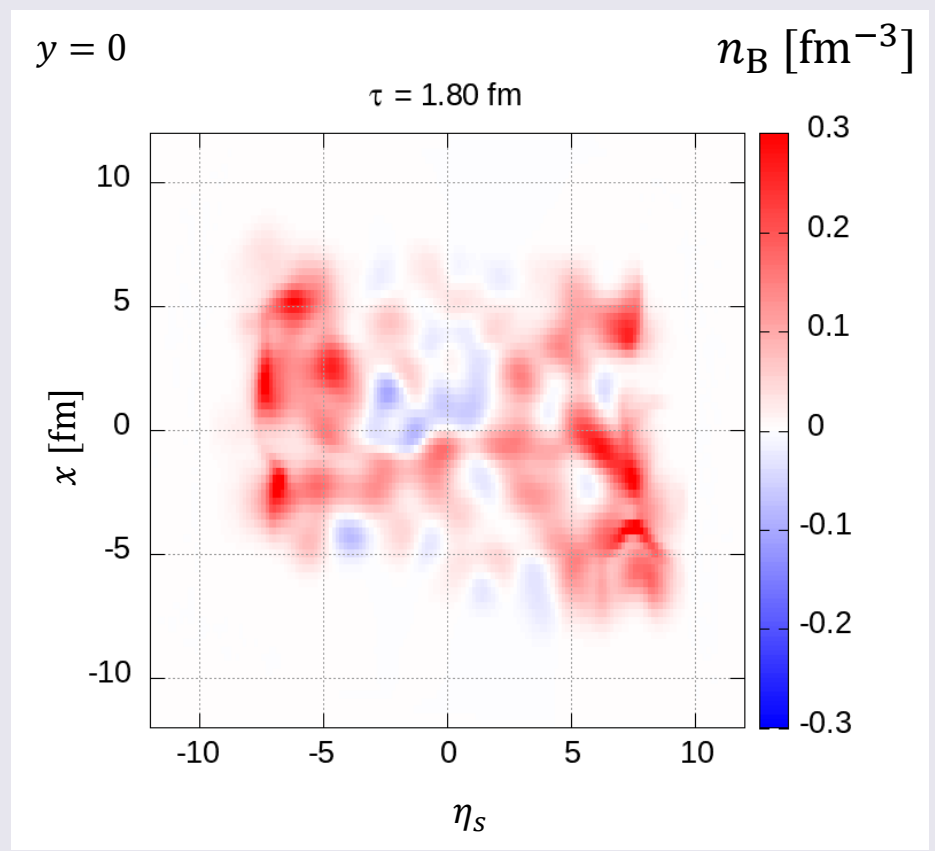
cf.) $y_{\text{beam}}(\sqrt{s_{\text{NN}}} = 2.76 \text{ TeV}) \approx 8$

- Large fluctuations of baryon number density even in midrapidity

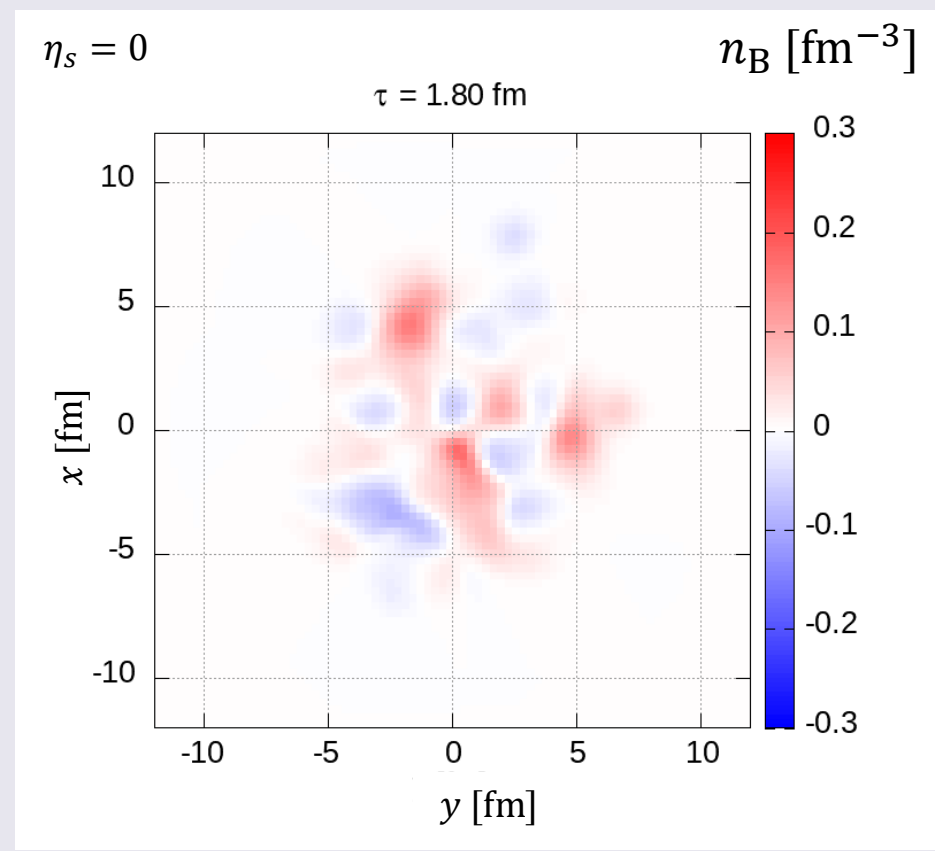
➡ Negative n_B region appears

Space-time evolution of core

Baryon number density (longitudinal profile)



Baryon number density (transverse profile)



- Large baryon number density is realized in forward rapidities $5 \lesssim |\eta_s| \lesssim 10$

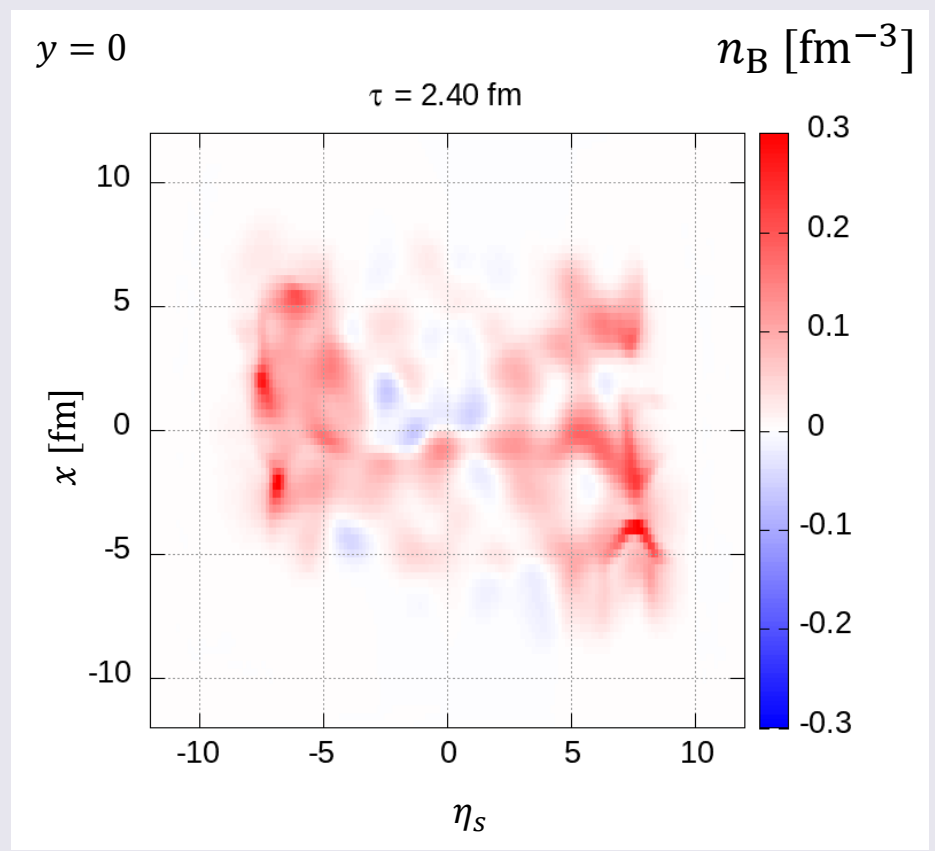
cf.) $y_{\text{beam}}(\sqrt{s_{\text{NN}}} = 2.76 \text{ TeV}) \approx 8$

- Large fluctuations of baryon number density even in midrapidity

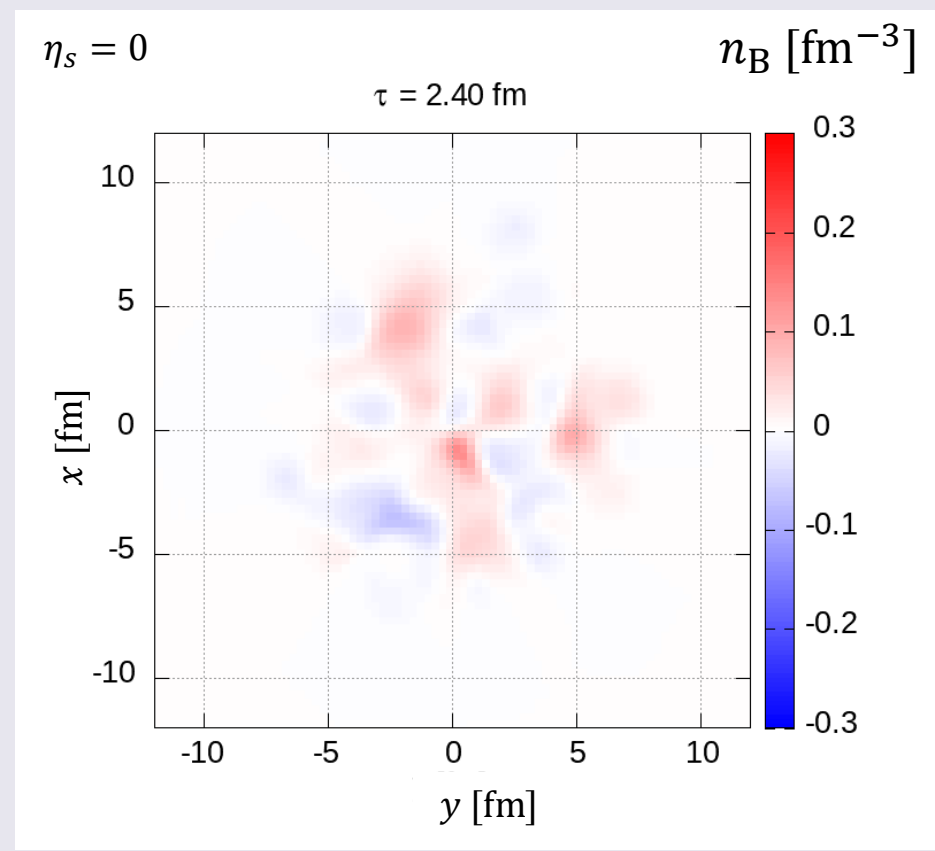
➡ Negative n_B region appears

Space-time evolution of core

Baryon number density (longitudinal profile)



Baryon number density (transverse profile)



- Large baryon number density is realized in forward rapidities $5 \lesssim |\eta_s| \lesssim 10$

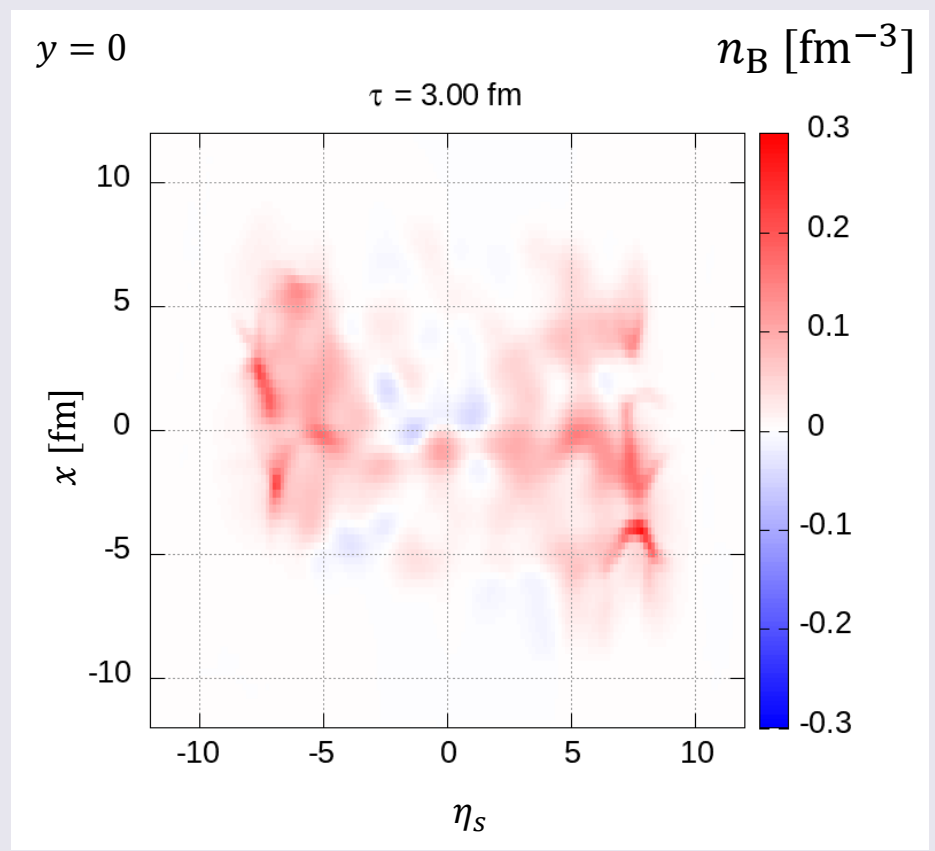
cf.) $y_{\text{beam}}(\sqrt{s_{\text{NN}}} = 2.76 \text{ TeV}) \approx 8$

- Large fluctuations of baryon number density even in midrapidity

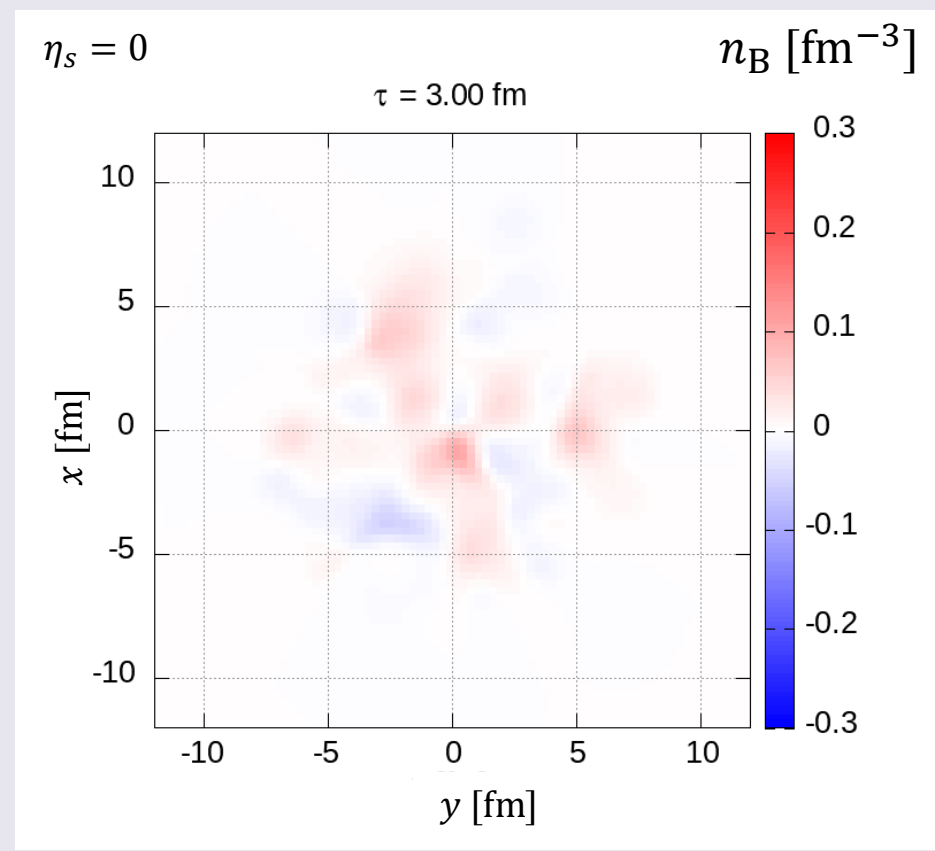
➡ Negative n_B region appears

Space-time evolution of core

Baryon number density (longitudinal profile)



Baryon number density (transverse profile)



- Large baryon number density is realized in forward rapidities $5 \lesssim |\eta_s| \lesssim 10$

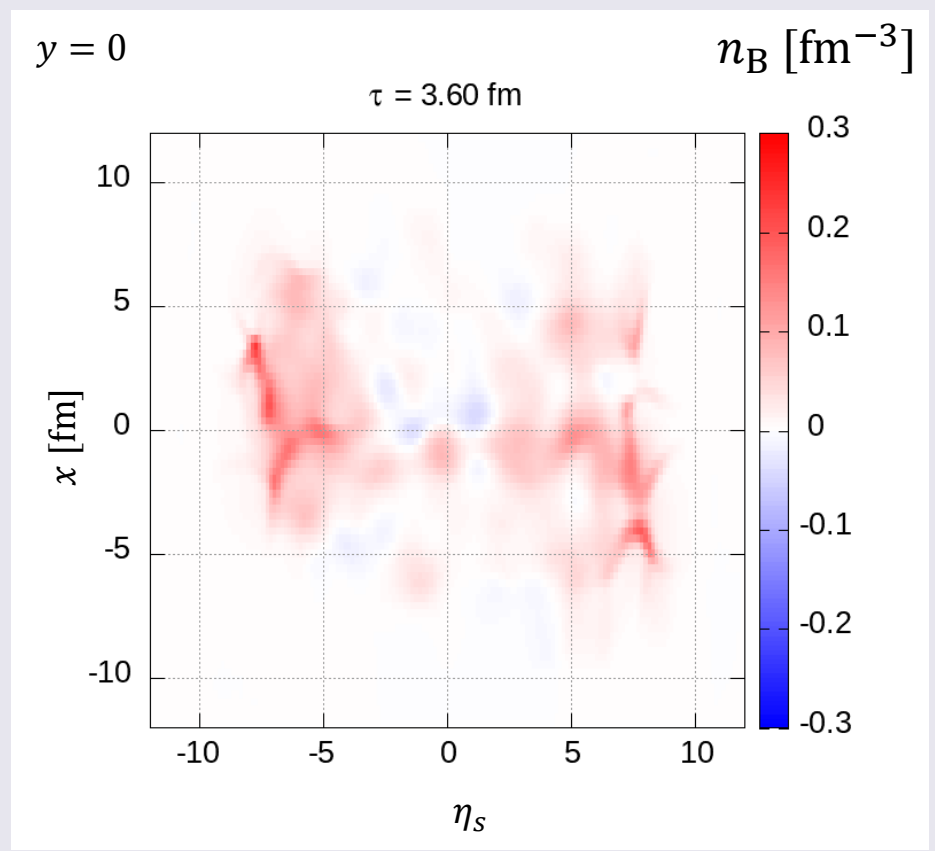
cf.) $y_{\text{beam}}(\sqrt{s_{\text{NN}}} = 2.76 \text{ TeV}) \approx 8$

- Large fluctuations of baryon number density even in midrapidity

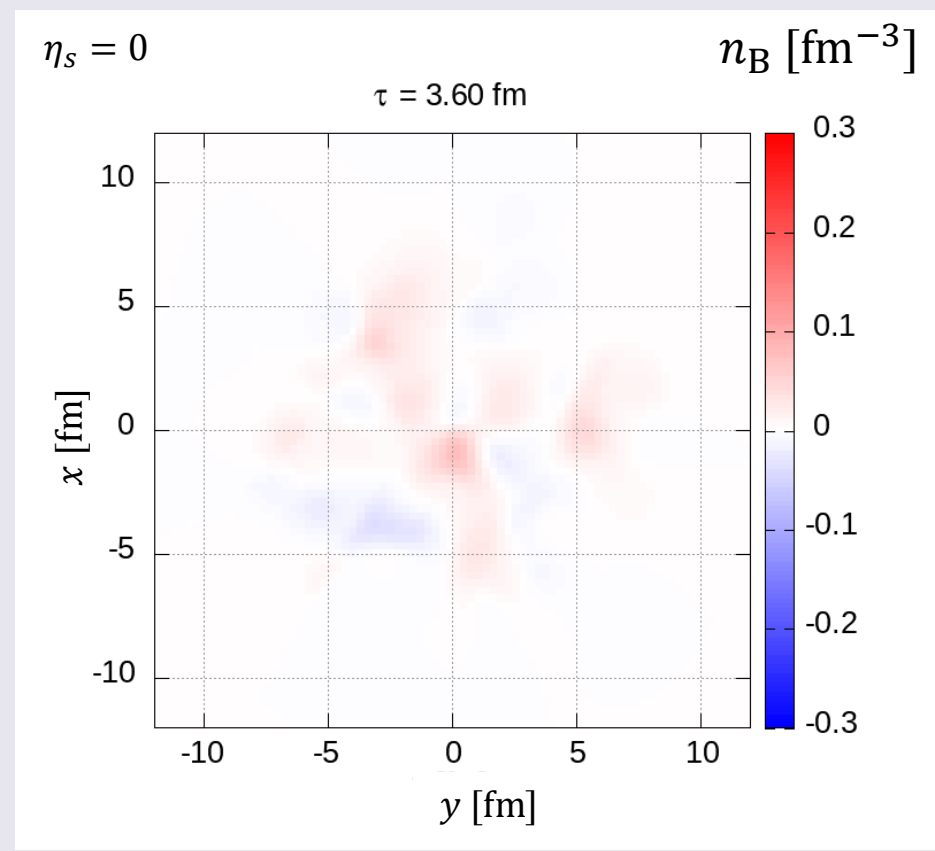
➡ Negative n_B region appears

Space-time evolution of core

Baryon number density (longitudinal profile)



Baryon number density (transverse profile)



- Large baryon number density is realized in forward rapidities $5 \lesssim |\eta_s| \lesssim 10$

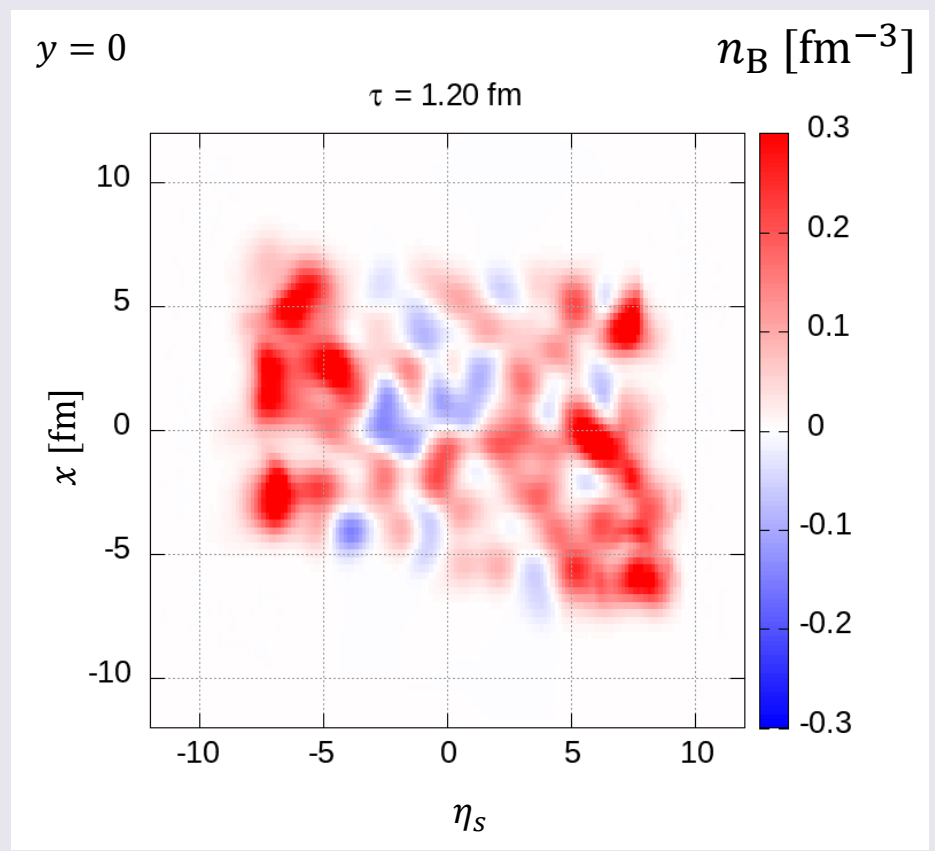
cf.) $y_{\text{beam}}(\sqrt{s_{\text{NN}}} = 2.76 \text{ TeV}) \approx 8$

- Large fluctuations of baryon number density even in midrapidity

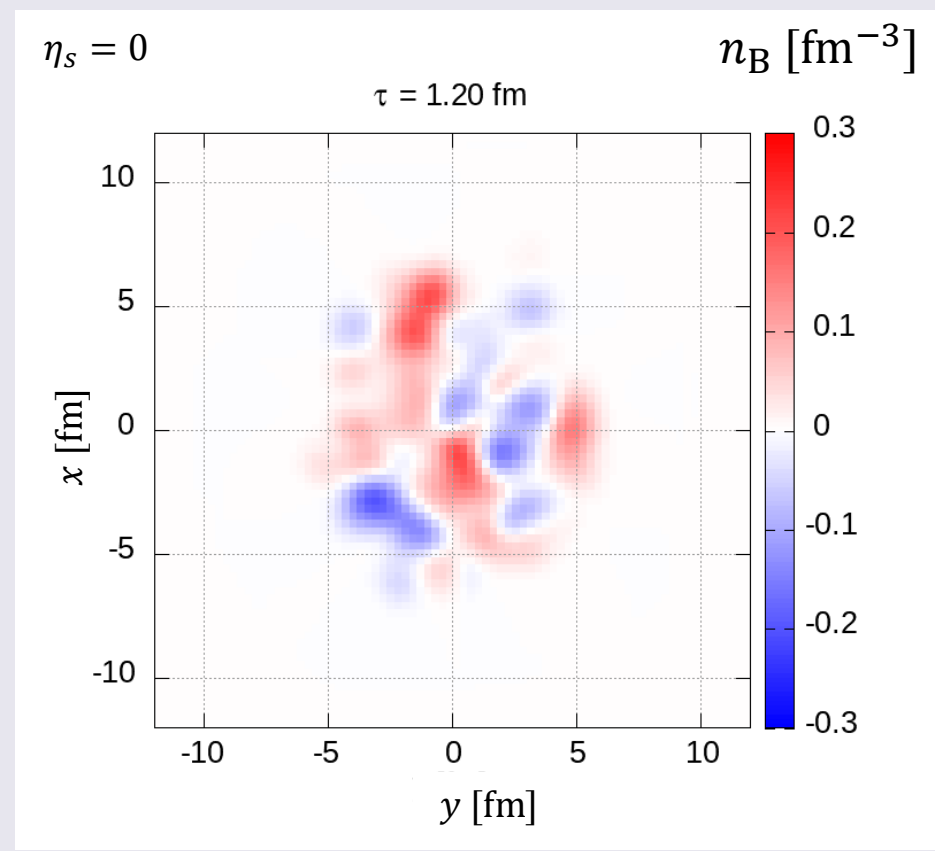
➡ Negative n_B region appears

Space-time evolution of core

Baryon number density (longitudinal profile)



Baryon number density (transverse profile)



- Large baryon number density is realized in forward rapidities $5 \lesssim |\eta_s| \lesssim 10$

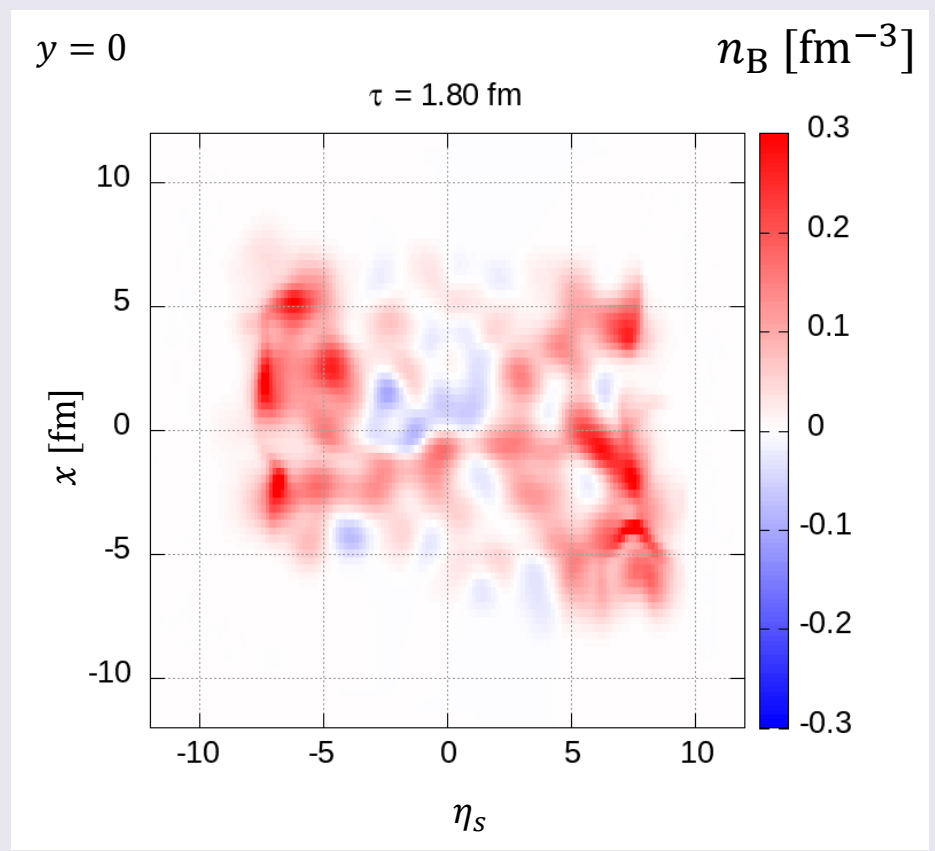
cf.) $y_{\text{beam}}(\sqrt{s_{\text{NN}}} = 2.76 \text{ TeV}) \approx 8$

- Large fluctuations of baryon number density even in midrapidity

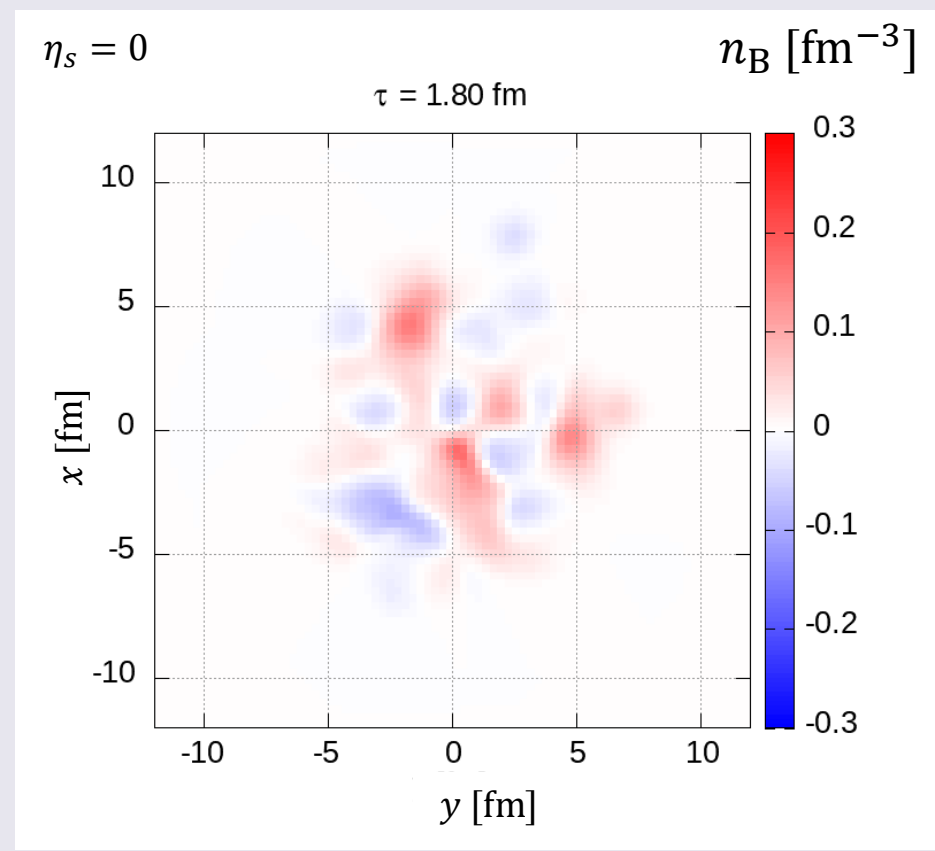
➡ Negative n_B region appears

Space-time evolution of core

Baryon number density (longitudinal profile)



Baryon number density (transverse profile)



- Large baryon number density is realized in forward rapidities $5 \lesssim |\eta_s| \lesssim 10$

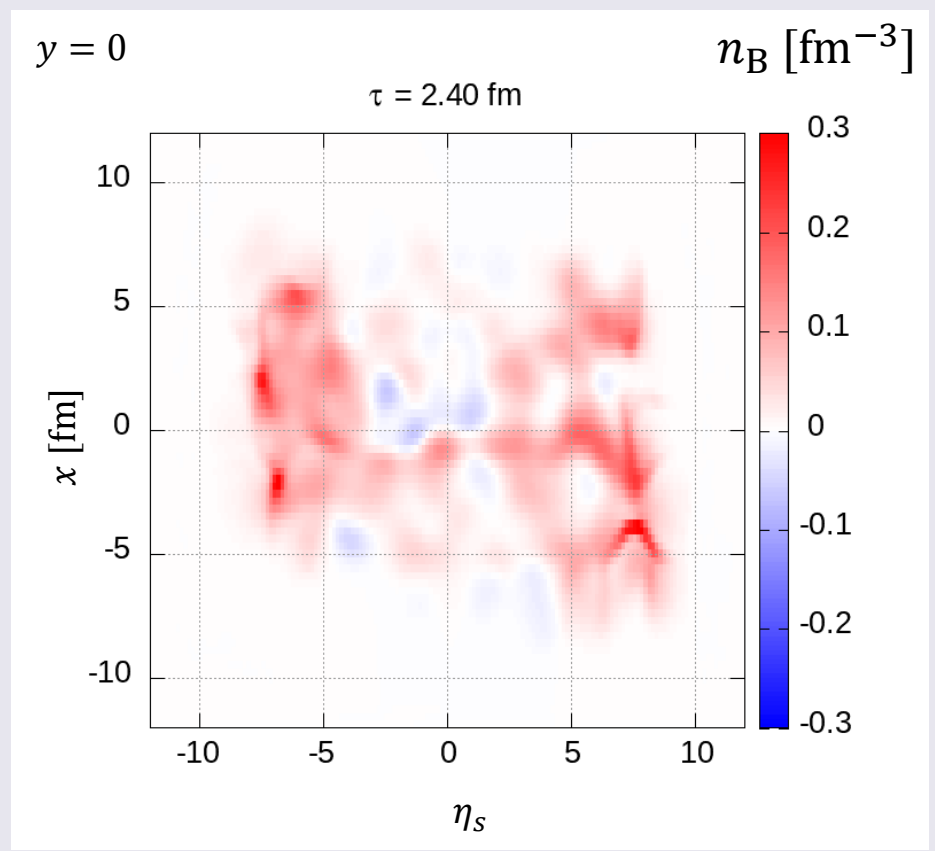
cf.) $y_{\text{beam}}(\sqrt{s_{\text{NN}}} = 2.76 \text{ TeV}) \approx 8$

- Large fluctuations of baryon number density even in midrapidity

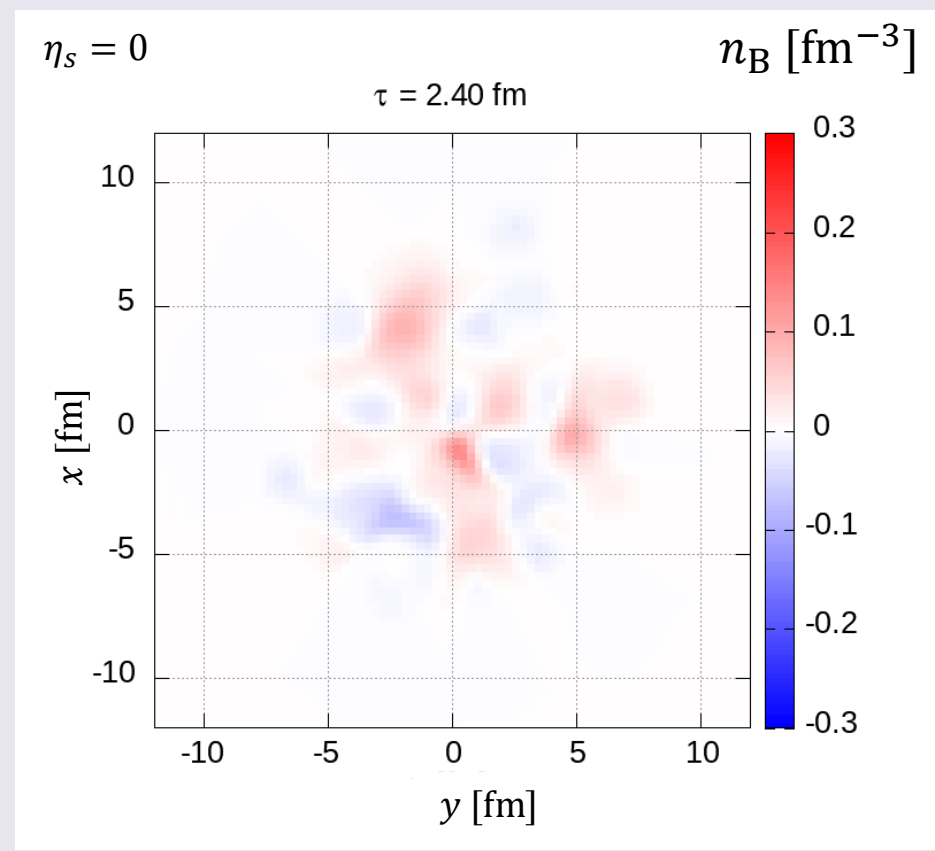
➡ Negative n_B region appears

Space-time evolution of core

Baryon number density (longitudinal profile)



Baryon number density (transverse profile)



- Large baryon number density is realized in forward rapidities $5 \lesssim |\eta_s| \lesssim 10$

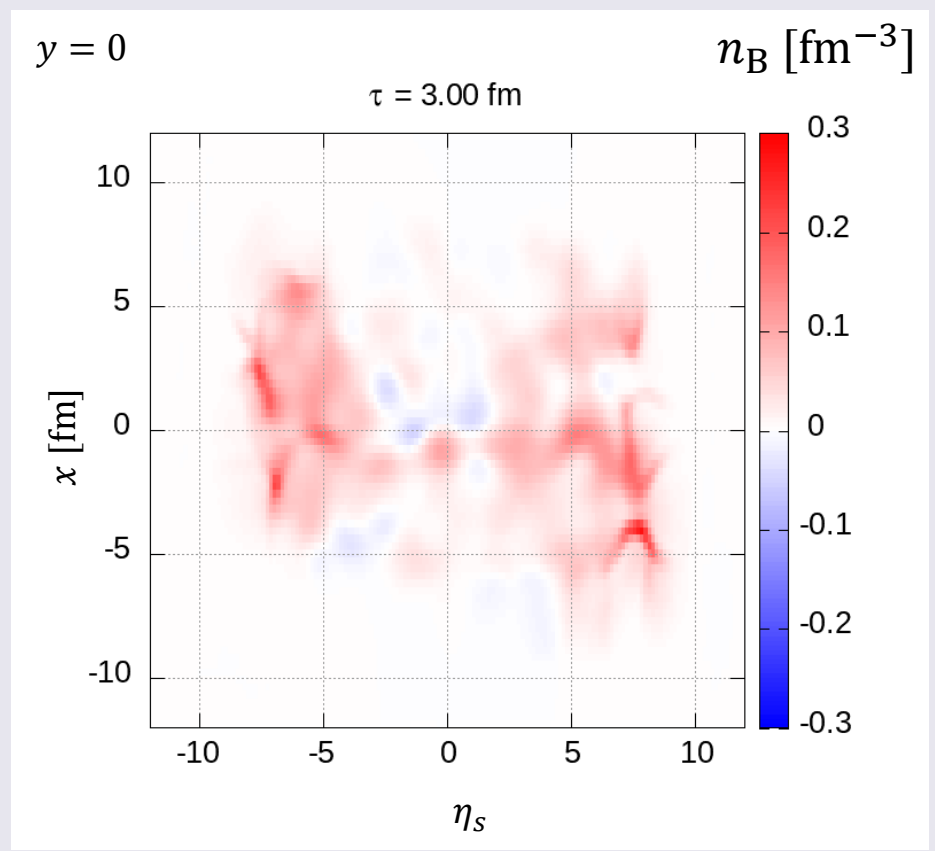
cf.) $y_{\text{beam}}(\sqrt{s_{\text{NN}}} = 2.76 \text{ TeV}) \approx 8$

- Large fluctuations of baryon number density even in midrapidity

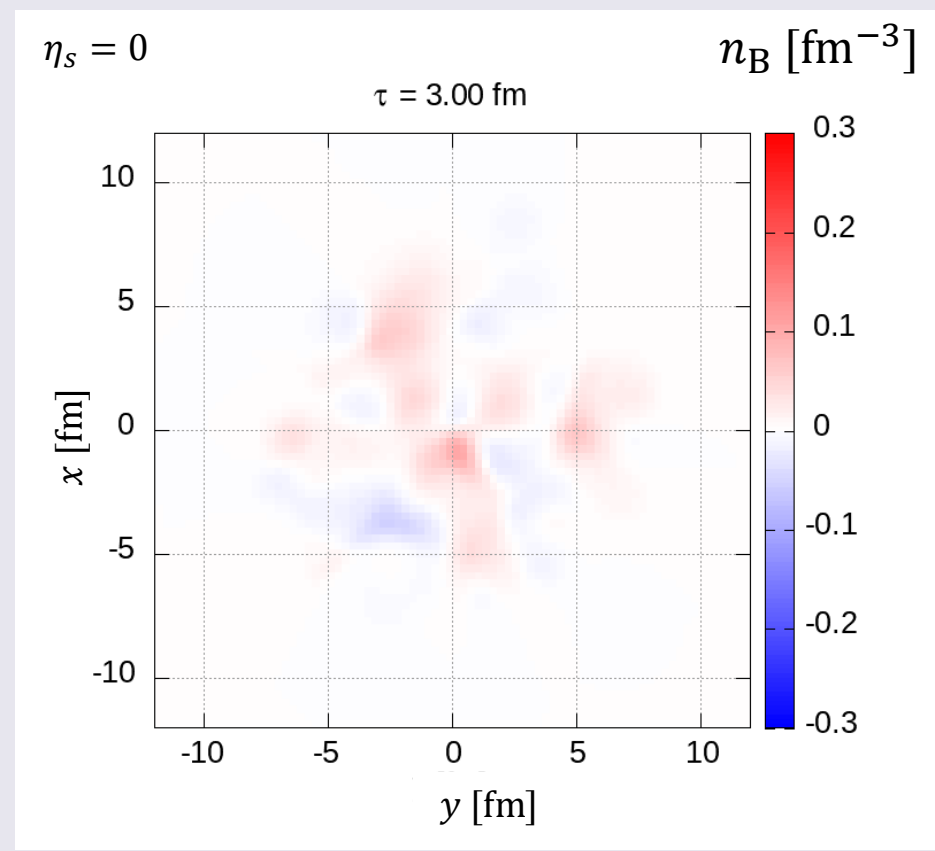
➡ Negative n_B region appears

Space-time evolution of core

Baryon number density (longitudinal profile)



Baryon number density (transverse profile)



- Large baryon number density is realized in forward rapidities $5 \lesssim |\eta_s| \lesssim 10$

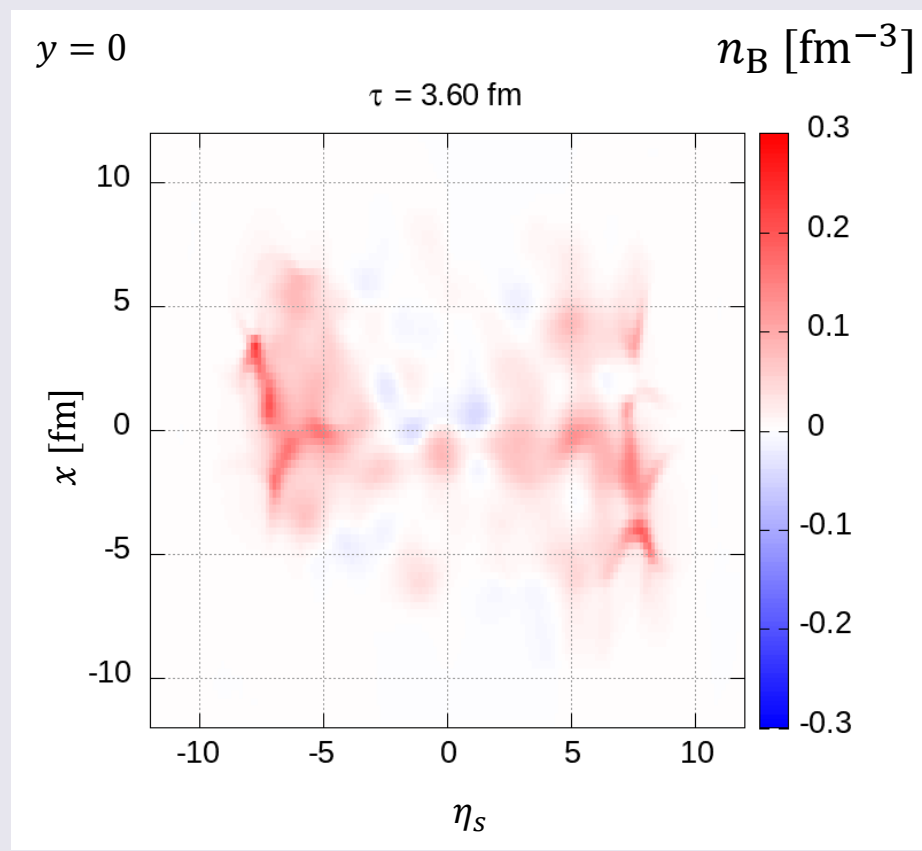
cf.) $y_{\text{beam}}(\sqrt{s_{\text{NN}}} = 2.76 \text{ TeV}) \approx 8$

- Large fluctuations of baryon number density even in midrapidity

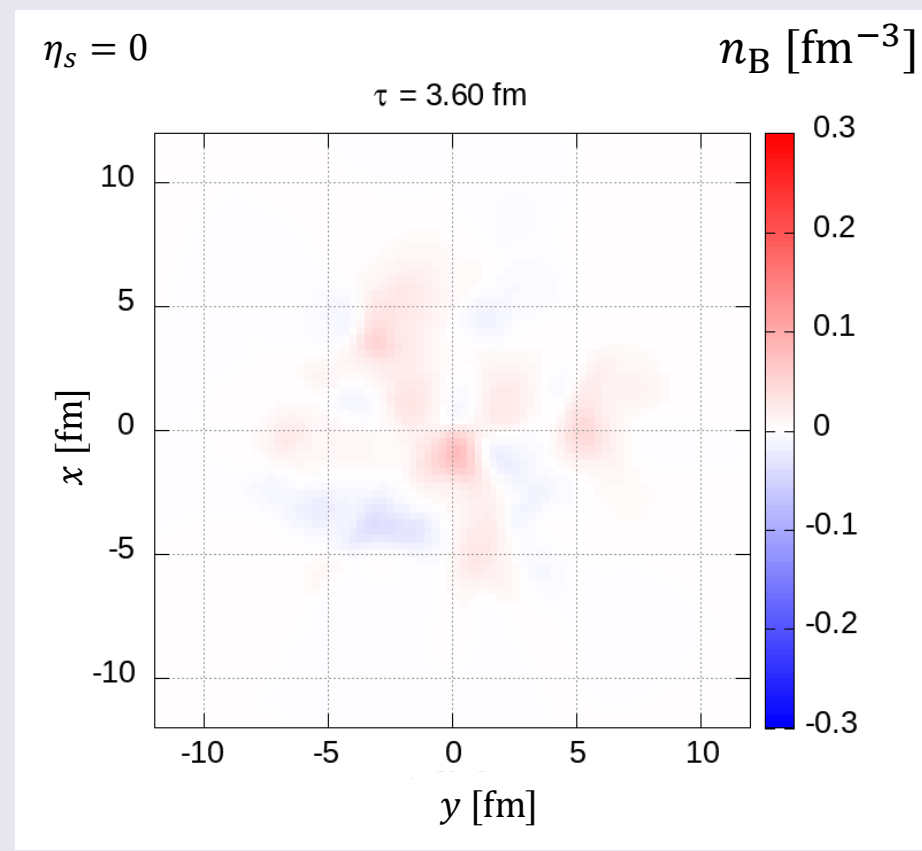
➡ Negative n_B region appears

Space-time evolution of core

Baryon number density (longitudinal profile)



Baryon number density (transverse profile)



- Large baryon number density is realized in forward rapidities $5 \lesssim |\eta_s| \lesssim 10$

cf.) $y_{\text{beam}}(\sqrt{s_{\text{NN}}} = 2.76 \text{ TeV}) \approx 8$

- Large fluctuations of baryon number density even in midrapidity

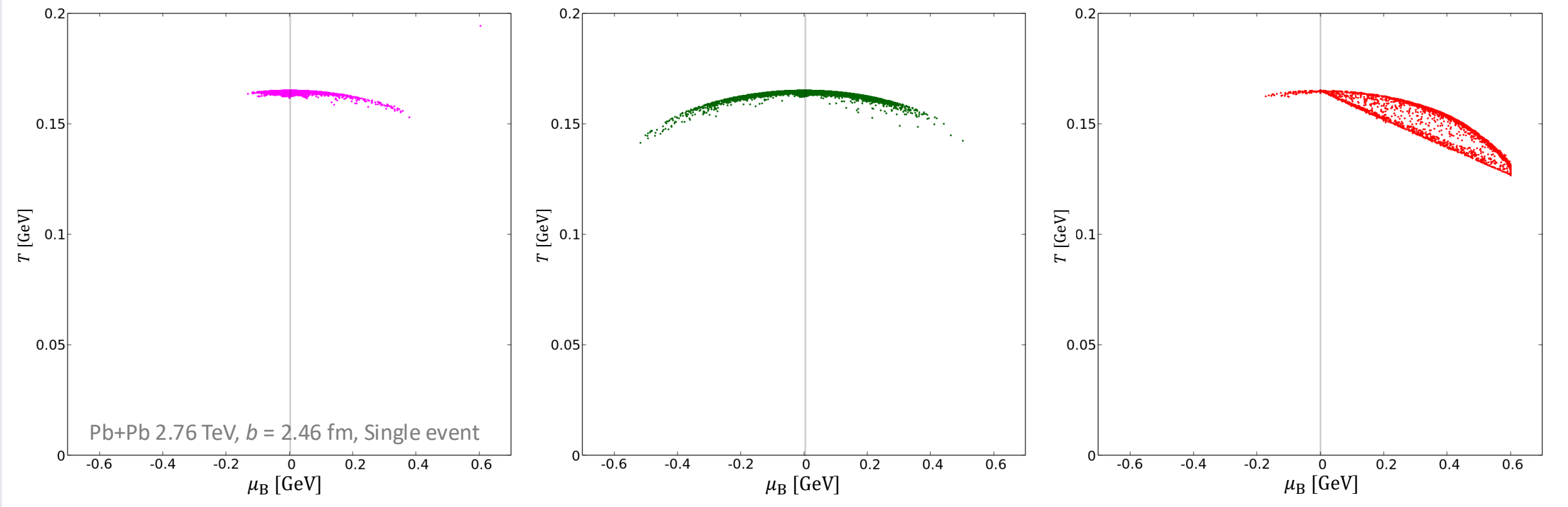
➡ Negative n_B region appears

Rapidity dependence of freezeout hypersurface

$-1 \leq \eta_s \leq 1$

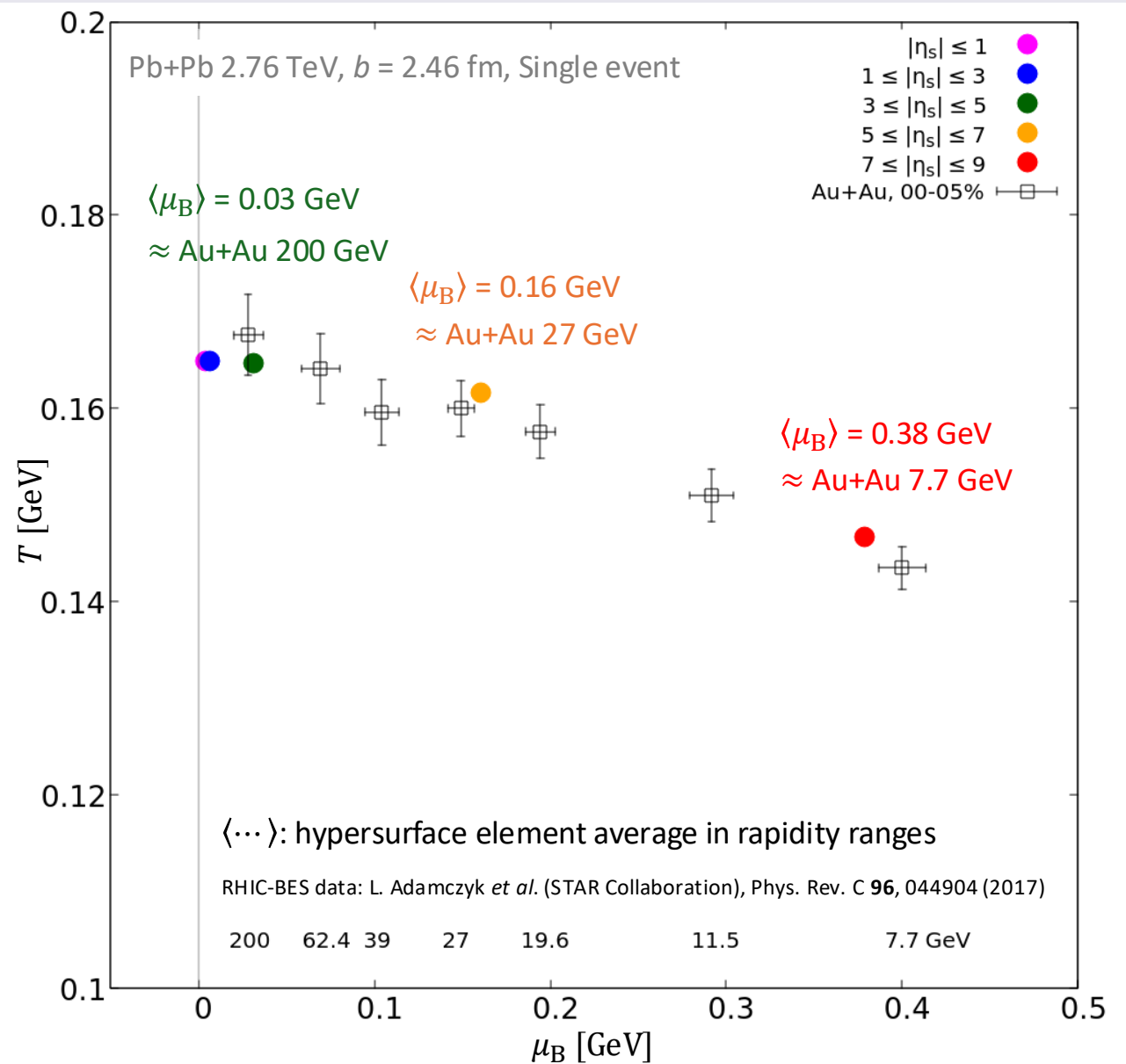
$3 \leq \eta_s \leq 5$

$7 \leq \eta_s \leq 9$



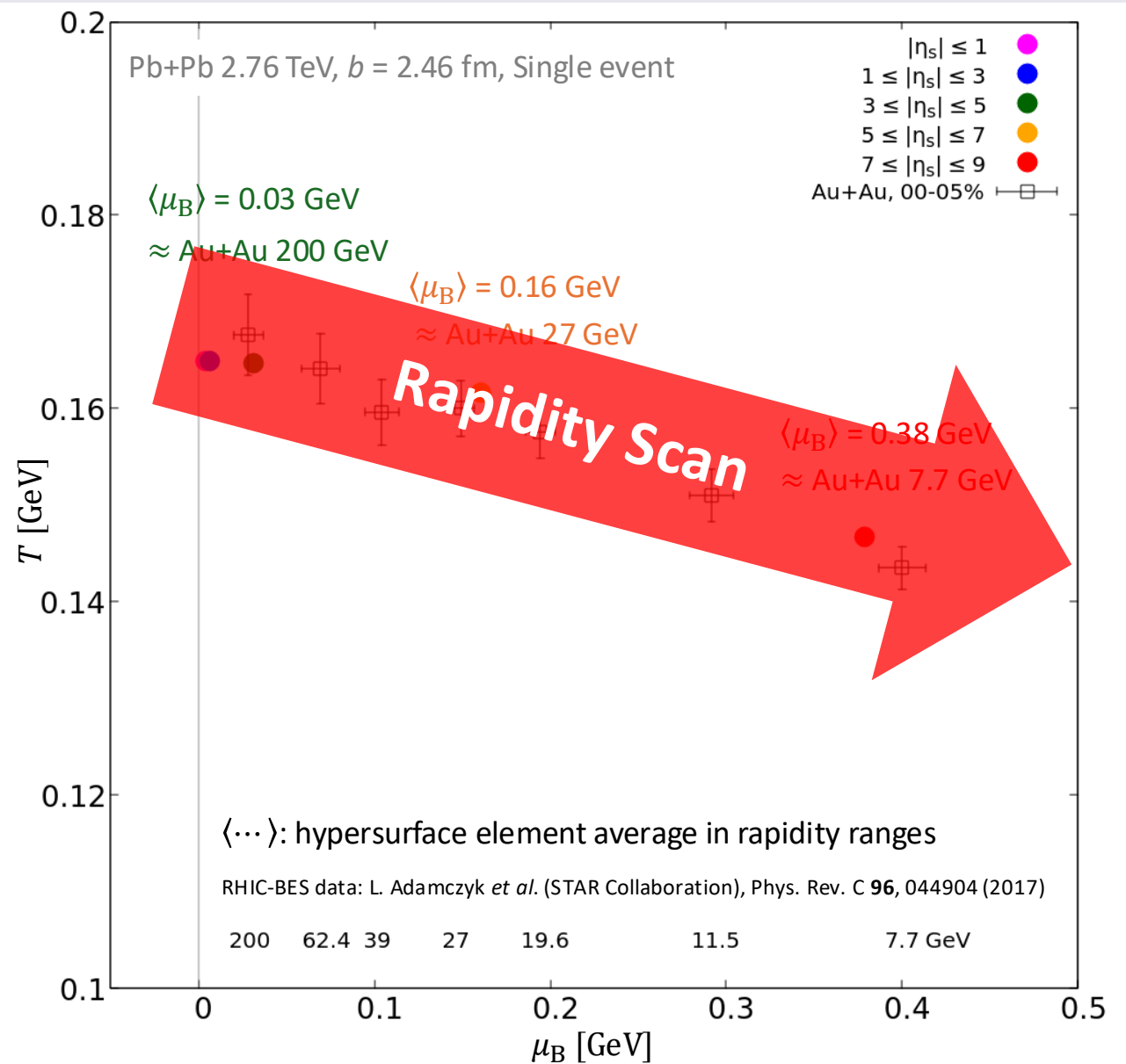
- Some hypersurface element has negative baryon chemical potentials
- Significantly large baryon chemical potentials in forward rapidities

Rapidity-averaged freezeout hypersurface



- Almost zero baryon chemical potential until $|\eta_s| \leq 5$
 ➔ \approx Au+Au 200 GeV
- Averaged-hypersurface in rapidity range $5 \leq |\eta_s| \leq 7$ exceeds $\mu_B = 100$ MeV
 ➔ \approx **Au+Au 27 GeV**
- Averaged-hypersurface in rapidity range $7 \leq |\eta_s| \leq 9$ exceeds $\mu_B = 300$ MeV
 ➔ \approx **Au+Au 7.7 GeV**

Rapidity-averaged freezeout hypersurface



- Almost zero baryon chemical potential until $|\eta_s| \leq 5$
 - ➔ \approx Au+Au 200 GeV
- Averaged-hypersurface in rapidity range $5 \leq |\eta_s| \leq 7$ exceeds $\mu_B = 100$ MeV
 - ➔ \approx **Au+Au 27 GeV**
- Averaged-hypersurface in rapidity range $7 \leq |\eta_s| \leq 9$ exceeds $\mu_B = 300$ MeV
 - ➔ \approx **Au+Au 7.7 GeV**

Rapidity scan is a strong tool for exploring the QCD phase diagram!!

Introduction

Model

Results

 **Summary and Outlook**

Summary and Outlook

Summary

- Extended the DCCI model to finite baryon number
 - ➡ descriptions of thermalized baryon number
 - ➡ Rapidity Scan!!
- Negative $n_B(\mu_B)$ region appears due to the depositions of anti-quarks
- At LHC energies, high baryon chemical potentials are realized in forward rapidities

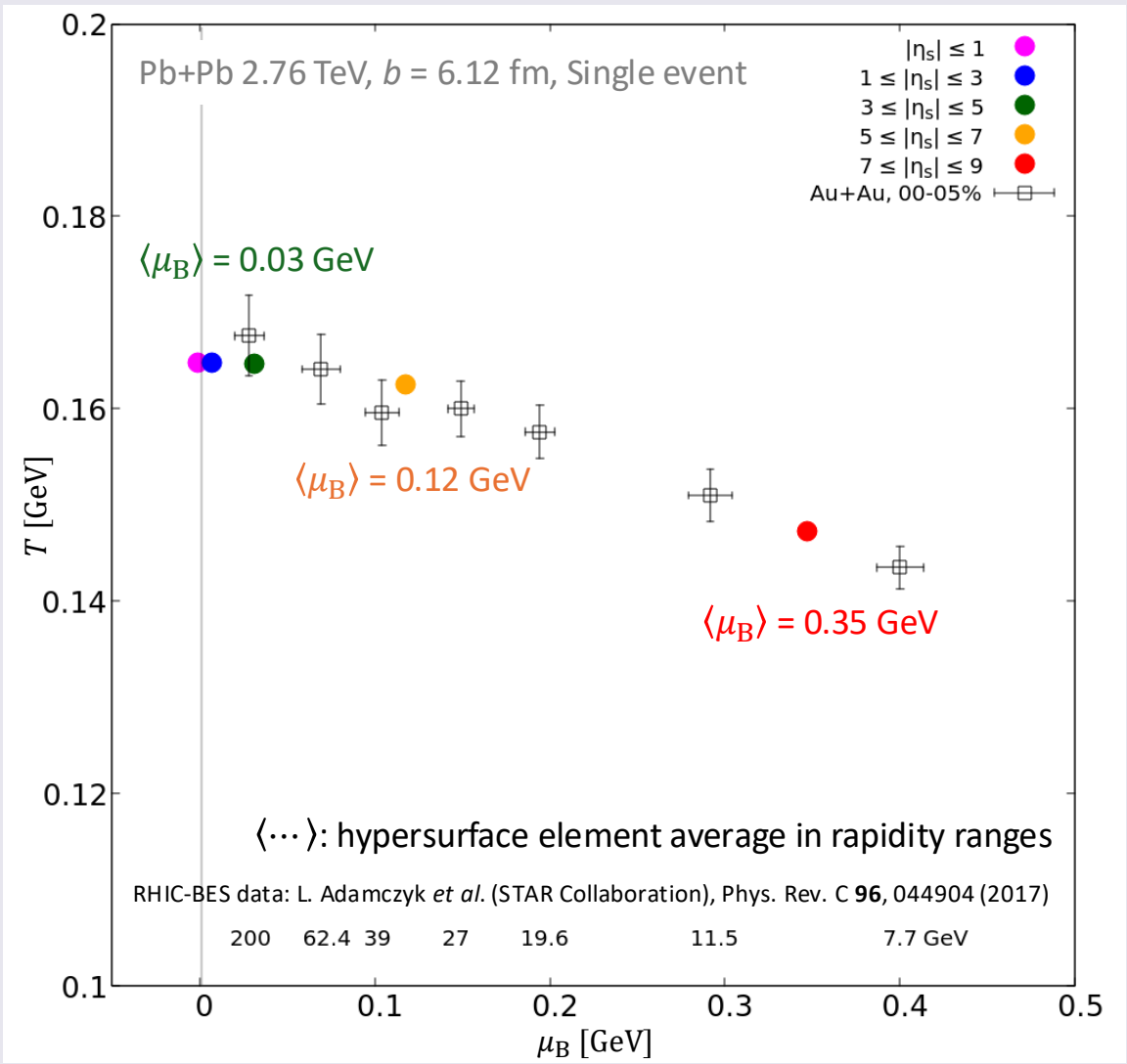
Outlook

- Centrality dependence
- Event-averaged analysis
- Baryon stopping

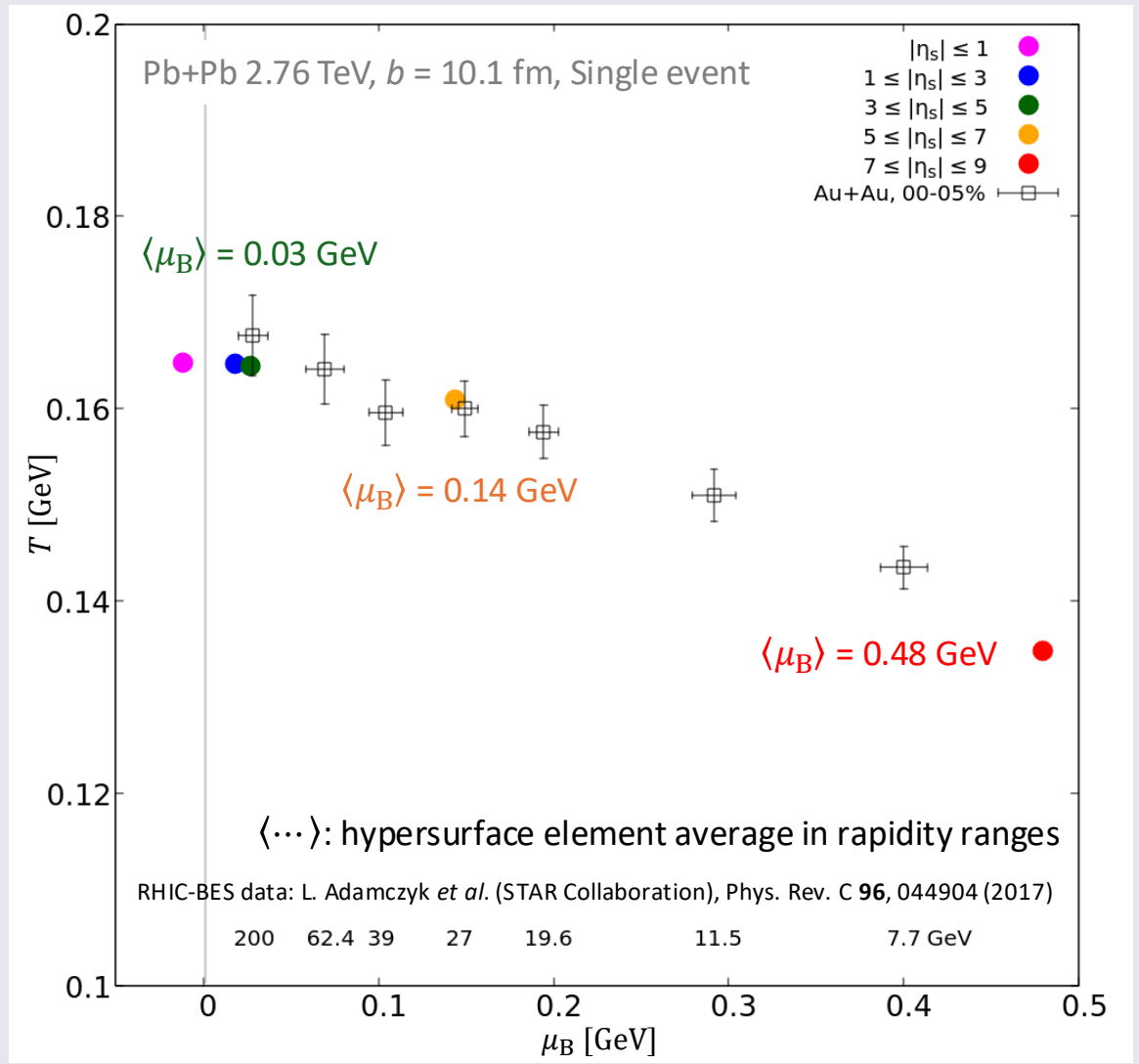
Backups

Rapidity-averaged freezeout hypersurface

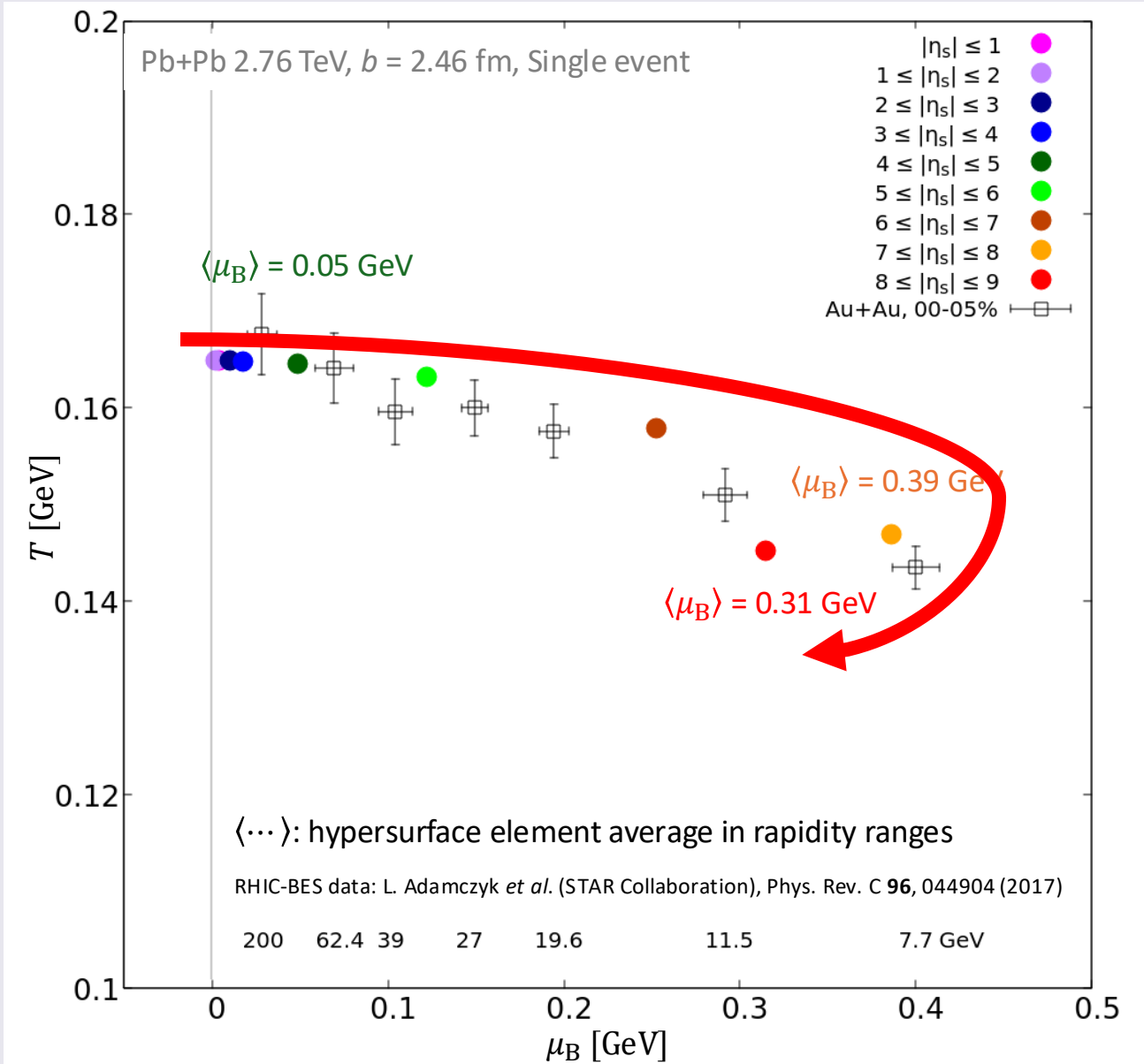
$b = 6.12$ fm



$b = 10.1$ fm



Rapidity-averaged freezeout hypersurface



● μ_B becomes maximum in $7 \leq |\eta_s| \leq 8$

cf.) $y_{\text{beam}}(\sqrt{s_{\text{NN}}} = 2.76 \text{ TeV}) \approx 8$

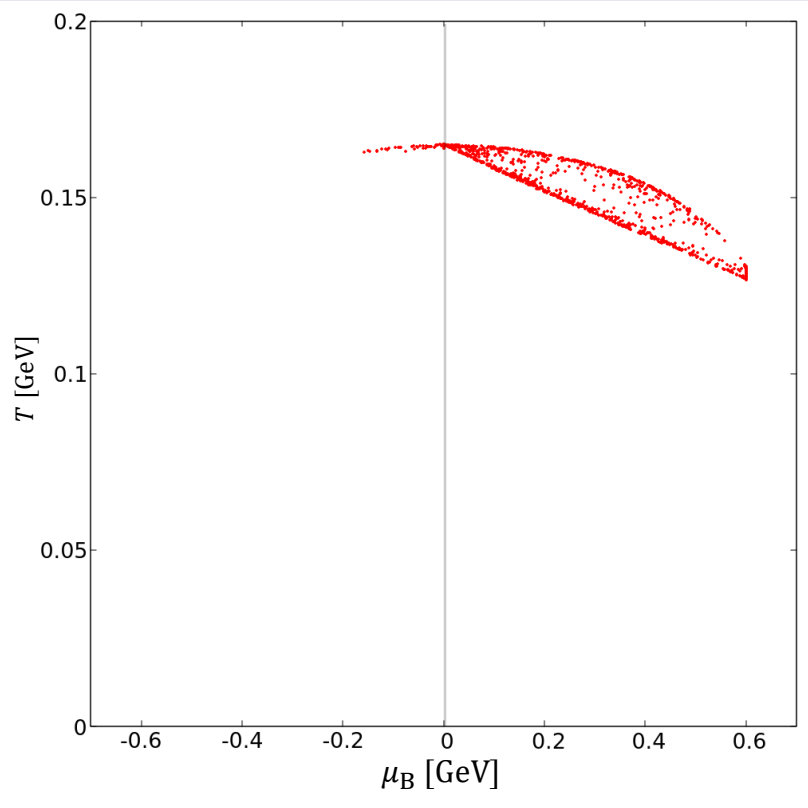
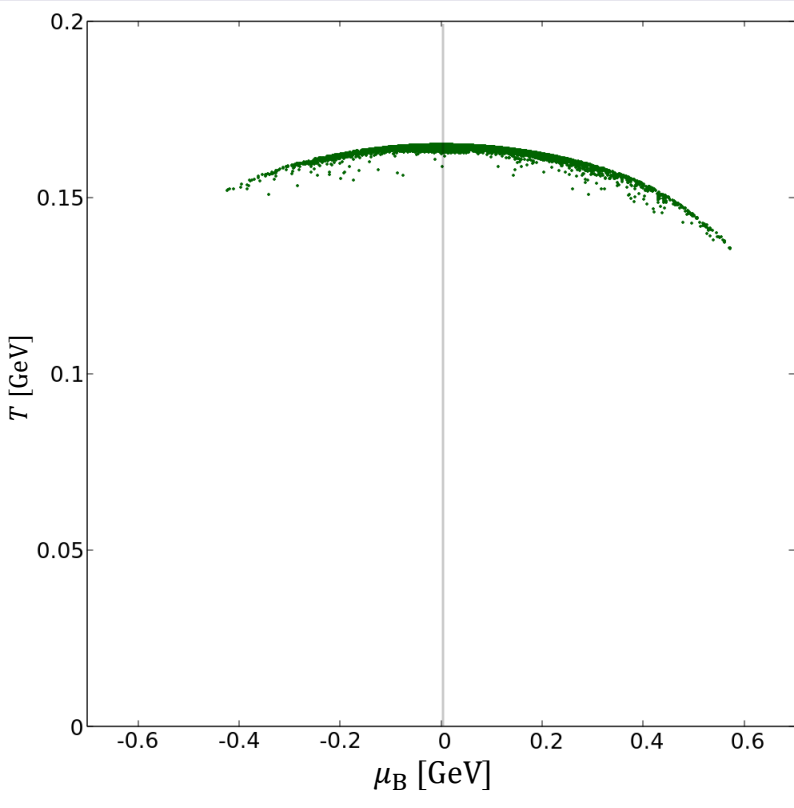
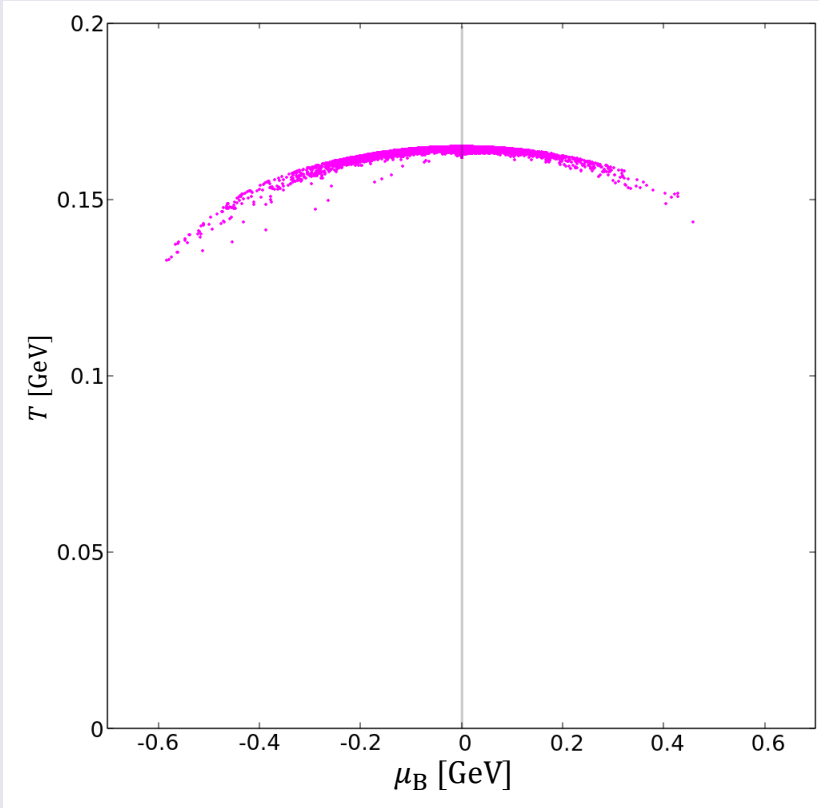
Rapidity dependence of freezeout hypersurface

Pb+Pb 2.76 TeV, $b = 6.12$ fm, Single event

$-1 \leq \eta_s \leq 1$

$3 \leq \eta_s \leq 5$

$7 \leq \eta_s \leq 9$



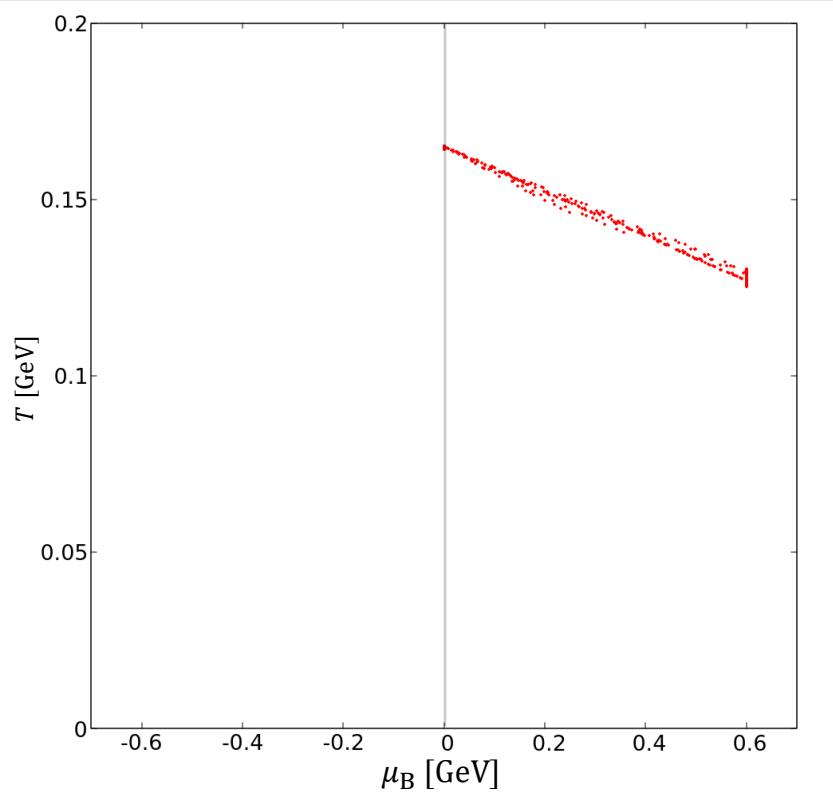
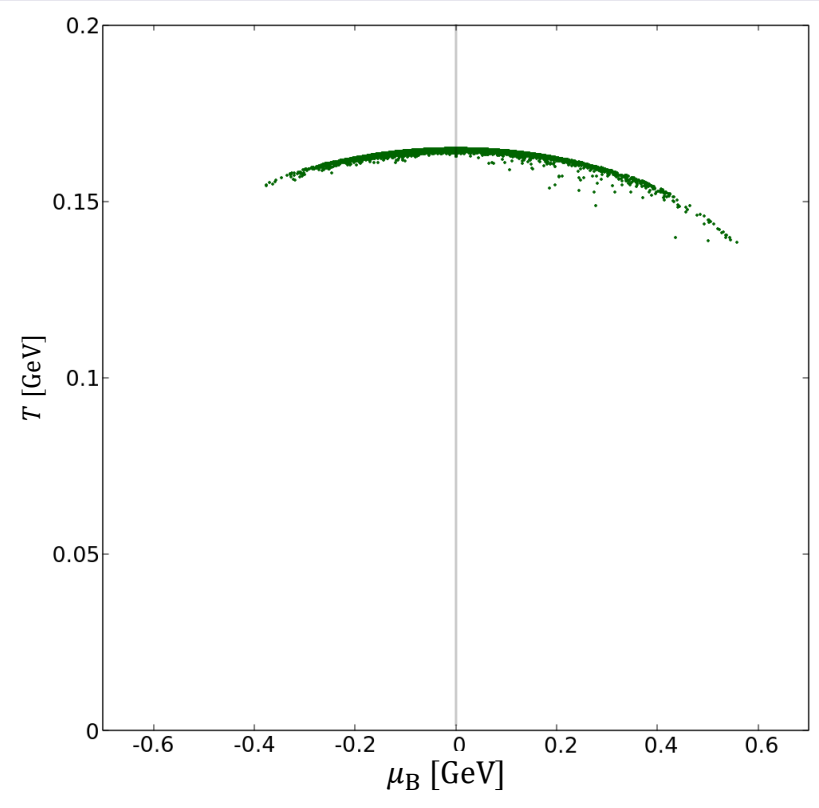
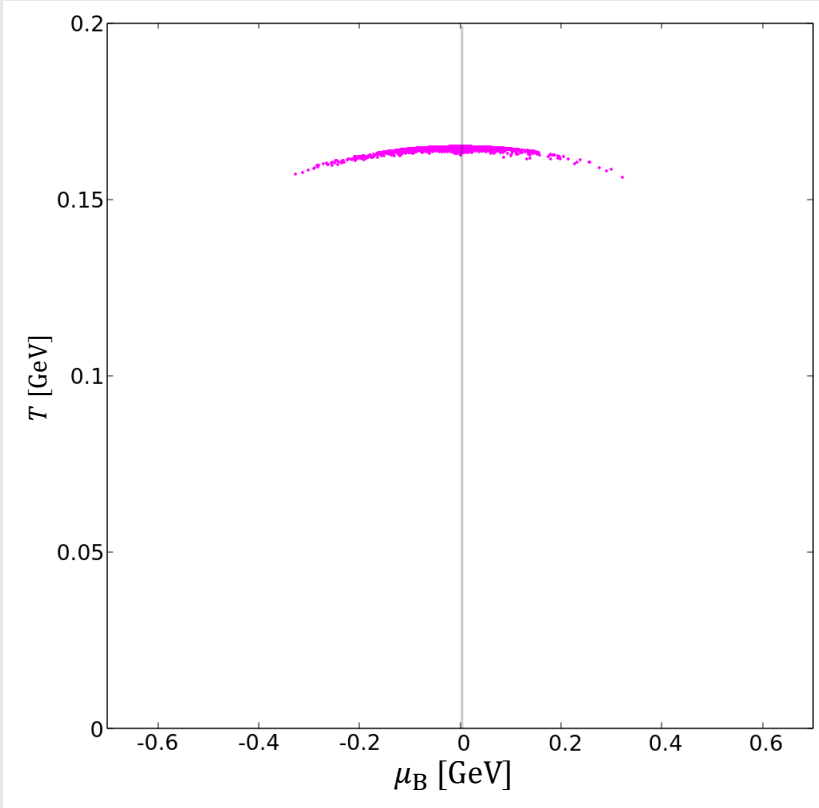
Rapidity dependence of freezeout hypersurface

Pb+Pb 2.76 TeV, $b = 10.1$ fm, Single event

$-1 \leq \eta_s \leq 1$

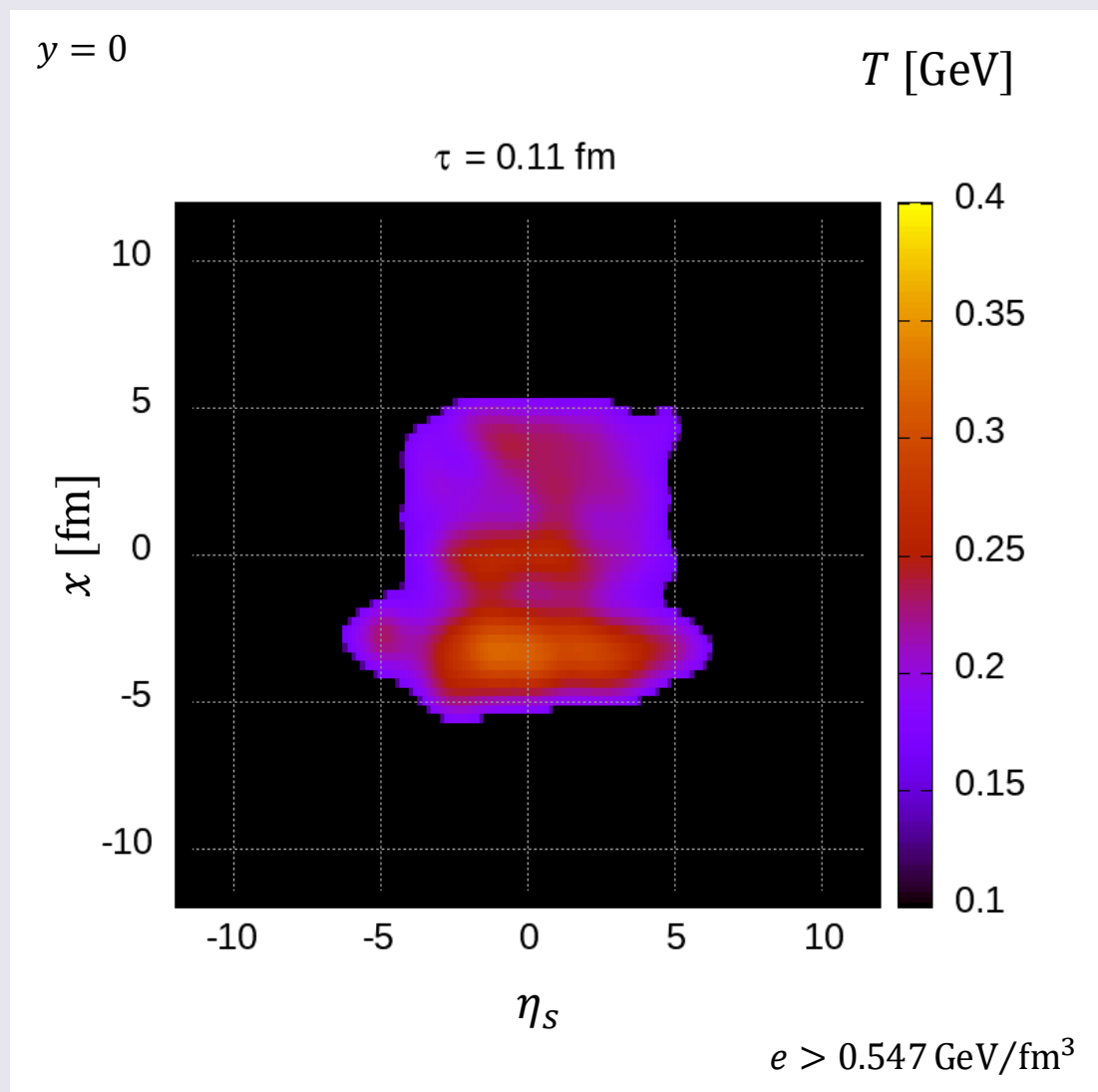
$3 \leq \eta_s \leq 5$

$7 \leq \eta_s \leq 9$

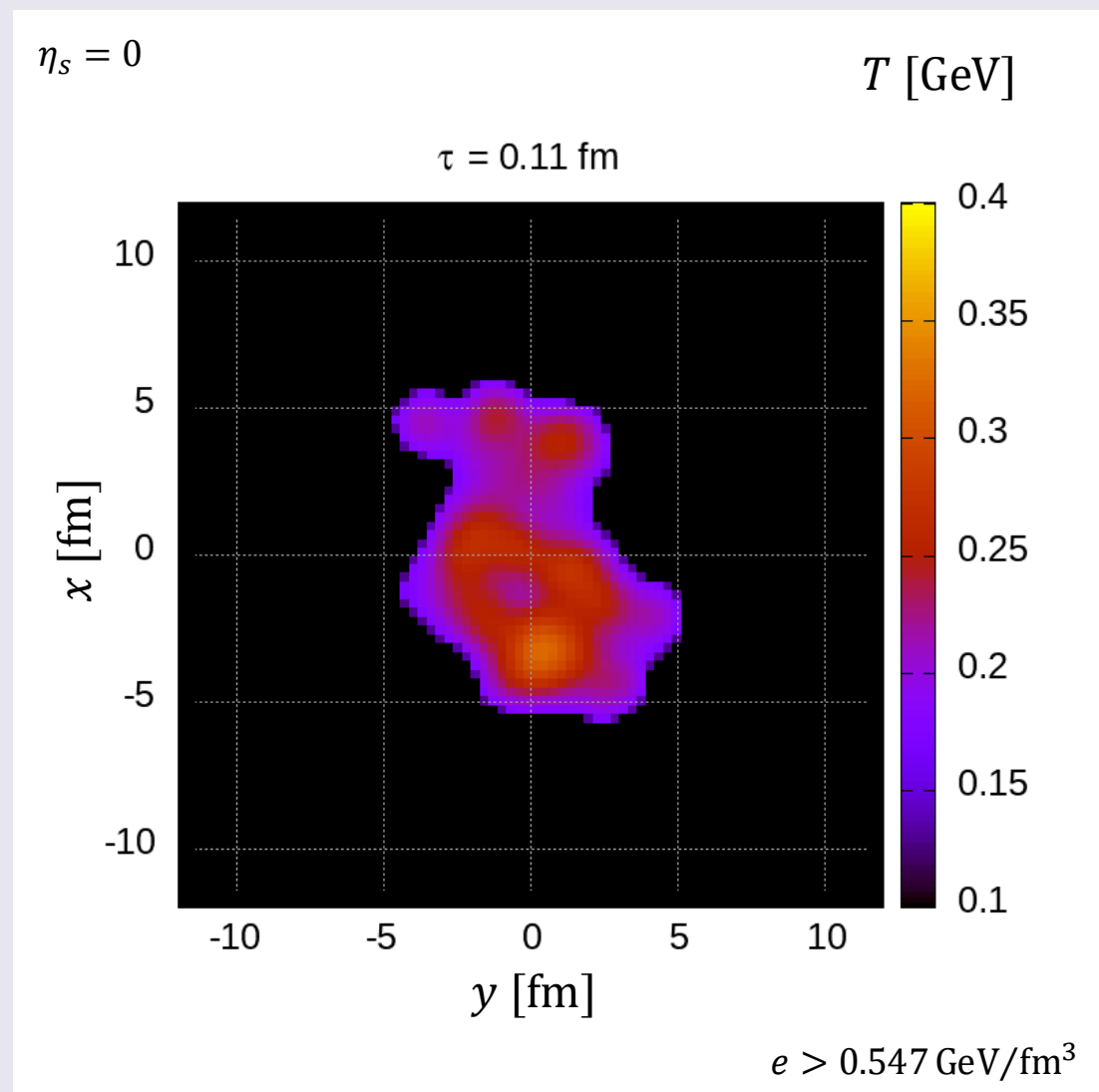


Space-time evolution of core

Temperature (longitudinal profile)

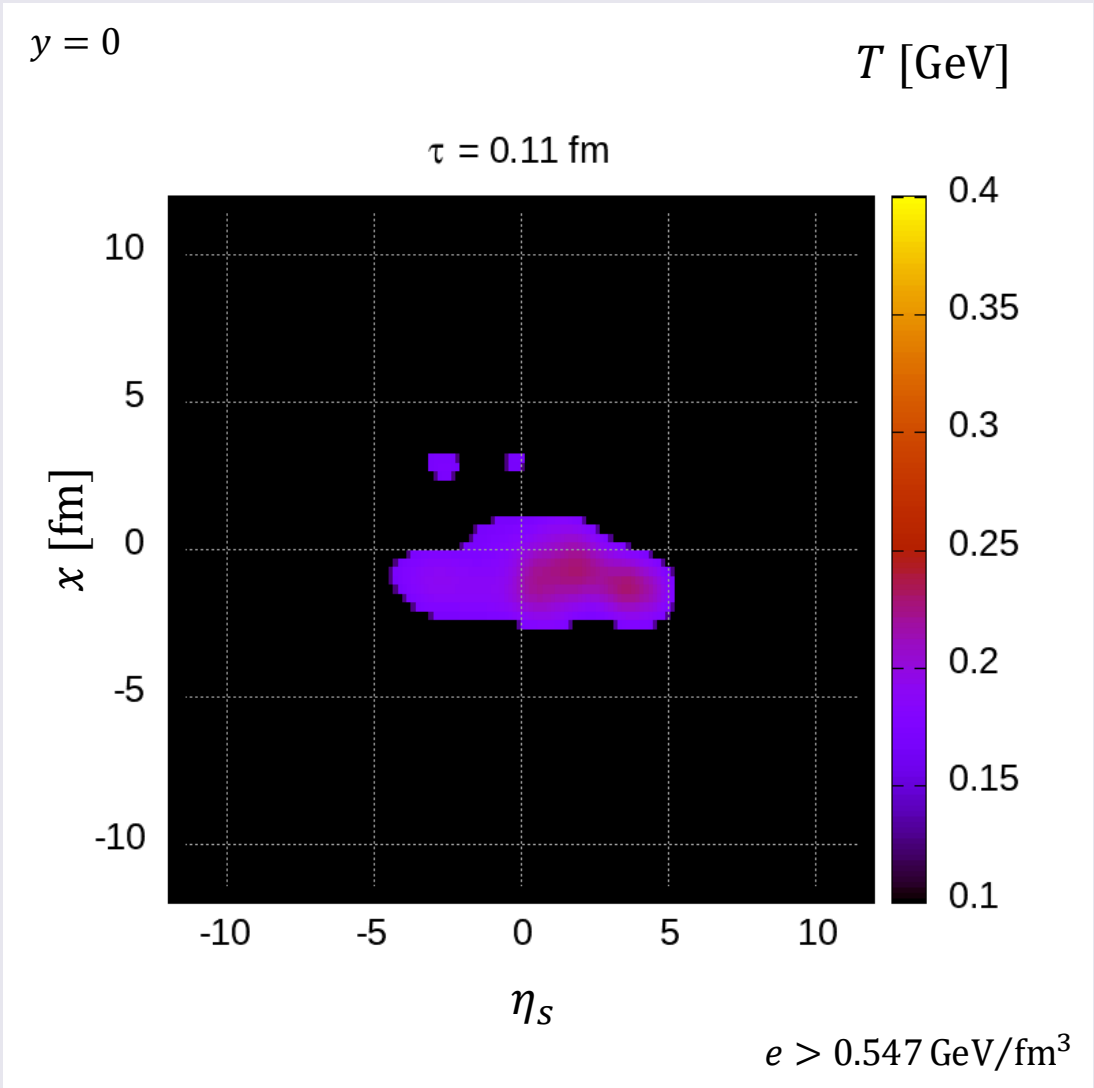


Temperature (transverse profile)

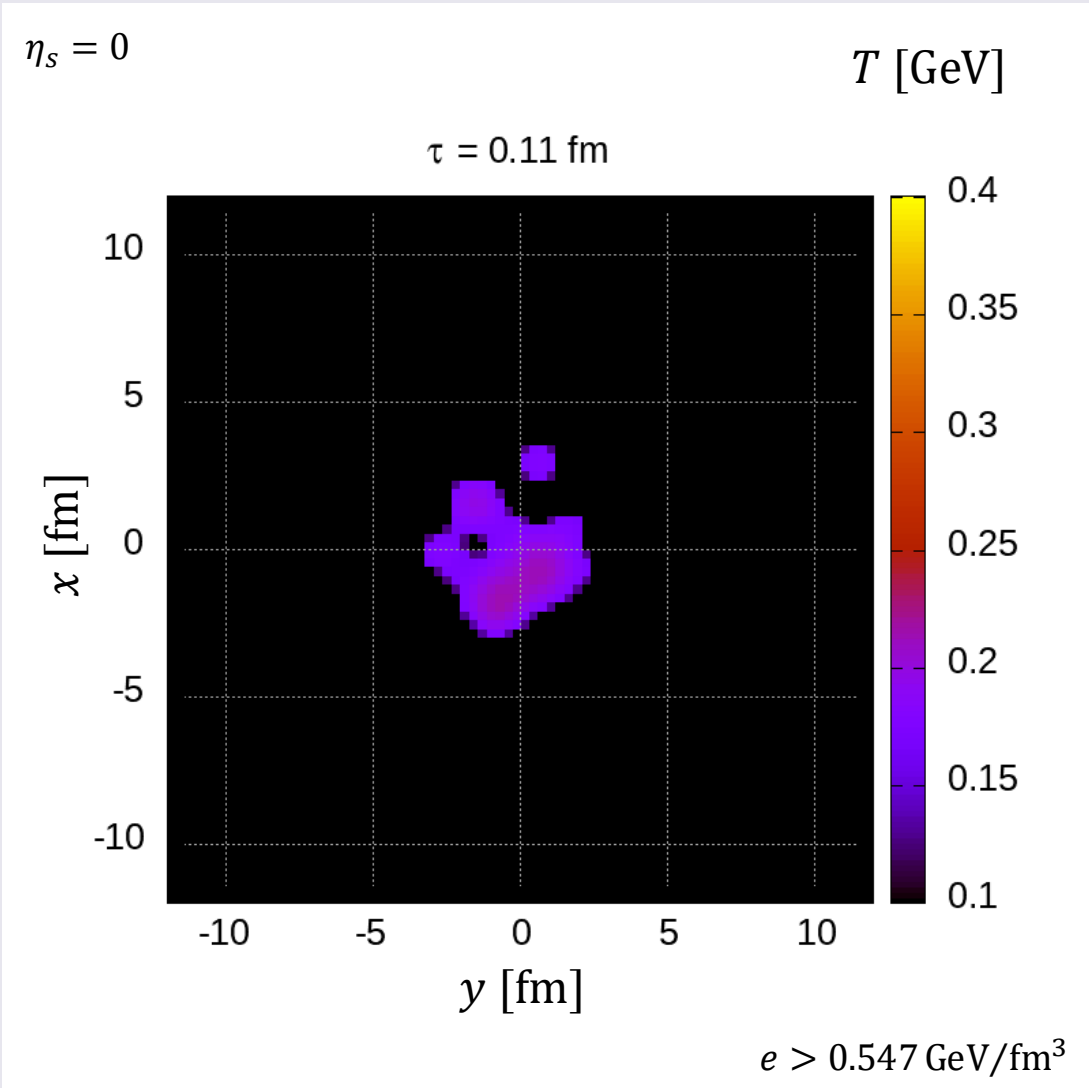


Space-time evolution of core

Temperature (longitudinal profile)

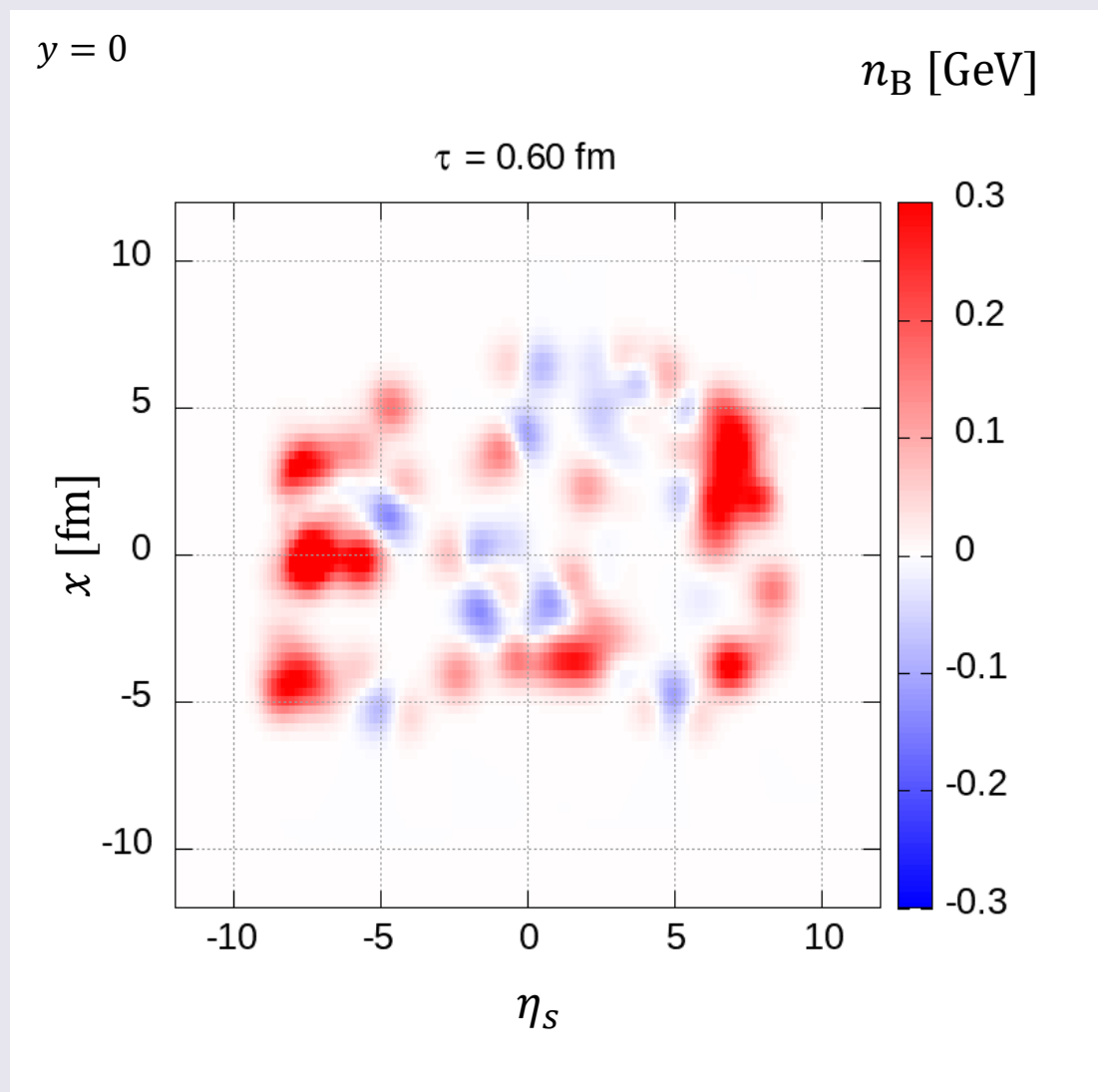


Temperature (transverse profile)

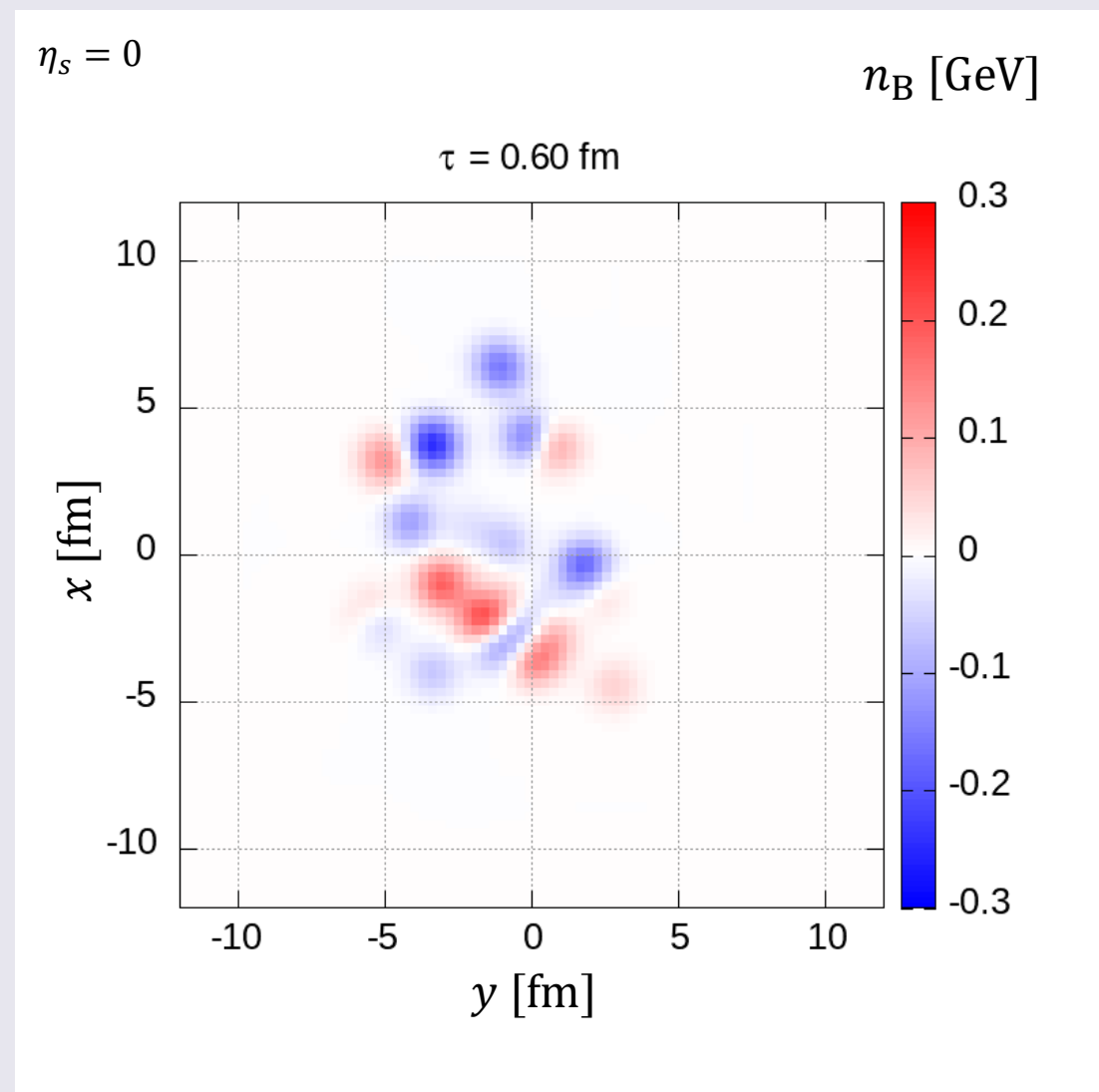


Space-time evolution of core

Baryon number density (longitudinal profile)

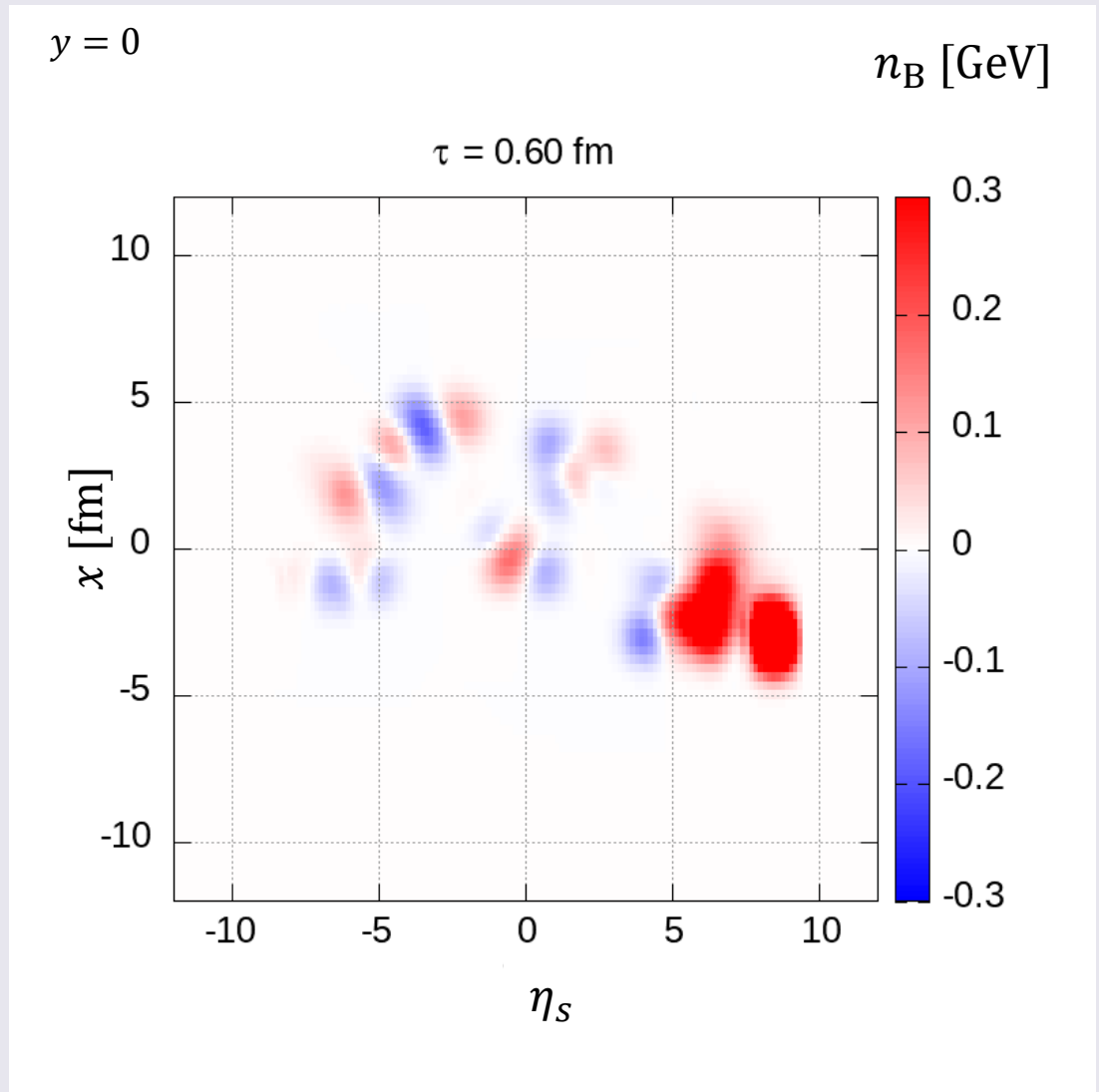


Baryon number density (transverse profile)

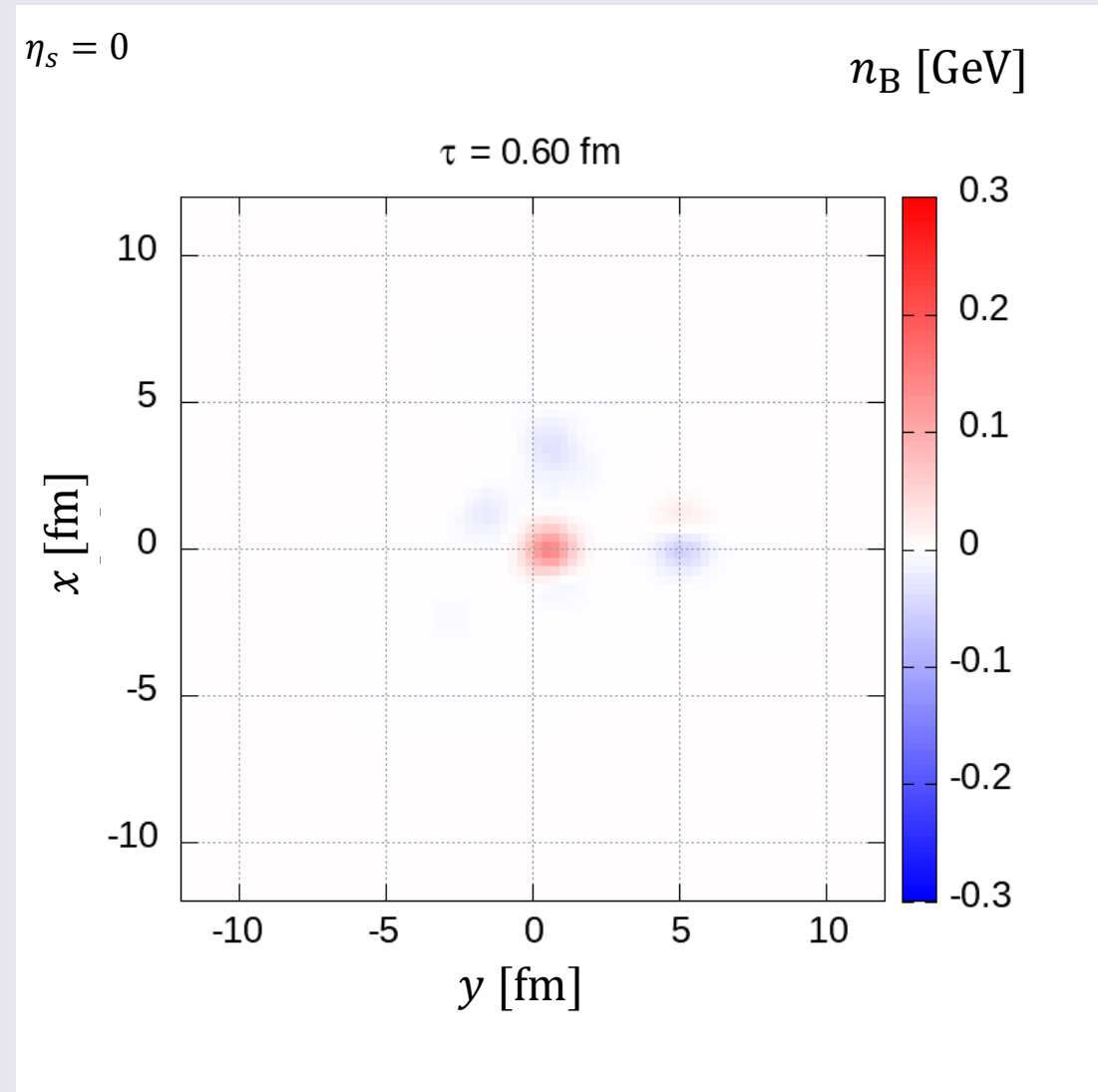


Space-time evolution of core

Baryon number density (longitudinal profile)

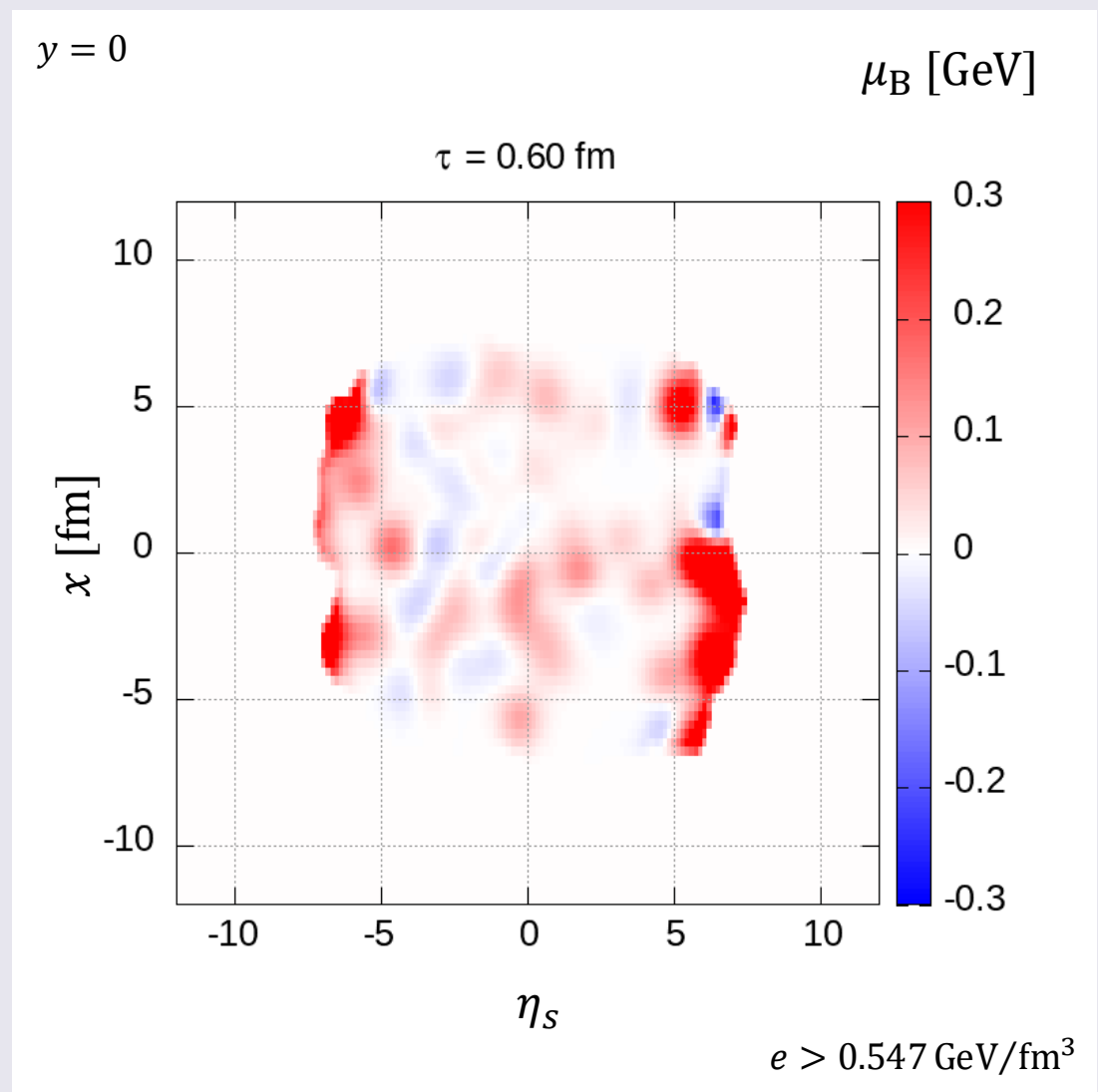


Baryon number density (transverse profile)

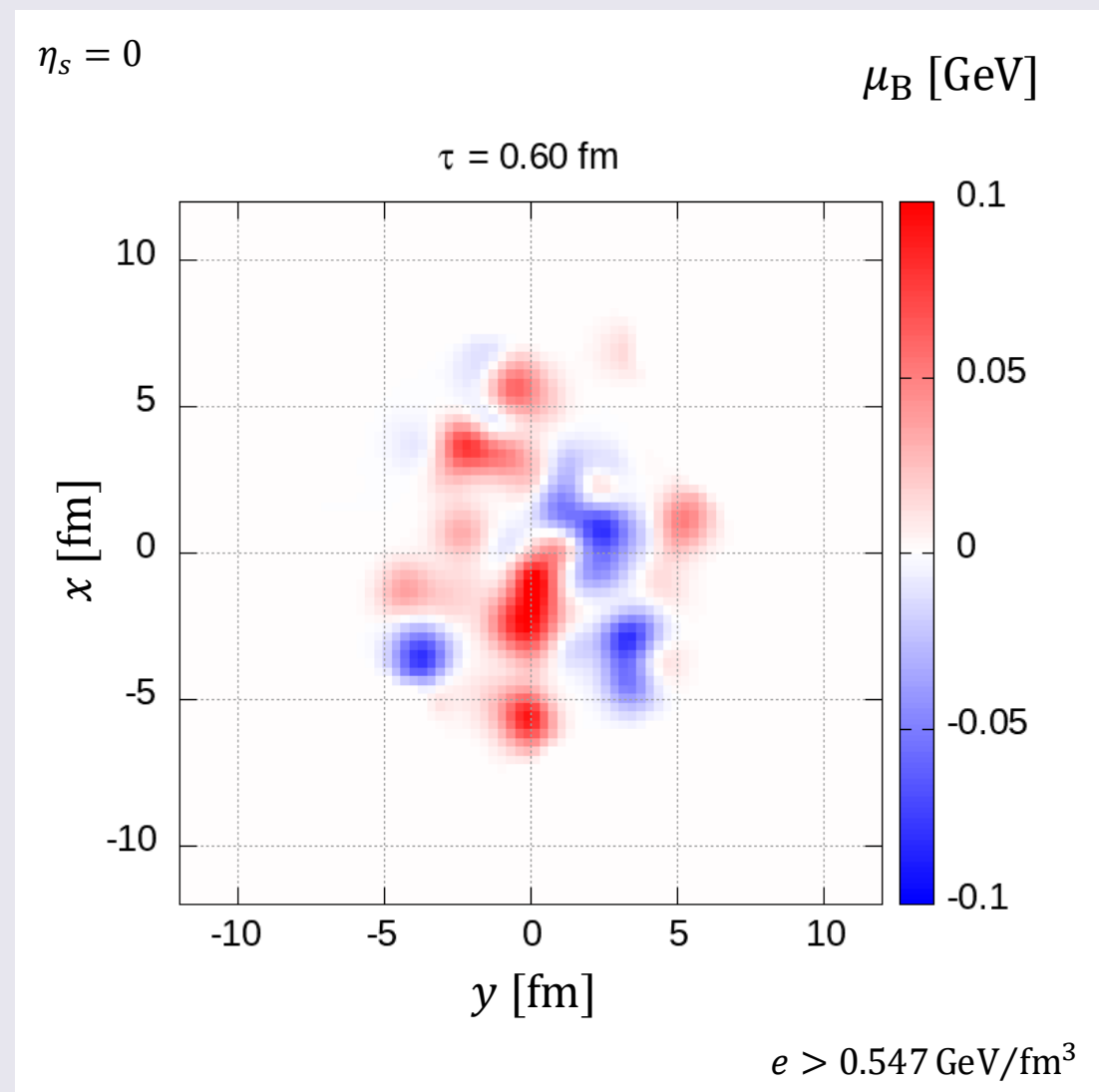


Space-time evolution of core

Baryon chemical potential (longitudinal profile)

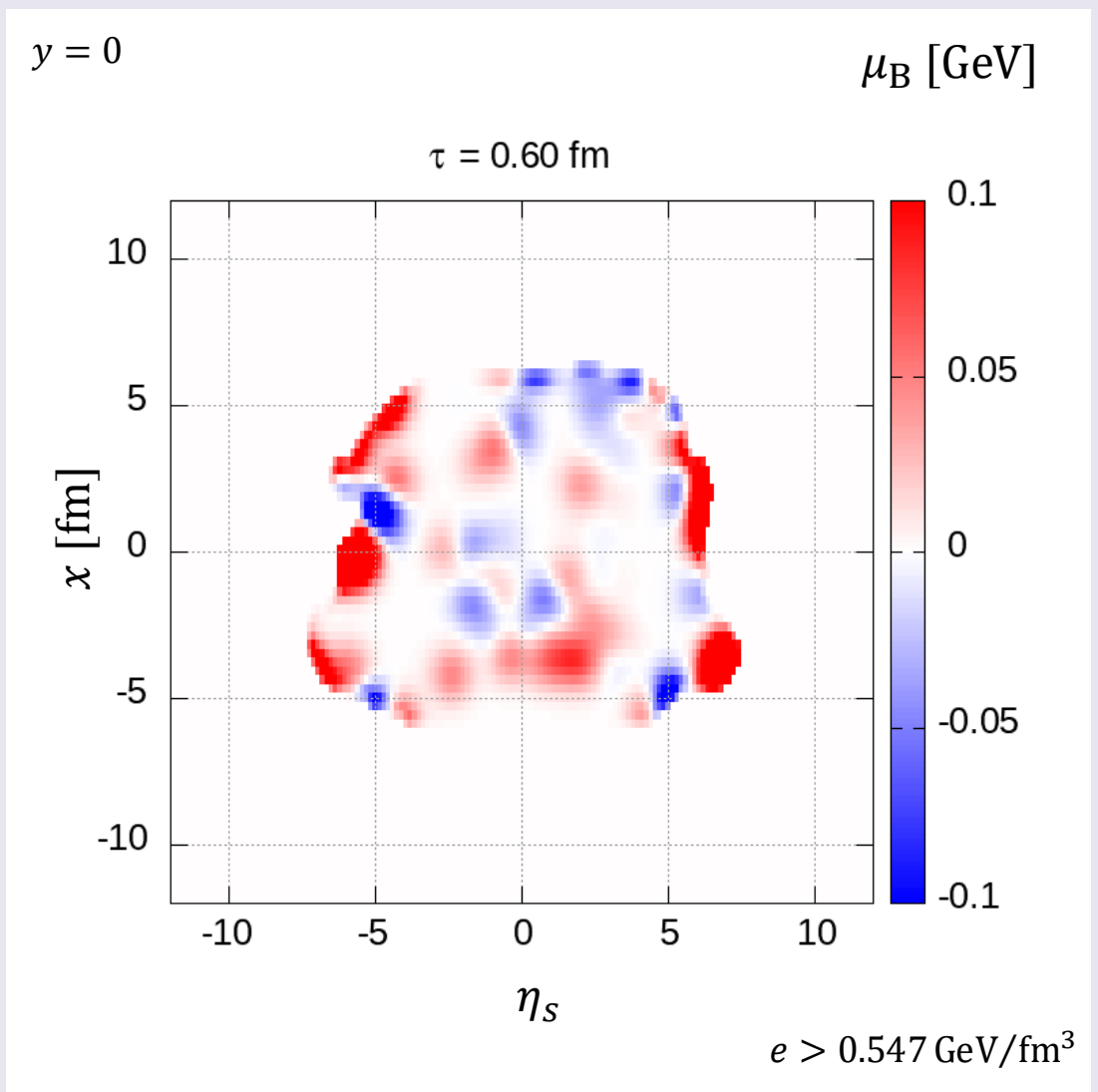


Baryon chemical potential (transverse profile)

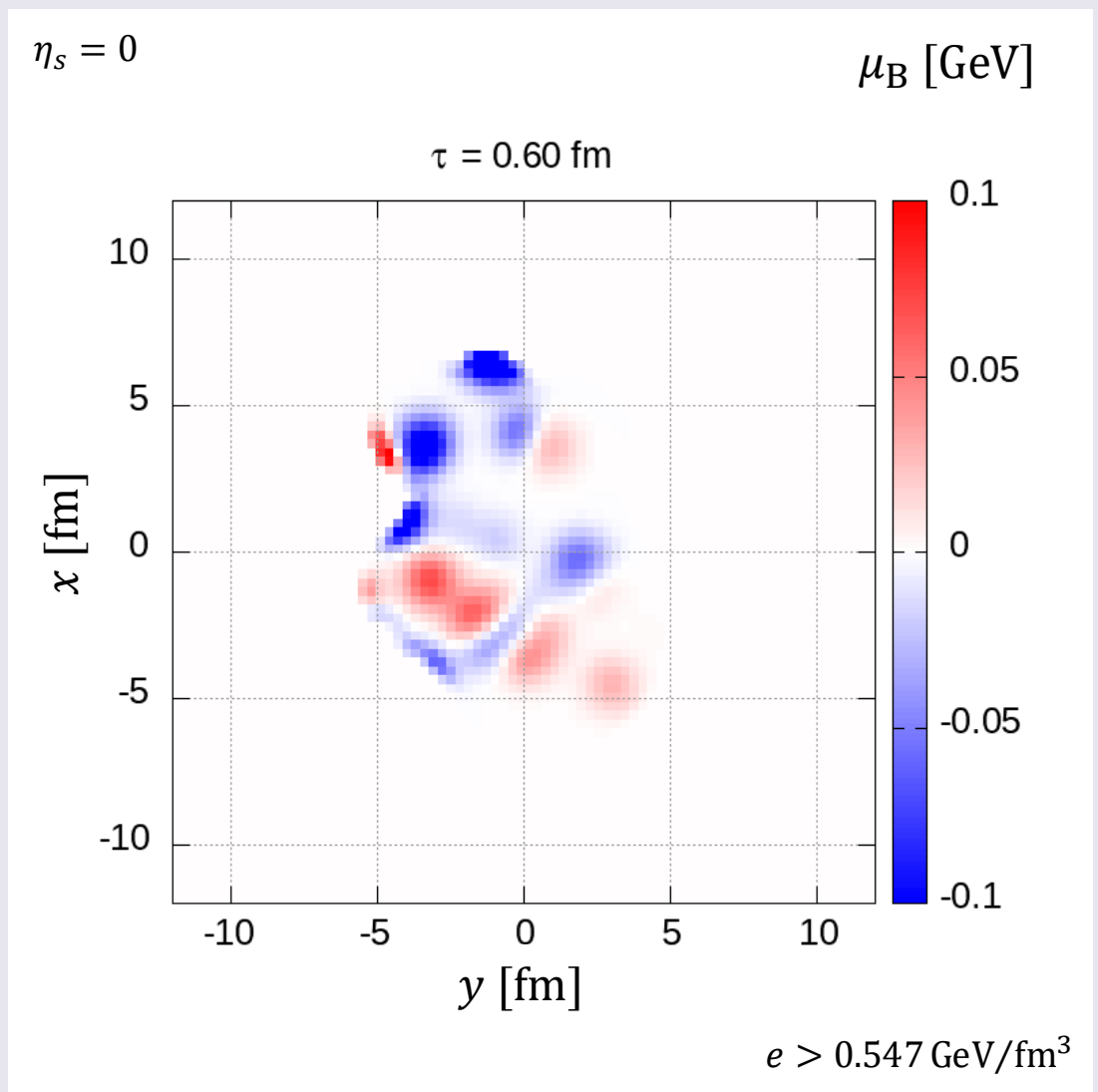


Space-time evolution of core

Baryon chemical potential (longitudinal profile)

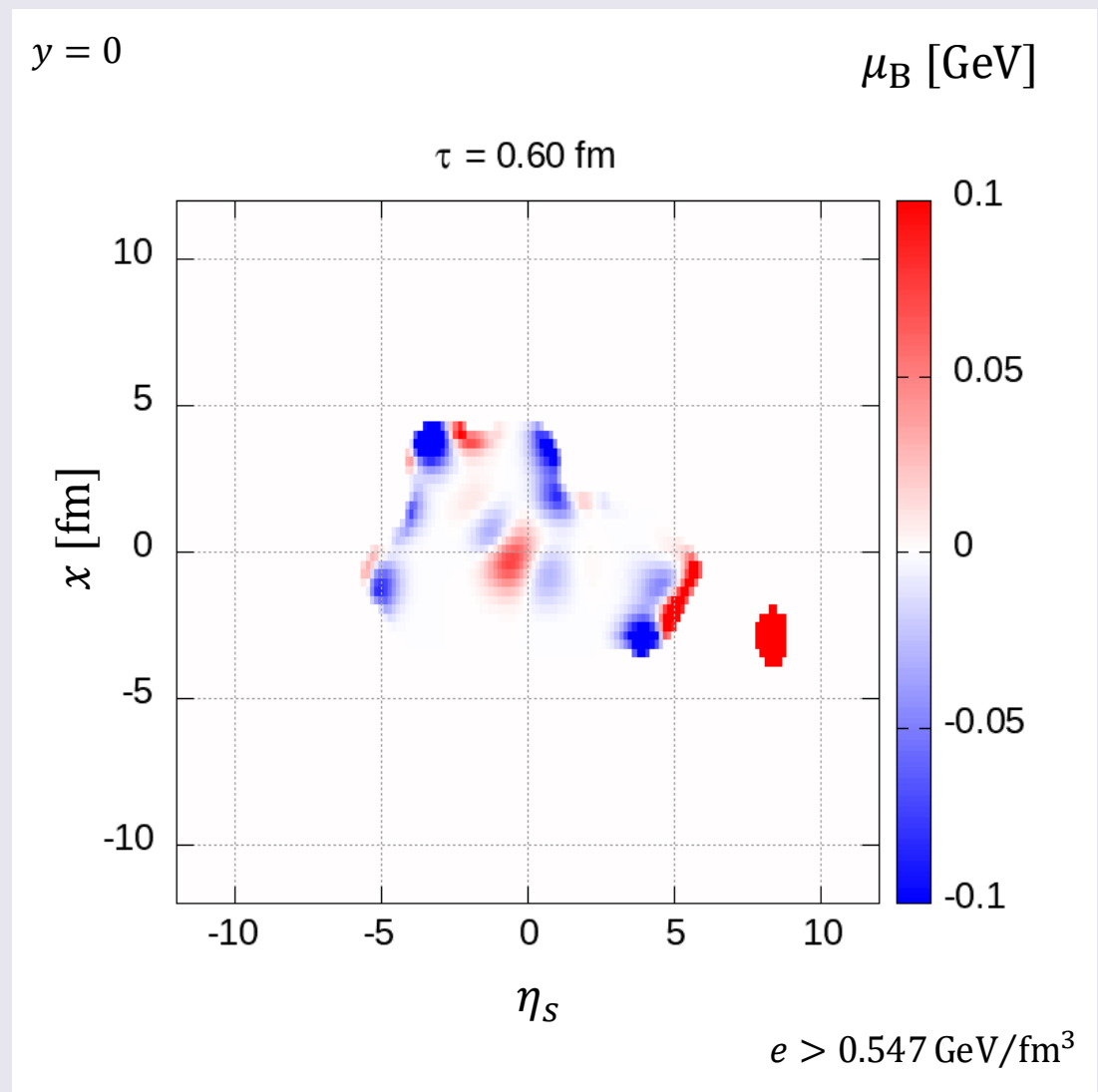


Baryon chemical potential (transverse profile)

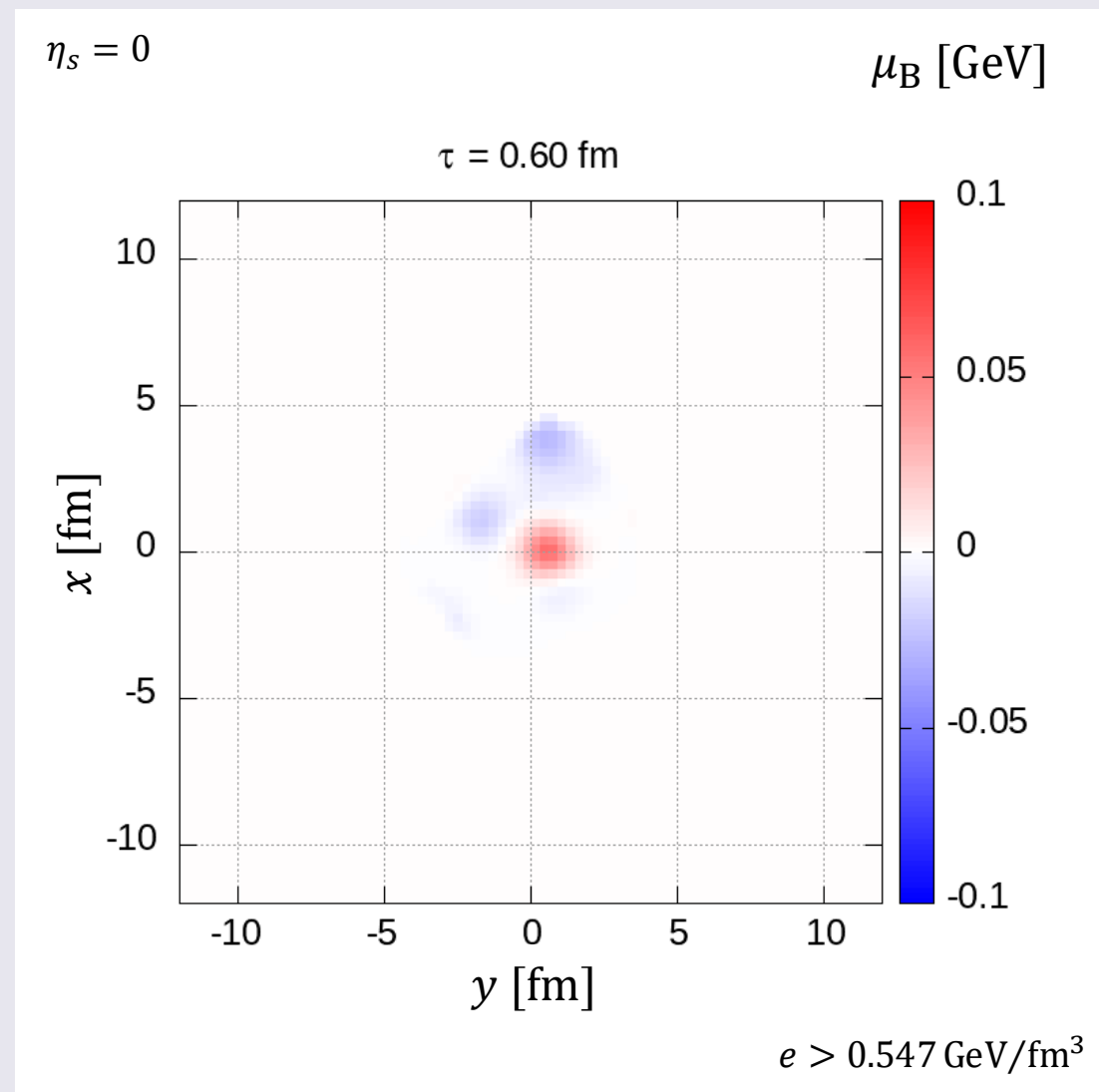


Space-time evolution of core

Baryon chemical potential (longitudinal profile)



Baryon chemical potential (transverse profile)



High baryon number density at LHC energies

Nuclear compression + CGC

Ming Li, Ph.D thesis, U. of Minesota (2018)

M. Li and J. I. Kapusta, Phys. Rev. C **99**, 014906 (2019)

- Solving classical gluon fields of receding nuclear remnants
 ⇒ Rapidity loss Δy of nucleons

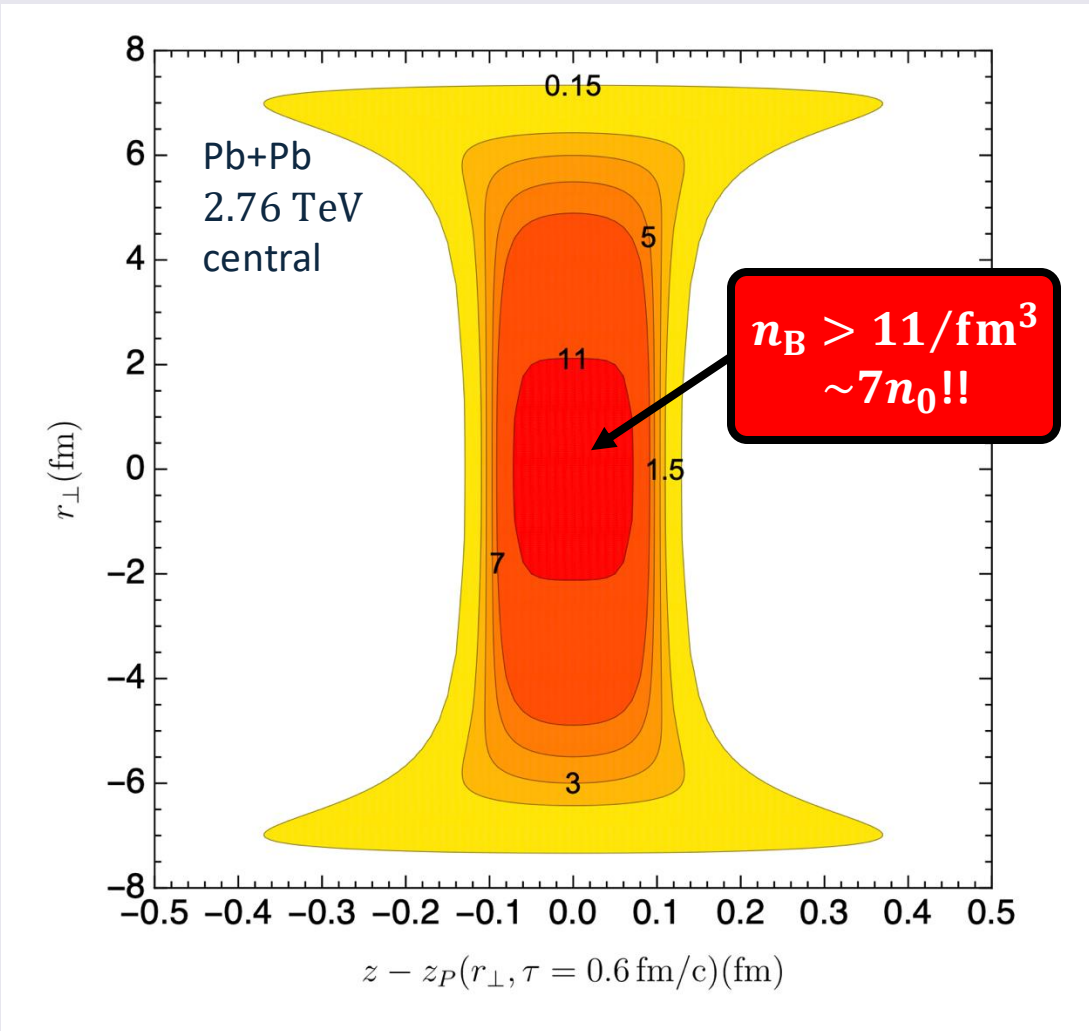
- Nuclear compression by Δy

$$n_B(x, y, z) \approx e^{\Delta y} \rho_A(x, y, ze^{\Delta y}) \text{ @high energy}$$

M. Gyulassy and L. P. Csernai, Nucl. Phys. A **460**, 723 (1986)

➔ **Extremely high baryon number density in the fragmentation regions of high-energy heavy ion collisions**

Baryon number density of compressed Pb



Source terms

Energy-momentum source term

$$\partial_\mu T_{\text{fluid}}^{\mu\nu} = j^\nu$$

$$j^\nu = - \sum_i \frac{dp_i^\nu(t)}{dt} G(\mathbf{x} - \mathbf{x}_i(t))$$

p_i^ν : Four-momentum of i_{th} parton

G : Gaussian function \mathbf{x}_i : Position of i_{th} parton

When i_{th} parton
deposit all energy
= dead parton

Baryon number source term

New!!

$$\partial_\mu N_{\text{fluid}}^\mu = \rho$$

$$\rho = - \sum_{i_{\text{dead}}} \frac{dB_{i_{\text{dead}}}}{dt} G(\mathbf{x} - \mathbf{x}_{i_{\text{dead}}}(t))$$

$B_{i_{\text{dead}}}$: Baryon number of $i_{\text{dead}}\text{th}$ parton

Phenomenological fluidization rate per particle in core-corona picture

$$\frac{dp_i^\mu}{d\tau} = - \sum_j^{N_{\text{scat}}} \rho_{i,j} \sigma_{i,j} |v_{\text{rel},i,j}| p_i^\mu$$

$\rho_{i,j}$: Effective density of j_{th} seen from i_{th}

$\sigma_{i,j}$: Cross section between i_{th} and j_{th}

$v_{\text{rel},i,j}$: Relative velocity between i_{th} and j_{th}

Low p_T / Dense

→ Core

High p_T / Dilute

→ Corona

NEOS-BQS

Taylor expansion using Lattice results (high T)

$$\frac{P}{T^4} = \frac{P_0}{T^4} + \sum_{l,m,n} \frac{x_{l,m,n}^{B,Q,S}}{l,m,n} \left(\frac{\mu_B}{T}\right)^l \left(\frac{\mu_Q}{T}\right)^m \left(\frac{\mu_S}{T}\right)^n$$

Hadron gas (low T)

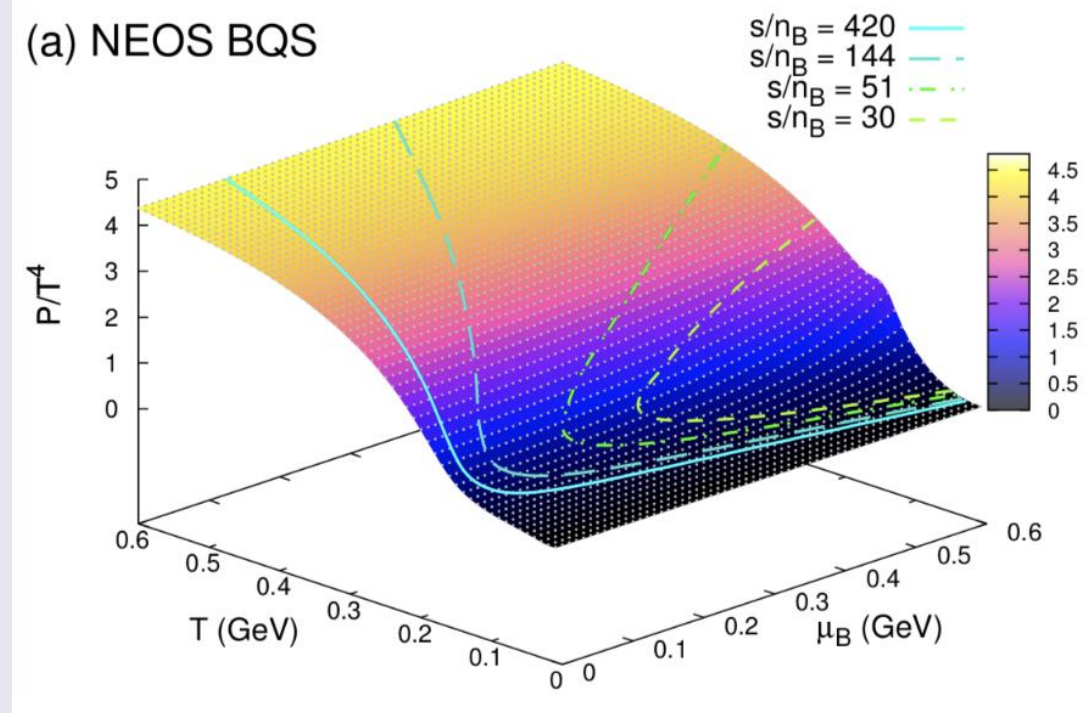
$$P = \pm T \sum_i \int \frac{g_i d^3p}{(2\pi)^3} \ln[1 \pm e^{-(E_i - \mu_i)/T}]$$

$$= \sum_i \sum_k (\mp 1)^{k+1} \frac{1}{k^2} \frac{g_i}{2\pi^2} m_i^2 T^2 e^{k\mu_i/T} K_2\left(\frac{km_i}{T}\right)$$

CONNECT

$$\frac{P}{T^4} = \frac{1}{2} [1 - f(T, \mu_J)] \frac{P_{\text{had}}(T, \mu_J)}{T^4} + \frac{1}{2} [1 + f(T, \mu_J)] \frac{P_{\text{lat}}(T, \mu_J)}{T^4}$$

(a) NEOS BQS



Constraints: $n_Q = 0.4n_B$, $n_S = 0$

$$e(T, \mu_B) = e(0.165 \text{ GeV}, 0) = 0.547 \text{ GeV}/\text{fm}^3$$

➔ e_{sw} for core

Hydrodynamic module in DCCI

Energy-momentum conservation

$$\partial_\mu T_{\text{fluid}}^{\mu\nu} = j^\nu$$

$$T_{\text{fluid}}^{\mu\nu} = e u^\mu u^\nu - p \Delta^{\mu\nu} \quad \leftarrow \text{ideal hydro}$$

$$j^\nu = - \sum_i \frac{dp_i^\nu(t)}{dt} G(\mathbf{x} - \mathbf{x}_i(t))$$

Baryon number conservation

$$\partial_\mu N_{\text{fluid}}^\mu = \rho$$

$$N_{\text{fluid}}^\mu = n_B u^\mu \quad \leftarrow \text{ideal hydro}$$

$$\rho = - \sum_{i_{\text{dead}}} \frac{dB_{i_{\text{dead}}}}{dt} G(\mathbf{x} - \mathbf{x}_{i_{\text{dead}}}(t))$$

$$G_{\text{Milne}} = \frac{1}{\sqrt{2\pi\sigma_\eta^2\tau^2}} \exp\left(-\frac{(\eta_{s,\text{parton}} - \eta_{s,i})^2}{2\sigma_\eta^2}\right) \times \frac{1}{2\pi\sigma_{xy}^2} \exp\left(-\frac{(x_{\text{parton}} - x_i)^2 + (y_{\text{parton}} - y_i)^2}{2\sigma_{xy}^2}\right)$$

Default: $\sigma_\eta = 0.5$, $\sigma_{xy} = 0.6$ fm

RHIC-BES data

L. Adamczyk *et al.* (STAR Collaboration), Phys. Rev. C **96**, 044904 (2017)

